ELECTRODE REACTION KINETICS DETERMINED BY CYCLIC VOLTAMMETRY AND RELATED STUDIES

SHACHAR NADLER

A Thesis

in

The Department

of

Chemistry

Presented in Partial Fulfillment of the Requirements
for the degree of Master of Science (Chemistry) at
Concordia University
Montreal, Quebec, Canada

June 1983

ABSTRACT

ELECTRODE REACTION KINETICS DETERMINED BY CYCLIC VOLTAMMETRY AND RELATED STUDIES

Shachar Nadler

A commercially available voltammetric system was evaluated and found suitable for cyclic voltammetry (CV) work. The initial assessment was carried out by evaluating the standard reaction rate constants (K_s) for the cadmium and zinc systems at the hanging-mercury-drop electrode (HMDE). The results obtained were in good agreement with values reported in the literature. The CV technique used is based on the anodic/cathodic peak potentials separation.

The versatility of CV was demonstrated from data collected from several chromium polypyridyl complexes. It was shown that pertinent data such as peak-height-to-concentration ratio and polarographic half-wave potentials can be easily determined from cyclic voltammograms. Three existing methods for computing $E_{1/2}$ were compared. Best results were obtained using a

technique based on the fact that $E_{1/2}$ occurs at a point 85.17% up the cathodic slope. Consequently, all the $E_{1/2}$ values needed for the computation of reaction rates were determined by this technique.

The reaction rate constants (K_f) for aqueous $[Cr(2,2'\text{-bipyridine})_3]^{+3}$ and $[Cr(4,4'\text{-dimethyl-}2,2'\text{-bipyridine})_3]^{+3}$ were evaluated by CV. These complexes display similar electrochemical behaviour in water; i.e. a reversible electron transfer is followed by an irreversible chemical reaction in the form of

$$O + ne \rightleftharpoons R \xrightarrow{K_f} Z.$$

K_f can be computed from its relation to the anodic/cathodic peak height ratio (i_a/i_c). Existing techniques for evaluating i_a/i_c were not applicable due to complication created by the "charging current." Consequently, a semiempirical method was developed to properly evaluate i_a/i_c. Using this technique, good results were obtained for the rate of reaction (K_f) for both complexes.

ACKNOWLEDGEMENTS

The author wishes to acknowledge above all the interest, expertise, and invaluable assistance of Professor J. G. Dick in connection with every aspect of the present work. Thanks are also due to Brinkmann Instruments LTD for lending the analytical system.

Appreciation is extended to Dr. N Serpone and Dr. M. Jamieson for supplying the chromium complexes and the initial pertinent information, to Dr. C. H. Langford for valuable advice on interpretation of data. Deep felt thanks go to Dr. S. J. Daunt for encouragement and numerous valuable discussions.

Thanks are also due to Mr. S. Seto for the regular "bull sessions" and for being the ideal lab partner, to my daughter Daphnee for helping with the tedious computer work, to Ms. V. Bozarth for typing the manuscript and finally to my friend Richard Shoemaker for an excellent job of proofreading.

THIS THESIS IS DEDICATED TO MY PARENTS

CLARA AND IULIUS NADLER.

TABLE OF CONTENTS

CHAPTER 3

THE STANDARD RATE CONSTANT FOR CADMIUM AND ZINC

CHAPTER 4

THE VERSATILITY OF CYCLIC VOLTAMMETRY

CHAPTER 5

THE RATE OF REACTION OF $Cr(bipy)_3$ AND $Cr(me_2\text{-}bipy)_3$ IN AQUEOUS SOLUTIONS

CHAPTER 6

APPENDIX A

APPENDIX B

APPENDIX C

LIST OF FIGURES

LIST OF TABLES

CHAPTER 1

INTRODUCTION

1.1 Introductory Remarks

Perhaps no other single instrumental method has had so profound an influence on analytical chemistry as voltammetry. Possessing both qualitative and quantitative capabilities, voltammetry has proven to be a powerful tool with a wide range of application from simple trace-metal determination in the low ppb range to the less mundane in vivo monitoring of brain chemistry (1,2, 3,4).

Rapid-sweep single and cyclic voltammetry is commonly used in the study of the redox behavior of chemical species as this applies to electrode reaction situations. In recent years, this relatively new branch of voltammetry has emerged as the most convenient method for the investigation of rate of reaction, electrode kinetics, and mechanism of reaction (5,6,7). This aspect of voltammetry is the focal point of this experimental work.

1.2 Experimental Objectives

This project has three experimental objectives:

Part A: To evaluate the suitability of a commercially available cyclic voltammetry (CV) unit in the determination of the standard rate of reaction for cadmium and zinc.

Part B: To demonstrate the general versatility of cyclic voltammetry.

Part C: To determine the rate of reaction for processes where a charge transfer is followed by an irreversible chemical reaction.

1.2.1 Part A: Instrumental evaluation on cadmium and zinc systems

Although the Metrohm voltammetric system will be evaluated throughout the experimental phase, the initial assessment as to accuracy and reproducibility will be made by determining the rate of reaction of simple and well-known processes; i.e., the standard rate constants (K_s) at the hanging mercury drop electrode (HMDE) for the cadmium and zinc systems:

$$Cd^{+2} + 2e \overset{K_s}{\rightleftharpoons} Cd(Hg)$$

$$Zn^{+2} + 2e \overset{K_s}{\rightleftharpoons} Zn(Hg)$$

The cadmium and zinc systems were chosen because:

(a) Their standard rate constants have been reported in the literature.

(b) Cadmium is a highly-reversible system, while zinc is a quasi-irreversible system.

(c) The difference in the reversibility of the two systems permits demonstration of the importance of both the slow and rapid sweep methods of approach in CV.

1.2.2 Part B: The versatility of cyclic voltammetry

This aspect of cyclic voltammetry will be demonstrated using four different chromium complexes:

$[Cr(bipy)_3](ClO_4)_3 \cdot \frac{1}{2}H_2O$

$[Cr(4,4'\text{-}me_2\text{-}bipy)_3](ClO_4)_3 \cdot H_2O$

$[Cr(terpy)_2](ClO_4)_3 \cdot 2\frac{1}{2}H_2O$

$[Cr(ph_2\text{-}bipy)_3](ClO_4)_3 \cdot 2H_2O$

When in non-aqueous media, these complexes are known to have four reversible oxidation state reactions. We shall see that the transitions between these states can be easily observed. In addition, it will be seen that other information, such as the peak current to concentration ratio and the polarographic half-wave potential ($E_{1/2}$) may be obtained concurrently. Three different methods of obtaining $E_{1/2}$ are compared.

1.2.3 Part C: The rate of reactions of $[Cr(bipy)_3]^{+3}$ and $[Cr(4,4'\text{-}me_2bipy)_3]^{+3}$ in aqueous solutions

Both these complexes demonstrate similar behavior in aqueous solutions; that is, following the first reduction wave, an irreversible chemical reaction occurs. The rate of reaction (K_f) for $[Cr(bipy)_3]^{+3}$ has been previously determined by a variety of techniques, including cyclic voltammetry.

Thus, while the rate of reaction for both these complexes will be determined here, that for $[Cr(bipy)_3]^{+3}$ will be used for comparison and calibration purposes only. The main emphasis of this experimental phase is, however, again on technique and instrumental evaluation.

CHAPTER 2

VOLTAMMETRIC PRINCIPLES AND INSTRUMENTATION

2.1 General Introduction

Much of the following is derived from the works of J. Heyrovsky (8), J. G. Dick (9), L. Meites (10), P. Delahay (11) and R. N. Adams (12).

Voltammetry may be defined as the study of the current-potential (i-E) relationships in an electrolytic medium as measured by the use of microelectodes. More specifically, it is the determination of the potential of a single microelectrode during the course of a sustained electron transfer at an electrode surface, i.e., while a net current flows through the electrochemical cell. The process usually involves the controlled application of potential and the measurement of the associated current flow situation--hence, the term "voltammetry." That branch of voltammetry which involves the use of a microelectrode of the dropping mercury form (dme) is called polarography.

2.1.1 The nature of the currents generated in voltammetry

The surface area of the microelectrode used in

these measurement processes is very small; consequently the currents under study are also very small, ranging from microampere to fractional nanoamperes. It follows then that voltammetric systems have to take into consideration several factors, such as:

(a) iR drop (ohmic behavior within the solution under study).

(b) the dependence of current flow on the electrode reaction rate, and

(c) the stability of the potential which, for all practical purposes, is kept constant when the current is measured.

The currents generated in voltammetry are generally a function of mass transfer processes. A discussion of voltammetry requires a clear understanding of these processes.

Electrode processes are reactions which consist of three consecutive steps.

1. Transfer of the species to be reacted to the electrode surface.

2. Electron transfer at the electrode surface.

3. Transfer of the species reaction product away from the electrode surface.

This last step may involve transfer of the reaction product into the mercury drop or into the solution. The overall rate at which an electrode reaction proceeds

depends generally on the kinetic parameters for these three steps. In addition, surface adsorption phenomena may also have to be considered, as well as problems arising from the coupling of the electron transfer process with subsequent, purely chemical reactions.

2.1.2 Mass transfer processes

These are processes or mechanisms which govern the distribution of the reaction species within the electrochemical reaction and, in particular, in the immediate neighbourhood of the working microelectrode surface. The three most important mass transfer modes in electrochemical work are:

(a) diffusion

(b) convection

(c) electrostatic migration.

Diffusion is observed whenever there exists a difference in solute concentration between two adjacent solution zones. The direction of solute diffusion is from the higher to the lower concentration zone, and the rate of diffusion at constant temperature is a function of the concentration difference. An associated definition is that diffusion occurs over zones of difference in chemical potential for a given species.

Convection results from mechanical or thermal stirring actions. The latter occurs as the result of

heating or cooling processes. The dme causes some convection (stirring) with the fall of each drop of mercury.

Migration is the motion of a charged species to (or away from) the charged working electrode. This mass transfer by electrostatic attraction complicates the interpretation of results obtained in voltammetry. The migration effect is minimized by providing, in the solution, in the case of cathodic microelectrode reduction processes, a concentration of a positively charged ion that will be attracted to the cathode but, in the solution medium involved, not discharged or reduced. The concentration of the salt providing such an ion, called the supporting electrolyte, will be high relative to the concentration of the species ([O]) in the bulk of the solution.

In single- and cyclic-sweep voltammetry, as in the case of classical D.C. polarography, diffusion is the principal method of mass transfer. It follows then that the diffusion current is also the only current of interest. However, in order to fully understand the current-potential relationship in single- and cyclic sweep voltammetry, it is important to comprehend these relationships in DC polarography.

2.2 Classical D.C. Polarography

D.C. polarography is based on Heyrovsky's findings (13), as reported in 1922, while investigating electrochemical processes at the dme. He found that, at particular potentials, the current flow between two electrodes (one of which was a dme) in an electrolytic cell is related to the concentration of one of the species present in the cell. With the advances of technology the polarographic system became the subject of numerous modifications, including a three electrode cell arrangement. The basic principle, however, remained the same, and polarography is commonly used for quantitative and qualitative analytical work.

Although the diffusion current is the only current of interest, it is not the only current existing at the dme. It is necessary to consider all current situations existing for the changing dme surface. Due to the nature of the dme, the flow rate of mercury into the drop throughout its lifetime is constant. However, while the volume of the drop increases at a constant rate, the surface area of the drop does not so change, as can be seen from Figure 2-1. As the drop grows, its surface area increases at first very rapidly, proportionally speaking, and this rate of growth falls off with time to drop dislodgement. At the same time, the drop surface moves into the solution, at first rapidly, and then slowly near the end of

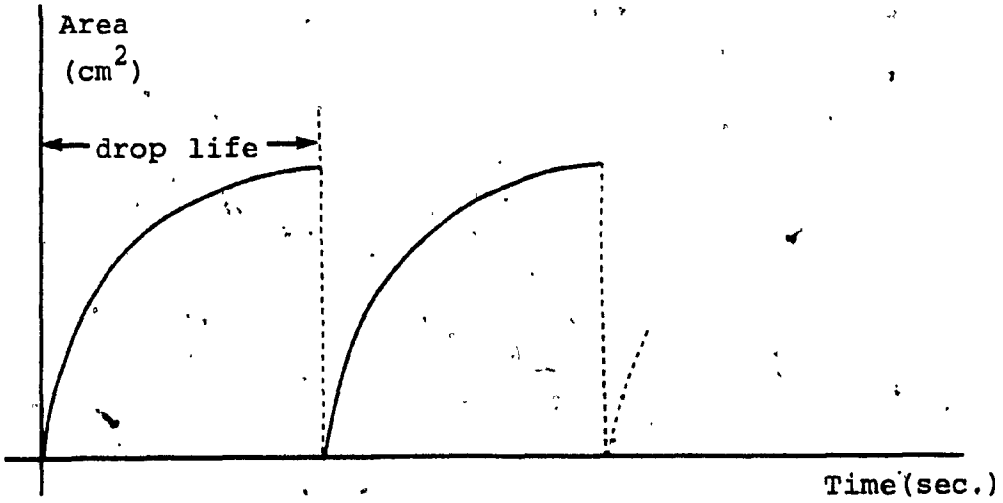

Figure 2-1: Surface growth of mercury drops as a function of time.

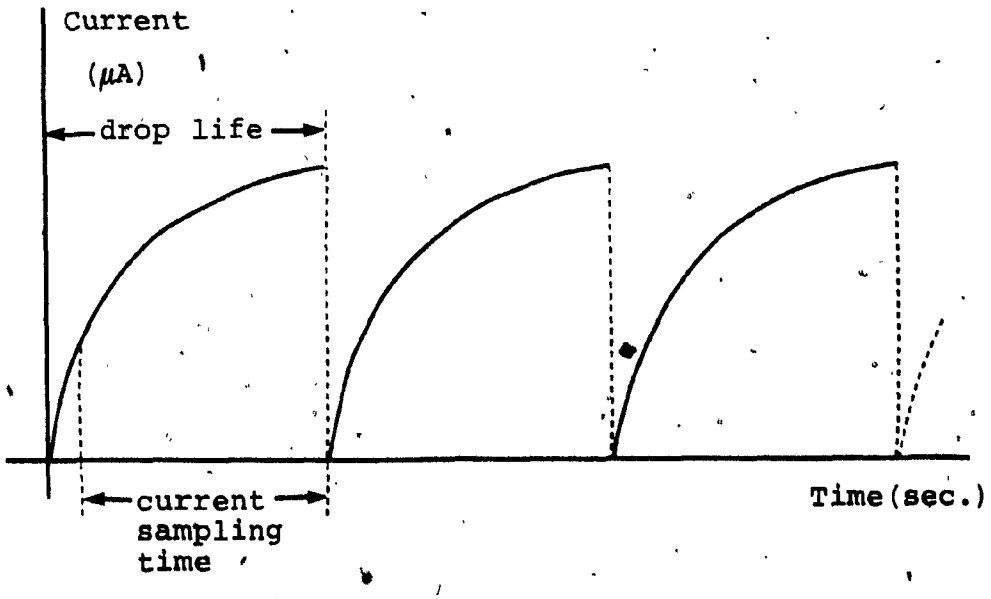

Figure 2-2: Current as a function of time at the dme.

the drop life. Both of these effects cause increases in the measured current. Such increases become minimal near the end of the drop life, when a concentration-depleted zone is formed at the electrode surface for the active species. The net current result is as shown in Figure 2-2. The sudden fall of the drop stirs the solution sufficiently to destroy the concentration gradient zone. As a result the current-time (i-t) curve remains the same for successive drops, again as shown in Figure 2-2. The depletion of reacting species within the electrolytic cell with successive drops is generally negligible.

As shown in Figure 2-2, current measurements are taken almost throughout the lifetime of each drop. From the nature of drop surface growth, however, it is evident that the current generated is to some extent due to the droplet expansion into the solution at the beginning of drop life and largely due to diffusion towards the end of drop life. A complete current potential curve (or wave) is obtained by determining the average current as a function of the dme potential as shown in Figure 2-3. The current corresponding to the upper plateau of the wave is generally referred to as the "diffusion current" (i_d). However, in cases where there is partial or total control of the current by a chemical reaction, the upper plateau is called the "limiting current." The expression "limiting current" is

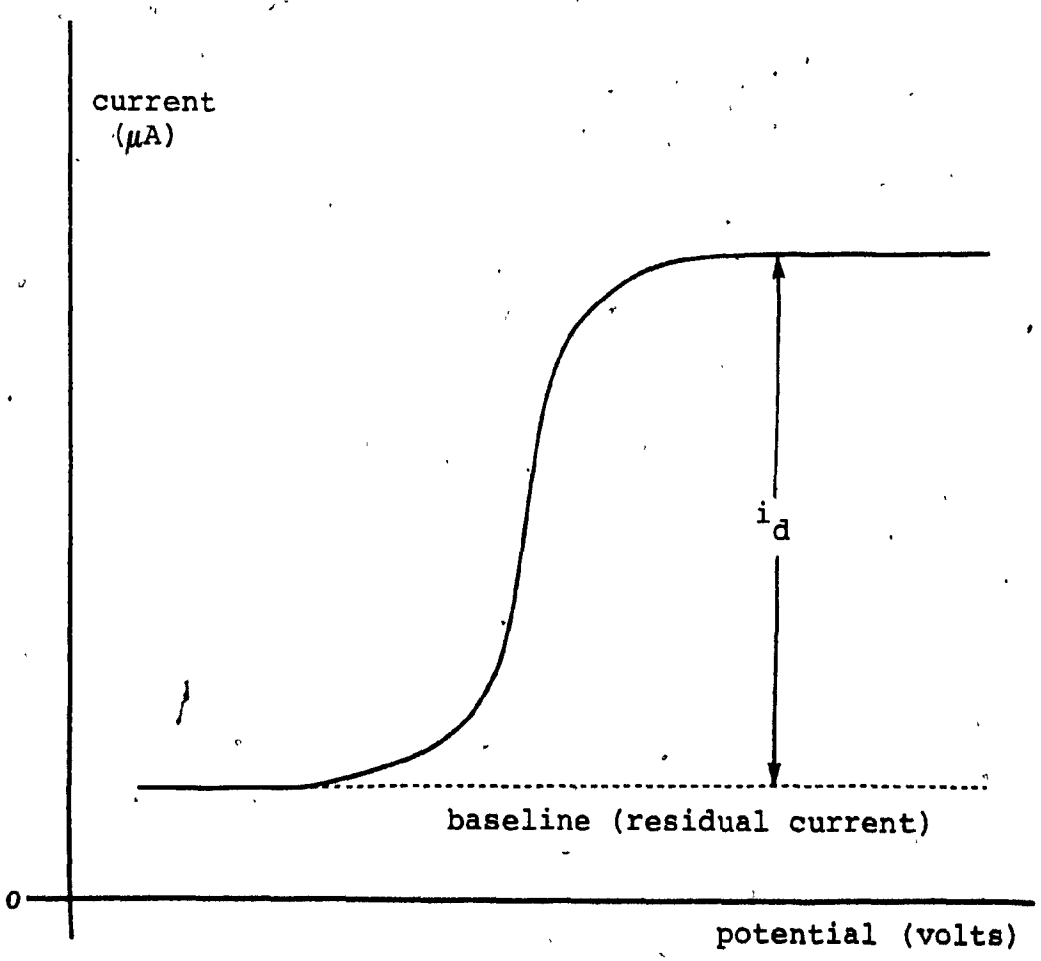

Figure 2-3: The polarographic wave.

also applicable to currents partially or totally controlled by convective transfer. The properties of these waves are very important from the analytical point of view, since the diffusion current is proportional to the concentration of the analyte.

The total height of a D.C. polarographic wave in the absence of any complicating factors is due to three separate contributions:

1. diffusion current (analyte)
2. impurities current
3. charging current.

The last two currents are often described as the residual current. The impurities current is due to reduction or oxidation of trace electroactive impurities in the solvent and supporting electrolyte. The charging current (i_c) is a small nonfaradaic current necessary to charge the electrical double layer of each individual mercury drop. Simply by recording a polarogram of the supporting electrolyte (blank) alone and subtracting it from the total limiting current, one obtains the desired diffusion current.

The correlation between the diffusion current (i_d) and the analyte concentration involves many factors, such as droplet boundary conditions, diffusion coefficients, and the electrochemical reactions involved. The earliest solution to the diffusion current/

concentration relationship was presented by Ilkovic (14). Over the years, several solutions evolved among which Equations 2-1 and 2-2 describe the commonly accepted solutions.

$$\bar{i}_d = \frac{1}{\tau}\int_0^{\tau} 709 n m^{2/3} t^{1/6} D_o^{1/2} C_o dt \qquad (2\text{-}1)$$

$$\bar{i}_d = 607 n m^{2/3} \tau^{1/6} D_o^{1/2} C_o \qquad (2\text{-}2)$$

where at 25°C:

$\bar{i}_d$=average diffusion current (μA)

n =number of electrons in the transfer

t =time (sec)

τ =drop life (sec)

m =rate of mercury flow (mg/sec)

D_o=diffusion coefficient (cm^2/sec)

C_o=concentration of analyte (mM)

The constants 607 and 709 are derived from the products of several factors such as Faraday's constant, the quantity π from the spherical equation and the density of mercury at 25°C.

The next important factor in D.C. polarography is the residual current. The major contributor to this current is the charging current, provided that dissolved oxygen has been removed from the solution by passage of an inert gas (e.g., nitrogen).

2.2.1. The charging current

Due to the adsorptive nature of the supporting electrolyte, positive electrolyte ions will migrate to the surface of the negative (potential) dme. Thus, the dme takes on a net positive charge which in turn attracts another layer of negative ions. This double layer, which does not involve electron exchange, behaves as a condenser (capacitor). With each drop formed, a certain current is needed to charge and establish this double layer. This quantity of electricity is usually referred to as the charging or capacity current. The equation for the charging current derived by Ilkovic (14) shows the following relationhips:

$$i_c = \frac{dQ}{dt}, \text{ and} \qquad (2\text{-}3)$$

$$\bar{i}_c = \frac{1}{\tau}\int_0^{\tau} i_c dt \qquad (2\text{-}4)$$

where i_c=charging current

$\bar{i}_c$=average charging current

t =time

τ =drop life

Q =charge quantity (coulombs).

The distorting effect of the charging current can be clearly seen from the ratio of capacity current to the peak (total) current.

$$\frac{\bar{i}_c}{i_p} = 2.3\text{x}10^{-8}\ \frac{v^{1/2}}{n^{3/2}C_o} \qquad (2\text{-}5)$$

where $v=\frac{dE}{dt}$ i.e., potential sweep rate (v/sec)

n =number of electrons

C_o=concentration of analyte.

Equation 2-5 provides information concerning the limit of detection of the D.C. method. In the practical sense, the limit of detection is reached when the diffusion current average approaches the charging current average. Experimental work at the dme (8,11) shows that the lower limit of detection, which is limited by the capacity current, is approximately 10^{-5}M. The i-E curves in Figure 2-4 demonstrate the effect of $\bar{I}_c$ on the total current read-out.

2.2.2 The polarographic half-wave potential ($E_{1/2}$)

This is another important quantity in polarography since it is a prime qualitative indicator.

Equation 2-2 is based on the assumption that $C_o(x=0)$ is negligible at the time the drop dislodges. In the case where $C_{o(x=0)}=0$, Delahay (11) shows that the Ilkovic equation becomes

$$\bar{I} = 607nm^{2/3}D_o^{1/2}\tau^{1/6}[C_o-C_{o(x=0)}] \text{ at } 25^oC \quad (2-6)$$

$$\text{or } \bar{I} = \bar{I}_d - 607nm^{2/3}D_o^{1/2}\tau^{1/6}C_{o(x=0)} \quad (2-7)$$

Now, considering the reaction $O + ne \rightleftharpoons R$, if one defines C_r as [R] at electrode surface,

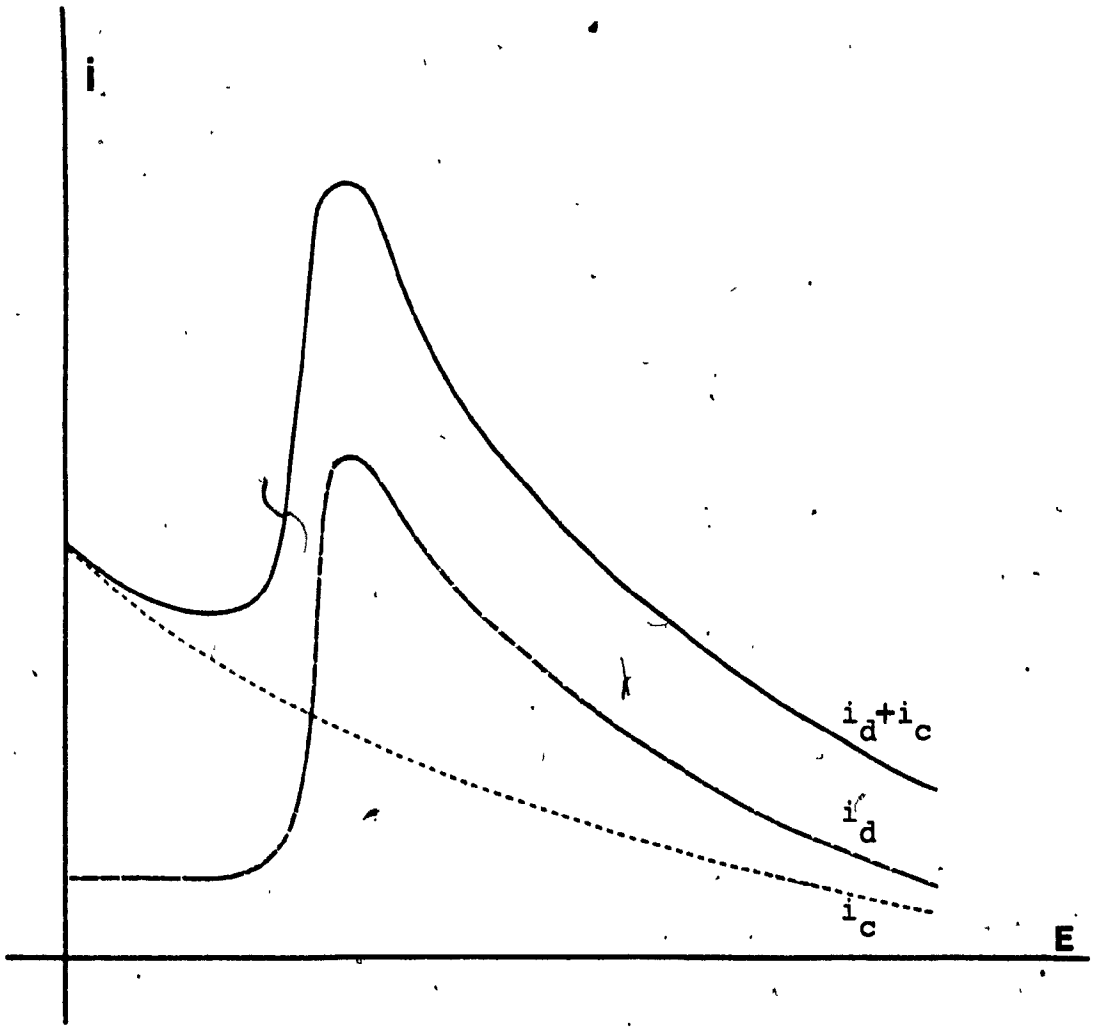

Figure 2-4: Distortion of current-potential curve by charging current (i_c)(Ref.11).

then $C_o - C_{o(x=0)} = C_{r(x=0)}$

Therefore, Equation (2-6) becomes

$$\bar{I} = 607nm^{2/3}D_r^{1/2}\tau^{1/6}C_{r(x=0)} \qquad (2\text{-}8)$$

from Equations 2-7 and 2-8

$$\frac{C_o}{C_r}(x=0) = \left[\frac{D_r}{D_o}\right]^{1/2} \frac{\bar{I}_d - i}{i} \qquad (2\text{-}9)$$

Applying the Nernst relationship, one obtains

$$E = E^o - \frac{RT}{nF}\ln \frac{f_r}{f_o}\left[\frac{D_o}{D_r}\right]^{1/2} + \frac{RT}{nF}\ln\frac{\bar{I}_d - i}{i} \qquad (2\text{-}10)$$

$$= E_{1/2} + \frac{RT}{nF}\ln\frac{\bar{I}_d - i}{i} \qquad (2\text{-}11)$$

where

$$E_{1/2} = E^o - \frac{RT}{nF}\ln \frac{f_r}{f_o}\left[\frac{D_o}{D_r}\right]^{1/2} \qquad (2\text{-}12)$$

and

E =electrode potential (vs. known reference)

E^o=standard potential for the O-R couple

$E_{1/2}$=half-wave potential

f =activity coefficient

D =diffusion coefficient

i =average current at any potential

$\bar{I}_d$=average diffusion current.

Hence, Equation 2-12 can predict and/or identify the potential at which a given species will react, and, in addition, Equation 2-10 describes the polarographic

wave by showing the relation between i-E and $\bar{i}_d$-E.

2.2.3 Differential pulse polarography (DPP)

The DPP technique was developed as an offshoot of square wave polarography where the general aim was to minimize the effects of the charging current. The technique involves the application of a fixed amplitude pulse at regular intervals on a slow potential sweep similar to that of D.C. polarography. The pulse is repeated for each drop and is synchronized with the point of maximum growth of the mercury drop. The system then samples the current flowing into the working electrode twice during each operating interval. The first current sample is taken just before the application of the potential pulse and would be equivalent to that obtained in normal D.C. polarography. Immediately after the current sampling, a pulse of potential (5 to 100mV amplitude) is applied to the electrode. This change in potential will, if the D.C. potential sweep is in the lower half of the S-wave forms, result in an increase in the current. If the potential sweep is in the upper half of the S-wave form, a current decrease will occur. To start with, additional current must flow to change the double layer capacitance of the electrode to the new applied potential. In addition and simultaneously, current may flow if the applied potential has changed to a

point where the equilibrium between O and R is shifted.

The applied pulse is maintained long enough to allow the capacitance current to decay to a low value. During this time the faradaic current also decays, but it does not drop below the diffusion-controlled level. Towards the end of the pulse life the current is sampled again. The difference between these two current samples is then amplified and presented as the output current in the i-E curve as shown in Figure 2-5. The peak height of this curve above the baseline is proportional to the concentration of the analyte.

The main advantage of this technique is the minimization of the influence of the charging current, since i_c is being subtracted in the difference between the two current samples. This provides an improved resolution and a better lower limit of detection, 10^{-7} to 10^{-8}M for most metallic cations (15, 16).

2.3 Rapid-Sweep Voltammetry

In conventional voltammetry/polarography the potential is changing in a slow linear ramp over a relatively long period of time, so that, in the intervals during which the current is measured, the potential can be considered stationary. In single and cyclic voltammetry techniques, the i-E relationship is obtained by the use of a rapid potential sweep. The sweep rate is

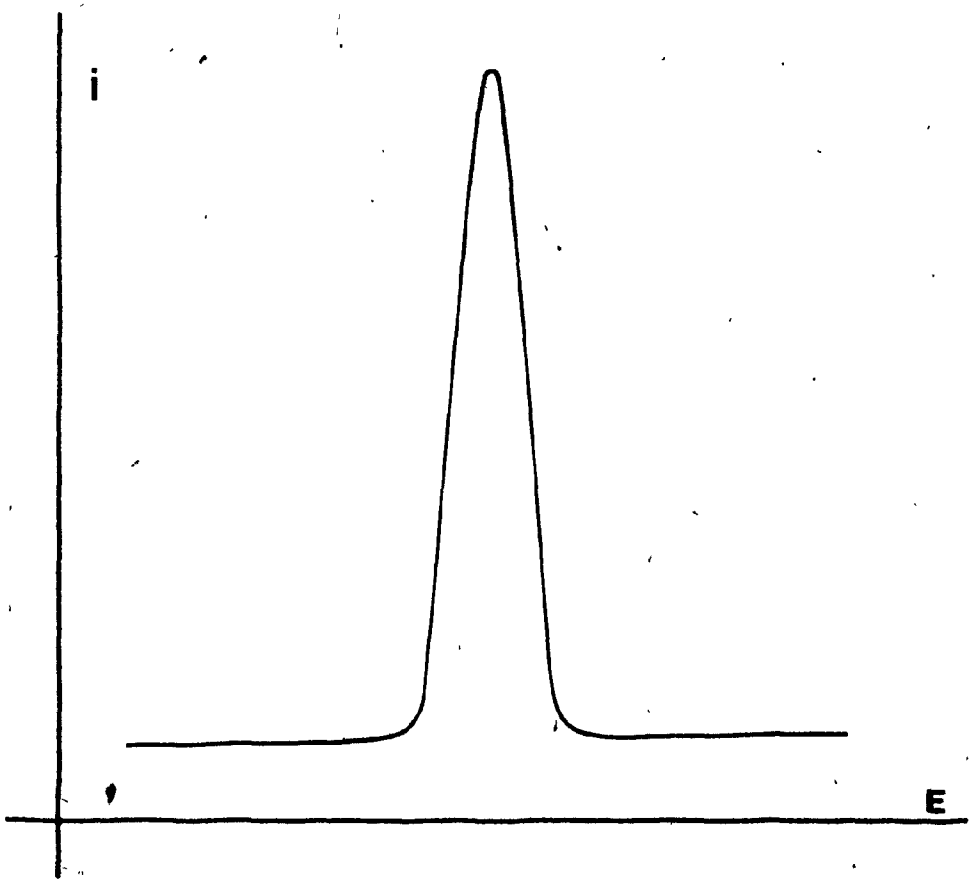

Figure 2-5: Current - Potential curve obtained from DPP.

usually of such a magnitude that the full range of potential (range of interest) can be covered within the lifetime of one Hg drop when the dme is used. As such, the dme can be considered as a stationary hanging mercury drop electrode (HMDE). In general, these techniques utilize stationary electrodes (e.g., HMDE or solid electrodes).

When discussing voltammetry with continuously variable (rapid sweep) potential, a distinction should be made between the i-E relations obtained in single sweep, multi-sweep and cyclic-sweep approaches.

2.3.1 Single-sweep voltammetry

The method derives its name from the fact that each drop (dme) during its life receives only one impulse of polarization potential, usually a saw-toothed sweep such as shown in Figure 2-6a. The production of very rapid voltage sweeps necessitates the use of electronic impulse generators which permit good linearity and variation of the sweep frequency within wide limits. For example, a frequency of 50Hz with an amplitude of 2 volts corresponds to a sweep rate of 600 volts/minute. The saw-toothed voltage must also have exact linearity, besides being as constant as possible in duration and amplitude.

Whereas in ordinary polarography the diffusion

current is independent of the speed of the voltage sweep, in rapid-sweep polarography the peak current is influenced by the rate of voltage sweep, as will be shown later. In addition, the choice of timing at which the impulse is applied to the dme is of utmost importance. In order to obtain good reproducible results, the impulse and drop-time must be exactly synchronized. This is achieved electrically by applying the potential with regular controlled intervals (delays) as shown in Figure 2-6b. Minimization of charging current is obtained by applying the potential pulse towards the end of the drop life. This consideration is not of interest when stationary electrodes are used.

If one considers the reduction of an analyte in an unstirred solution containing an excess of background electrolyte, so that linear diffusion is maintained, the Nernst relation is assumed to be applicable to the electrode process. The sweep voltage can be represented by

$$E = E_i - Vt \qquad (2\text{-}13)$$

where E_i = initial potential (volts)

V = rate of potential sweep (volts/sec.)

t = electrolysis interval (sec.).

No reduced substance is assumed to exist at t=0; hence, with the exception of the variable potential Vt,

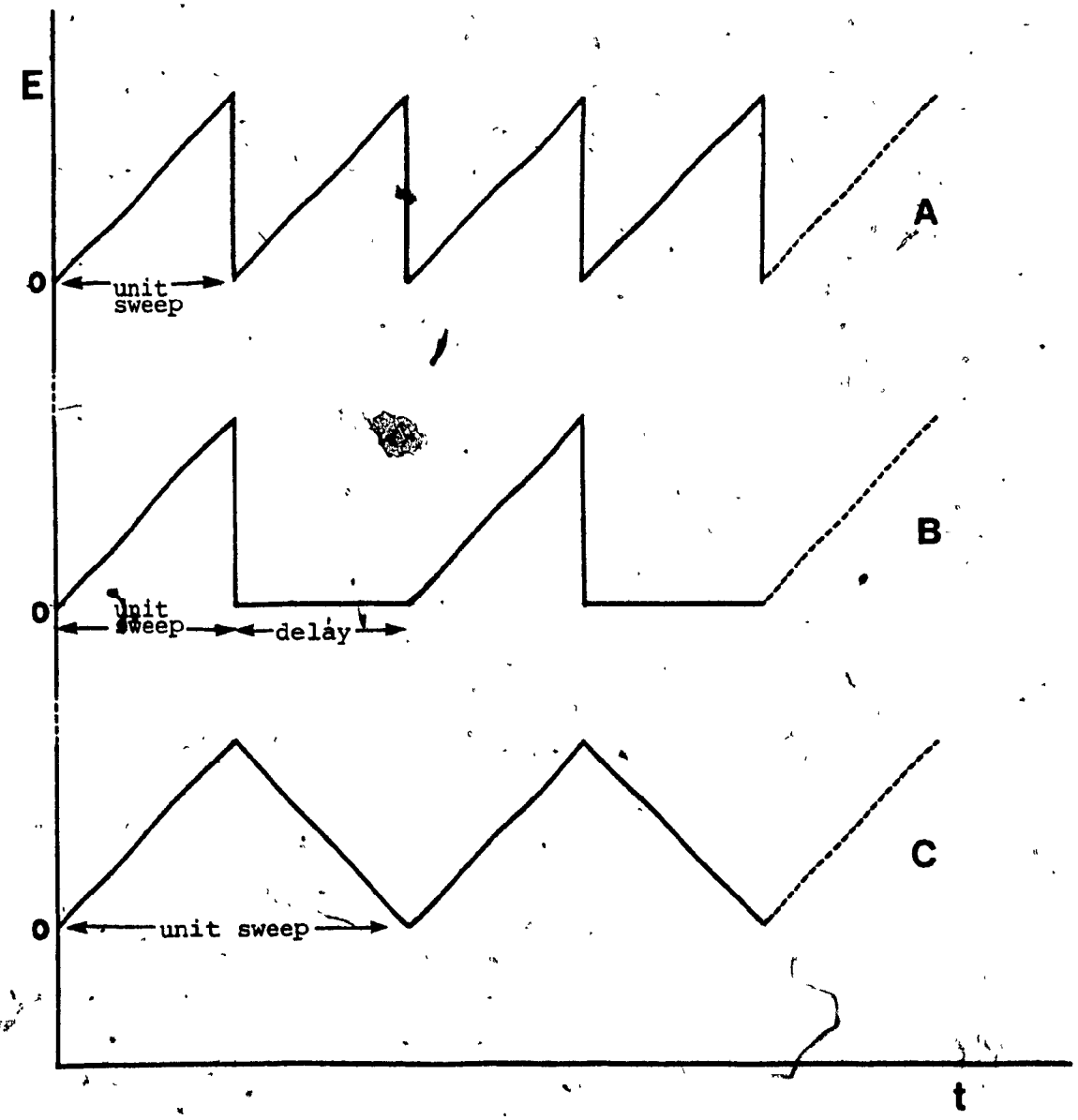

Figure 2-6: Types of potential sweeps in rapid scan voltammetry.

A. sawtoothed wave for single & multisweep methods
B. sawtooth with delay between sweeps
C. isosceles triangle for cyclic voltammetry.

conditions are identical to those for conventional polarography.

The diffusion problem for rapid-sweep polarography was first solved and translated into a current potential relationship independently by Randle and Sevcik (17,18). The i-E curve exhibits a maximum or peak, and the peak current is given by

$$i_p = Kn^{3/2}AD_o^{1/2}C_bV^{1/2} \qquad (2\text{-}14)$$

where i_p=peak current (amperes)

A =electrode surface area (cm^2)

K =Randle-Sevcik constant

C_b=concentration of analyte (moles).

It should be noted that the peak current (i_p) is directly proportional to the concentration and the sweep rate.

The i-E curves obtained from single-sweep polarography are commonly called peak polarograms, and the technique became known as peak voltammetry. This is due to the nature of the electrode process. In this technique, the full process occurs within the lifetime of a single mercury drop or at a stationary electrode. Consequently, as the potential sweep passes the peak potential (E_p), the electrode process results in a depletion of depolarizer (analyte) in the vicinity of the electrode so that the system displays a current drop, as can

be seen in Figure 2-7.

The single-sweep polarogram may be characterized by the peak potential (E_p) or the half peak potential ($E_{p/2}$). The latter is defined as the potential at which $i=i_p/2$. The relationships between charge transfer and peak height, location, and shape and their correlation to the polarographic half-wave potential, were derived by Matsuda and Ayabe (19) as follows:

For reversible processes at 25°C,

$$E_p = E_{1/2} - \frac{0.029}{n}V \qquad (2\text{-}15)$$

$$E_{p/2} = E_{1/2} + 109\frac{RT}{nF} = E_{1/2} + \frac{0.028}{n}V, \qquad (2\text{-}16)$$

$$E_p - E_{p/2} = -\frac{0.057}{n}V \qquad (2\text{-}17)$$

$$\text{or } |E_p - E_{p/2}| = \frac{0.057}{n}V \qquad (2\text{-}18)$$

It can be seen from Equation (2-18) that the peak polarogram of a reversible system is sharp, spanning a voltage range of roughly 0.12 volts for a one electron transfer system. The peak potential in a reduction process is 0.029/n volts more cathodic than the corresponding $E_{1/2}$, and the half peak potential is 0.028/n volts more anodic. In practice, the peak for a reversible process at a stationary electrode is fairly broad and extends over a range of several millivolts. Hence, it is sometimes convenient to use the half peak

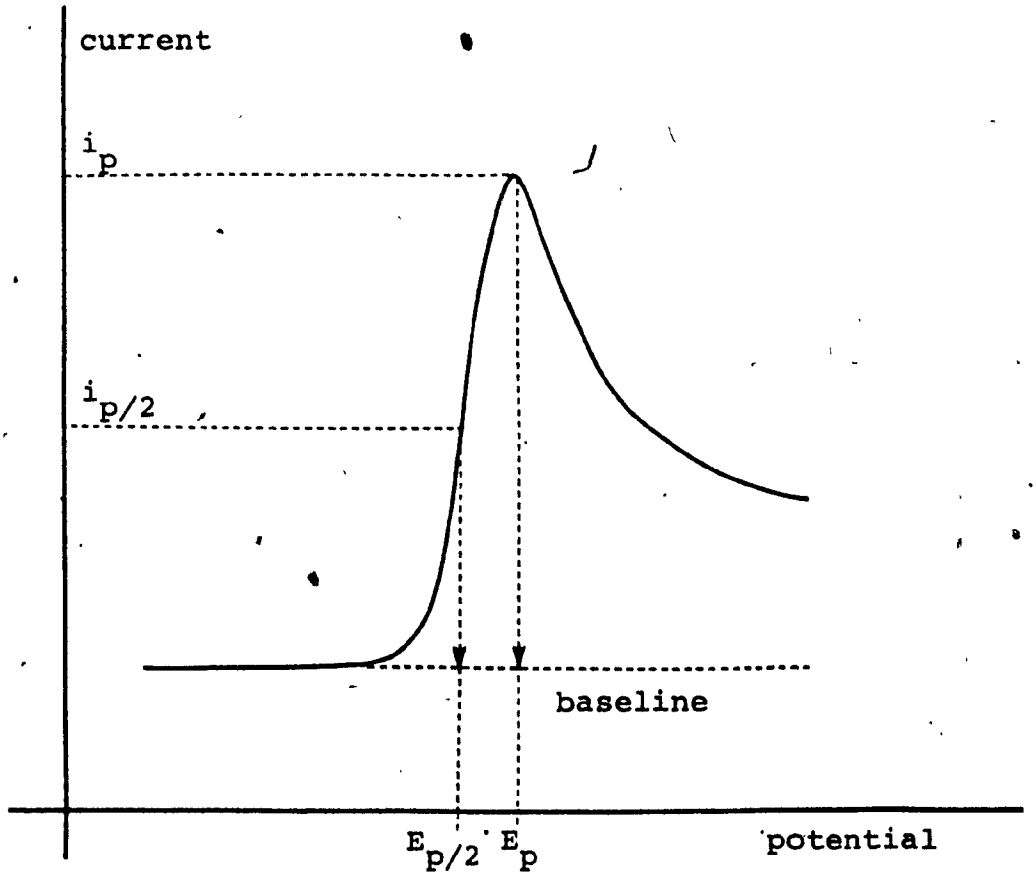

Figure 2-7: Current - potential curve of a rapid, single sweep process.

potential (Equation 2-16) as a reference point (20), although this has no direct kinetic or thermodynamic significance. In addition, it has been shown that the polarographic $E_{1/2}$ can be estimated from a reversible stationary electrode polarogram, based on the fact that it can be found at a point 85.17% up the cathodic slope (21).

The equations for totally irreversible systems are much more involved, and no simple relationship exists between E_p and $E_{1/2}$. One has to consider the rate of electron transfer and its relationship to the rate of potential sweep, etc. For simple quasi irreversible cases, it has been shown (5,19) that one obtains:

$$E_{p/2}-E_p = \frac{0.048}{\alpha n}V \qquad (2\text{-}19)$$

where; α =charge transfer coefficient (rate). It can be seen that as αn decreases the peak polarogram becomes more spread out and rounded at the maximum.

Finally, the Randle-Sevcik constant, K in Equation 2-14, has been shown to be a function of the experimental parameters, i.e., electrode type and shape, cell structure and the nature of analyte and supporting electrolyte. Consequently, K has a range from $2X10^5$ to $3X10^5$ coulombs/$(volt)^{1/2}$.

2.3.1.1 Current as a function of applied potential

The most up-to-date treatment of the i-E relation in rapid-sweep voltammetry was carried out by Nicholson and Shain (21,22). A study of a large number of electrodes and electrolyte solutions yielded a numerical solution to the electrode boundary and diffusion values. This numerical solution gave rise to a current function which, when multiplied by the ordinary parameters of electrode processes, yields the current as a function of applied potential. In its final form the equation can be written in terms of the current function χ'.

For reversible processes:

$$i = 602n^{3/2}AD^{1/2}V^{1/2}C(\chi') \qquad (2\text{-}20)$$

where $\chi' = \pi^{1/2}\chi(at)$

$at = \frac{nF}{RT}(Ei-E)$

$(Ei-E)$ can be replaced by $(E-E_{1/2})$

A = electrode surface area (cm^2)

D = diffusion coefficient (cm^2/sec)

V = rate of potential sweep (volts/sec)

C = concentration of analyte (moles)

E = Ei-Vt potential (volts) at any given time

E_i = initial potential (volts).

This relation can be readily modified to fit the irreversible case by replacing $n^{3/2}$ by $n(\alpha n)^{1/2}$ and

using somewhat modified χ'.

From Equation 2-20, Nicholson also derived theoretical treatments for rates of reaction, transfer coefficients, applications to processes with coupled chemical reactions, and for electron transfers preceding or following chemical reactions; however, single sweep voltammetry, by itself and especially in the case of solid electrodes, is severely limited in the study of electrode processes. Consequently, these aspects of single sweep voltammetry wil not be covered here.

2.3.1.2 Multi-sweep techniques

In the multi-sweep technique, the i-E curve is repeatedly recorded while the applied potential undergoes its periodic variation with time. This technique is used mainly under very rapid scan conditions and in cases where the technology to record a single sweep is not available. The main drawback to this technique, however, lies in the fact that, with each successive sweep, there occurs a depletion of analyte concentration in the vicinity of the stationary electrode and, consequently, a corresponding decrease in peak current.

2.3.2 Cyclic voltammetry

Cyclic voltammetry (CV) employs an isosceles triangular wave shown in Figure 2-6c. Hence, the potential decreases at the same rate as it increases. Two

polarograms are thus produced, one representing reduction and the other oxidation, with both occurring during one unit sweep or cycle. Each polarogram is, of course, the same as would be obtained from single-sweep voltammetry. However, the height and position of the anodic (oxidation) peak of the polarogram will depend on the switching potential, E_{sw}, being applied, as shown in Figure 2-8.

Cyclic voltammetry is not commonly used for analytical purposes due to the cost factor and availability of more sensitive techniques. However, due to the nature of the technique, CV can be employed as an excellent tool for the study of electron transfer reactions, kinetics and mechanisms of complex reactions. Within its working range of analyte concentration, CV also can be applied for qualitative and quantitative analysis with results somewhat better than D.C. polarography.

In CV there are definite correlations between the separation of peaks (ΔE_p), peak height ratios and the general polarogram shape to the nature of the electrode reaction and chemical processes. For example, Equation 2-15 shows that E_p for reduction is 0.029/n volts more cathodic than $E_{1/2}$. Correspondingly, E_p for the oxidation of the same species will be 0.029/n volts more anodic than $E_{1/2}$. Hence, the potential increment between the peaks for a reversible system will be (11,

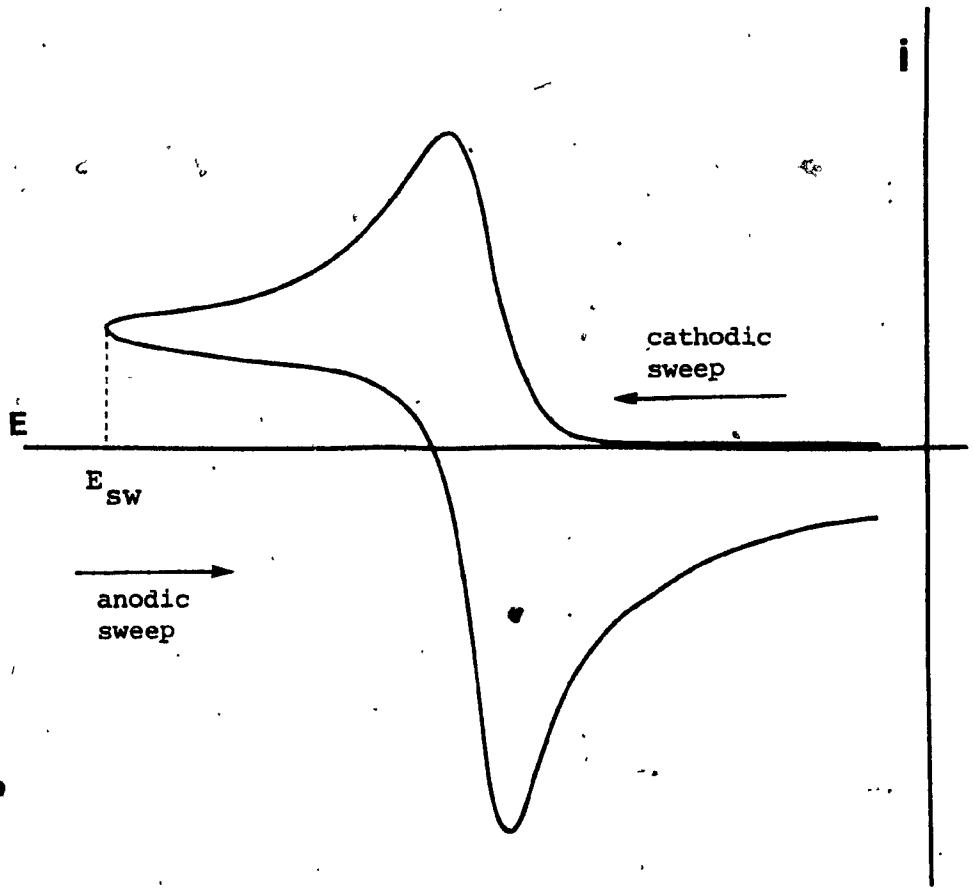

Figure 2-8: Current - Potential curve obtained from cyclic voltammetry.

19):

$$E_{p(o)}-E_{p(r)} = 2(0.029/n)=0.058/n \text{ volts} \qquad (2\text{-}21)$$

Consequently, peak separation becomes a function of the reversibility of the reaction, and a $n\Delta E_p$ of equal to or less than 60mV indicates a highly reversible reaction. Some of these correlations will be described and demonstrated in subsequent chapters.

Finally, in a manner similar to that for single sweep work, a distinction should be made between the first two or three cycles and continuing cycles. In the absence of a coupled chemical reaction, continuing cycles merely alter gradually the concentration profile near the electrode surface. The anodic and cathodic peaks change slightly in shape and decrease in size until a steady-state condition is achieved. Most of the work in this thesis will be based on data obtained from single-cycle CV.

2.4 Electrode Systems

In the analytical cell of a modern voltammetric system the potential and its corresponding current are controlled and monitored by the use of a three electrode system. These are the working electrode, the reference electrode and the auxiliary electrode as hereafter described.

2.4.1 Working electrodes

In voltammetry, the term "working electrode" (WE) is reserved for that electrode at which the primary polarographic reaction occurs (i.e., the electrode at which the species of interest is either oxidized or reduced). However, strictly speaking, any electrode may be called a working electrode whenever a net current flows through the cell.

A number of working electrodes have been employed, and these may be classified as follows:

a. Dropping mercury electrodes (dme)

b. Stationary electrodes

   1. quiet solutions

   2. stirred solutions

   3. flowing electrolyte

c. Rotating electrodes

d. Vibrating electrode systems.

Working electrodes can also be classifed according to the electrode material. These are often selected on the basis of price, of durability, and, most importantly, from the viewpoint of their effect on the overall product yield, purity and effective working potential range. Common WE materials are mercury electrodes (dme or HMDE), platinum, gold, carbon, graphite and thin-layer mercury electrodes.

The size and shape of the working electrode are

also of considerable importance, since they govern the nature of the mass transfer action and other parameters of the electrochemical process.

2.4.2 Reference electrodes

The potential within the analytical cell (i.e., the potential of the WE) is measured with respect to a reference electrode. This latter involves a half-cell having a known and stable potential. The most frequently used reference electrode (REF.) is the standard calomel electrode. For certain purposes the silver-silver chloride (Ag/AgCl) system is useful. Mercury-mercurous sulfate and lead amalgam-lead sulfate systems have been used.

All the reference half cells used in polarography/voltammetry can be coupled to any type of WE. There are no specific types peculiar to stationary or solid electrodes. The potential of the chosen reference electrode is standarized by measurement against a standard hydrogen electrode or a fixed potential system.

In general, unless another system is specifically required, the standard calomel (SCE) system is used, since much of the polarographic half-wave potentials ($E_{1/2}$) in the literature is reported versus SCE.

2.4.3 Auxiliary electrodes

Originally polarography work was carried out in

a cell containing only two electrodes--a working and a reference electrode. In such systems the reference electrode was often exposed to large currents (flowing through the cell). These currents could damage the sensitive reference electrodes. Consequently, a three electrode cell was developed. Here one speaks of an opposed working electrode or auxiliary electrodes (AUX). Hence, in an oxidation process the WE is the anode and the AUX acts as cathode, and it follows that the opposite is true in reduction processes. The potential of the auxiliary electrode is seldom of interest. It serves to carry the current between the working and auxiliary electrodes so that no excessive currents need be passed through the reference electrode. In the three-electrode system, the reference electrode measures the potential applied to the working electrode under the practically zero-flow current conditions obtained by high-impedence circuitry. Thus the potential reported as being applied to the WE is the actual potential applied. The most commonly used AUX electrode materials are platinum, gold, mercury pool, glassy carbon and carbon paste.

2.5 Instrumentation

The following equipment and instruments were used in the various phases of the experimental work.

2.5.1 Electrodes: Metrohm series

Working electrodes (WE)

EA-290: a micrometer capillary electrode (HMDE) manually set to give a hanging mercury drop of radius 0.265, 0.333, 0.384, 0.423mm, etc.

EA-267: a carbon paste electrode

EA-276: a glassy carbon electrode

Auxiliary electrodes (AUX)

EA-285: platinum microelectrode

EA-202: platinum wire electrode

Reference electrodes (REF)

EA-402: standard calomel (saturated KCL) electrode

EA-427: Ag/AgCl (saturated KCl or NaCl) electrode

EA-437: double junction electrode; Ag/AgCl (saturated KCl)

2.5.2 Polarographic/voltammetric instrumentation

The polarograph used was a multipurpose research instrument. The following describes only those operating functions and parameters applicable to this experimental work.

Polarograph	Metrohm E506 Polarecord
Polarography stand	Metrohm E505/1 stand
Operating modes used	DPP and DC for cyclic voltammetry
Potential range	-3.0 to +2.0 Volts in 1mV steps
Potential range steps	125, 250, 500, 1000 (per 250mm)
Potential scan rate	±0.04 mV/s minimum to ±40.0 mV/s and -60 mV/s maximum
Current sensitivity	DC; 0.1, 0.15, 0.25. . . . 1.0 nA/mm to . . . . 5.00 A/mm
	DP; 0.01, 0.015, 0.025 . . . .0.1 Na/mm to. . . . 0.5 A/mm
Drop life	0.4, 0.6, 0.8, 1.0, 1.2, 1.4, 2.0, 3.0, 4.0, 5.0, 6.0 seconds
Pulse amplitude	±100 mV in 1mV steps
Pulse duration	60 msec.

2.5.3 Wave Function generator (for CV)

Function generator	Metrohm Model E-612 VA scanner

Function	Isosceles or sawtoothed signal
Delay	Between waves; 0 to 10 seconds
Cycle control	1,2,4,8 cycles or multicycle
Amplitude control	Controlled by initial (U) and final (ΔU) voltage settings. Each with a range of $\pm$2.000 volts, thumbwheel control allowing 1mV increments
Sweep rate	Dial control; 1mV/sec to 1000 V/sec
Cycle trigger	Manual start or external signal start

2.5.4 Data acquisition (for CV)

Oscilloscope	Tektronix model 465. Dual channel with polaroid camera for multisweep fast scan.
	Tektronix model 564B (3A72, 344) storage oscilloscope for fast scan single sweep

X-Y record	H.P., model 7001 AM, for slow-sweep single and multi-sweep scans

2.5.5 Circuit description for cyclic voltammetry set-up

The equipment used for cyclic voltammetry is coupled in the manner shown in Figure 2-9. The dotted line represents the optional triggering mechanism used to synchronize the signal generator and recording device with the drop life when the dme is used.

This coupling permits the potential across the electrodes to be governed by the function generator, while the resulting currents are monitored by the polarographic unit. Although the initial, maximum and final potentials are controlled by the function generator, it is possible to shift the full triangular wave both positively or negatively. This is controlled by the initial potential setting on the polarographic unit. Consequently, the potential sweep of the CV system is extended to cover a range of from +4 volts to -5 volts.

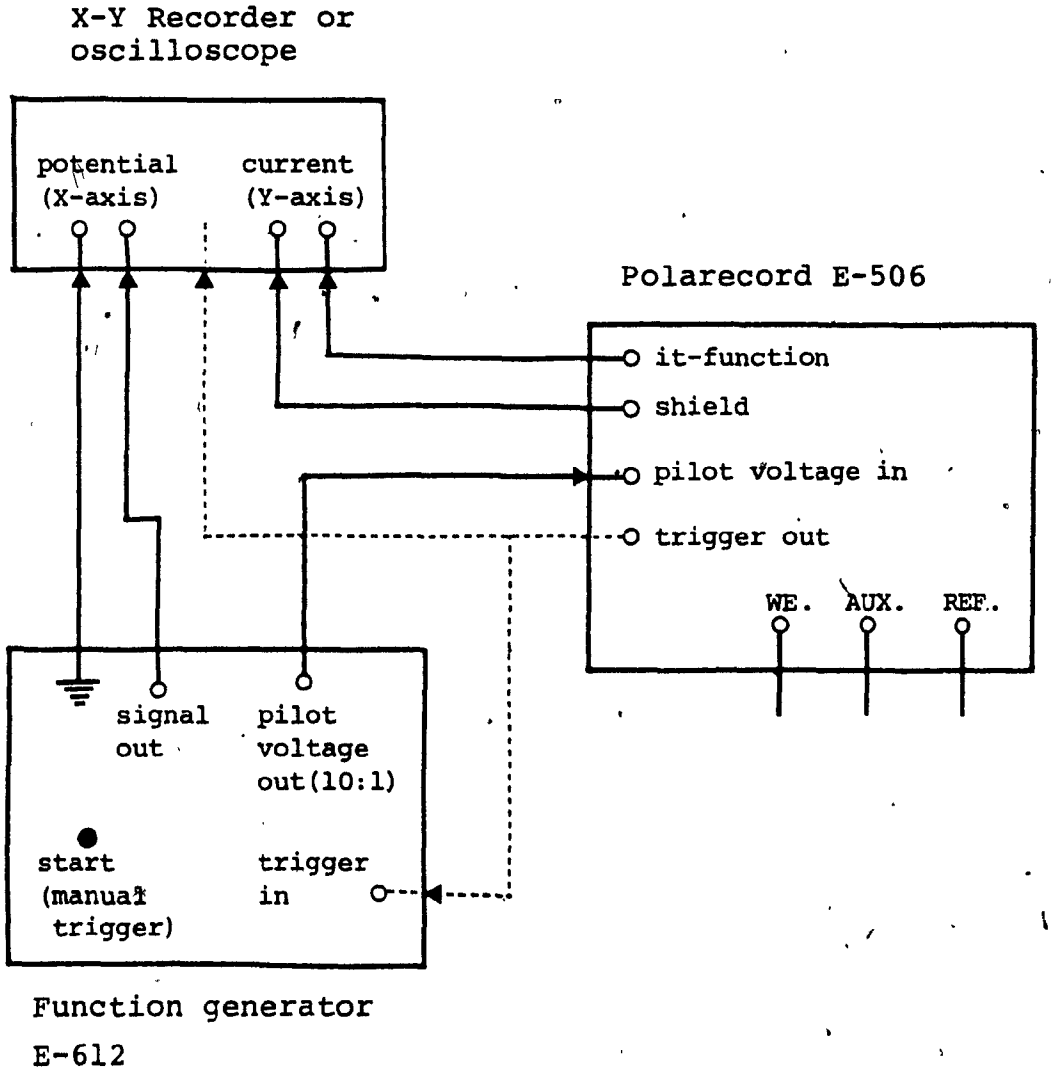

Figure 2-9: Instrumental coupling for cyclic voltammetry.

CHAPTER 3

THE STANDARD RATE CONSTANTS FOR CADMIUM AND ZINC

3.1 Introduction and Theory

The following is based on the principle that electrochemical processes which appear to be reversible at one frequency (sweep rate) may be made to exhibit kinetic behavior at higher frequencies as indicated by increased separation between the cathodic and anodic peak potentials.

Nicholson (23) has used the separation of peak potentials to measure standard rate constants for electron transfer in simple processes of the type $O + ne \rightleftharpoons R$ (i.e., processes which are not complicated by preceding or following chemical reactions). Application of the absolute rate theory to the electrode process and a numerical solution of an integral equation provided a correlation of the separation in peak potentials ΔEp with a function ψ given by:

$$\psi = \gamma^{\alpha} \frac{K_s}{[\pi D_o a]^{1/2}} \qquad (3\text{-}1)$$

where: α = electron transfer coefficient

$$\gamma = \left[\frac{D_o}{D_r}\right]^{1/2}$$

D =diffusion coefficient (cm^2/sec)

K_s=standard rate constant (cm/sec)

$$a = \frac{nFV}{RT}$$

V =potential sweep rate (volts/sec)

and π, F, R, T have their usual meanings and values.

Using the approximations $\gamma^{\alpha} = 1, D_o = 1X10^{-5} \frac{cm^2}{sec}$ and F/RT=39.2 one obtains a practical relationship between ψ, K and V, which is useful for estimating the sweep rates required to evaluate a given process. The simplified relationship becomes:

$$\psi = 28.5 \frac{K_s}{V^{1/2}} \qquad (3\text{-}2)$$

The variation of ΔE_p with ψ was derived by iteration (23) to give a working curve. The curve shown in Figure 3-1 indicates that a ψ value of 0.5 is about optimum for measurement purposes. Thus:

$$0.5 = 28.5 \frac{K_s}{V^{1/2}} \qquad (3\text{-}3)$$

Using the above, one can either "tune in the rate constant" by increasing the sweep rate or, if the system already shows a peak separation in excess of reversible ($\Delta E_p > 60mV/n$) behavior, vary the sweep rate to obtain ΔE_p values which fall within the working

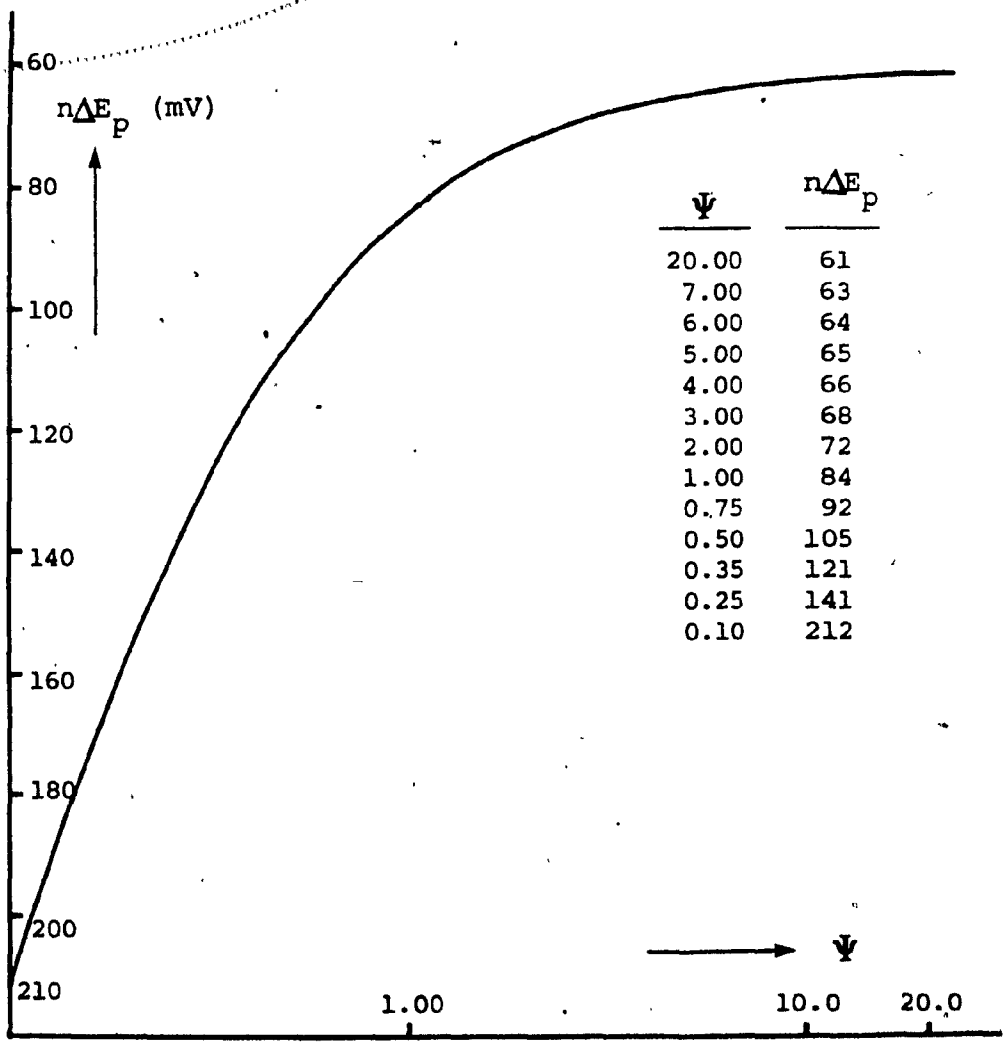

Ψ	nΔEp
20.00	61
7.00	63
6.00	64
5.00	65
4.00	66
3.00	68
2.00	72
1.00	84
0.75	92
0.50	105
0.35	121
0.25	141
0.10	212

Figure 3-1: Nicholson's working curve; $n\Delta E_p$ Vs. ψ (Anal. Chem.,37,1351(1965)).

range of ψ. For quite reversible reactions, the value of V should be increased to yield ψ values between 0.35 and 0.80, with 0.50 being about optimum. For quasi irreversible reactions, the range may be extended to lower values (e.g., 0.20 to 0.80). It should be noted, however, that for very slow rates or for irreversible systems this technique is useless. Usually such processes show only one peak (reduction or oxidation) or peaks with ΔEp outside the working range of ψ.

This technique is applied in the following determinations of the reduction standard rate constants for cadmium and zinc.

3.2 Experimental

3.2.1 Preparation of analyte and supporting electrolyte

The sample solutions in duplicate for both cadmium and zinc were prepared as indicated in Appendix A-1 to yield:

$2X10^{-4}M$ $CdSO_4$ in 1M Na_2SO_4 pH 6.0 (unadjusted)

and $3X10^{-4}M$ Zn^{+2} in 1M KCl pH 2.2 (unadjusted).

Na_2SO_4 and KCl were chosen as supporting electrolyte in order to facilitate the comparison of results with literature values obtained under similar conditions.

3.2.2 Preparation of the working curve and equations

The working curve was constructed as per Nicholson's (23) tabulated values as described in Appendix A-2.

Equation No. 3-1 was simplified by isolating K_s and evaluating all pertinent parameters as follows:

Starting with $\alpha = 0.25$ (Ref. 23) for cadmium

$$D_o = 0.72 \times 10^{-5} \text{ cm}^2/\text{sec} \quad \text{(Ref. 24)}$$

$$D_r = 2.07 \times 10^{-5} \text{ cm}^2/\text{sec} \quad \text{(Ref. 24)}$$

$$\gamma = \left(\frac{D_o}{D_r}\right)^{1/2} = \left(\frac{0.72}{2.07}\right)^{1/2} = 0.590$$

$$\gamma^{\alpha} = \gamma^{0.25} = 0.876$$

$$a = \frac{nFV}{RT} = 39.2 \text{ nV at } 23^{\circ}\text{C}$$

$$K_s = \frac{\psi [n(39.2)(0.72 \times 10^{-5})]^{1/2} v^{1/2}}{0.876}$$

and since n=2

$$K_s = (4.807 \times 10^{-2})\, \psi\, v^{1/2} \text{ at } 23^{\circ}\text{C} \qquad (3\text{-}4)$$

similarly for zinc, with

$$D_o = 0.72 \times 10^{-5} \text{ cm}^2/\text{sec} \quad \text{(Ref. 24)}$$

$$D_r = 1.57 \times 10^{-5} \text{ cm}^2/\text{sec} \quad \text{(Ref. 24)}$$

and $a = \frac{nFV}{RT} = 39.1$ nV at 24°C

one obtains

$$K_s = (4.637X10^{-2})\,\psi\, v^{1/2} \text{ at } 24^{o}C \qquad (3\text{-}5)$$

3.2.3 Apparatus and experimental parameters

All measurements were made with a three electrode cell circuit as described in Chapter 2, consisting of:

WE: HMDE (radius 0.265 mm)

AUX: Pt (platinum microelectrode)

REF: Ag/AgCl (saturated KCl)

The detectors were the Tektronix 465 and 564B oscilloscopes for fast scan, single-cycle and multicycle, and the HP 7001AM X-Y recorder for slow single scan.

3.3 Results and Discussion: Cadmium

The determination of the standard rate constant for the reaction of cadmium was carried out using both single-cycle and multicycle (steady-state) experiments. For all experiments an initial potential of -0.480 volts vs. Ag/AgCl was used, and the amplitude of the triangular wave was always 160 mV.

3.3.1 Results obtained from rapid-sweep CV

Preliminary sweeps on the cadmium samples indicated that optimum results could be obtained using potential sweep rates in the range of 30 to 100 volts/sec. Consequently, the experiment was designed so

as to obtain results from potential sweeps of 40, 60, 80 and 100 volts/sec.

Results for the reduction of $2X10^{-4}M$ cadmium in 1M Na_2So_4 are summarized in Tables 3-1 and 3-2 for single and multicycle respectively. The bulk of the data and pertinent computed values are listed in Appendix A-3. After statistical treatment of data, the final values for the standard rate of reaction obtained for cadmium at 23°C are as follows:

by single-cycle CV $K_s = 0.22 \pm 0.02$ cm/sec

by multicycle CV $K_s = 0.20 \pm 0.03$ cm/sec

The values of K_s in Table 3-1 agree reasonably well with Nicholson's results in Table 3-3 and with determinations made by other methods (25). The computation of K_s may be best demonstrated by an example. The polarogram in Figure 3-2 shows a typical redox cycle of sample 2 at 60 V/sec multicycle. The oscilloscope and the Polaroid camera were adjusted so that the horizontal axis read 0.1 V/cm. Now, from the polarogram, $\Delta Ep=48mV$, and since $n=2$, $n\Delta E_p=96mV$. From the working curve (Appendix A-2) one obtains a ψ value of 0.655 for $n\Delta E_p=96mV$. Thus using Equation 3-4,

$$K_s = (4.807X10^{-2})(0.655)(60)^{1/2} = 0.24 \text{ cm/sec}$$

Although the differences in standard rate constant values obtained by the multicycle and single-cycle approaches are within experimental error,

Table 3-1: Standard rate (Ks) determinations for the reduction of cadmium using single-cycle CV.

scan rate volt/sec.	n ΔEp mV.	Ψ	Ks cm./sec.
40	91	0.78	0.23
60	98	0.63	0.23
80	107	0.48	0.21
100	114	0.41	0.20

Table 3-2: Standard rate (Ks) determination for the reduction of cadmium using multicycle CV.

scan rate volt/sec.	n ΔEp mV	Ψ	Ks cm./sec.
40	93	0.73	0.22
60	98	0.62	0.23
80	109	0.46	0.20
100	123	0.34	0.17

Table 3-3: Nicholson's Ks values for the reduction of cadmium using single-cycle CV (Anal. Chem. 37,1351(1965))

scan rate volt/sec.	n ΔEp mV	Ψ	Ks cm./sec.
48	94	0.70	0.25
60	98	0.61	0.25
90	108	0.48	0.24
120	115	0.41	0.23

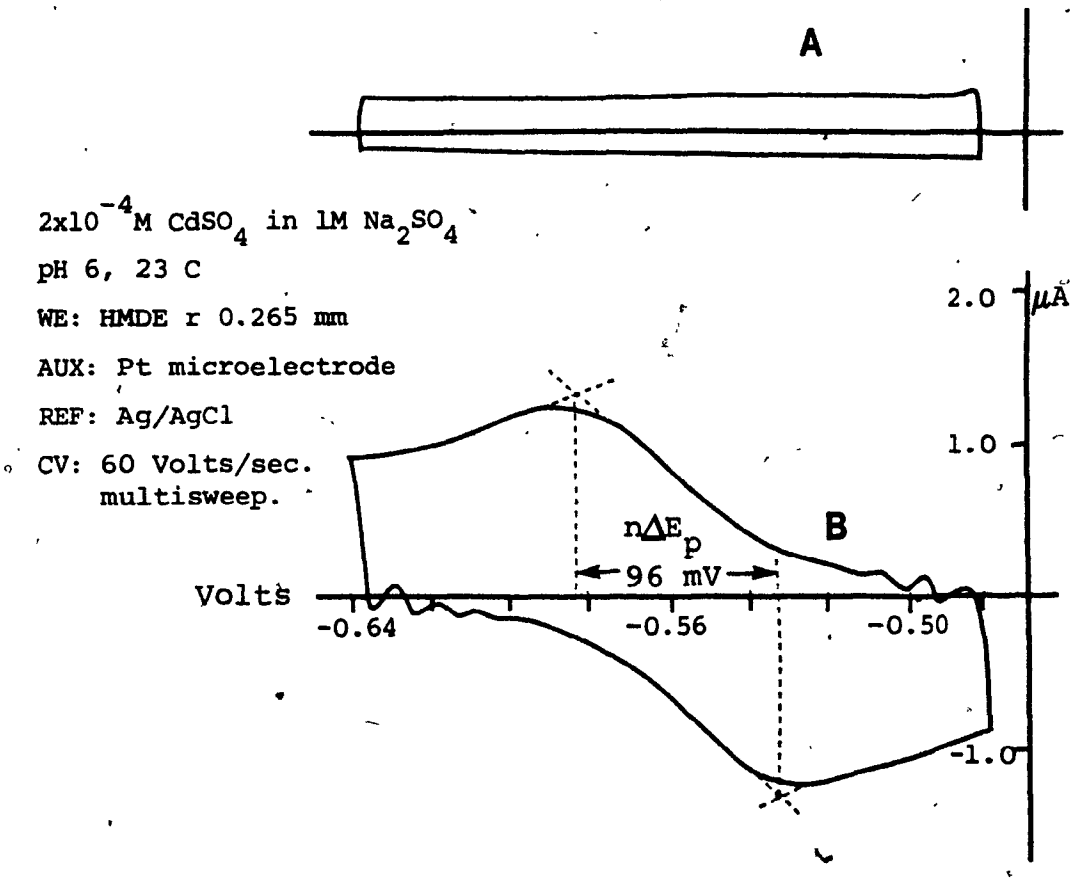

Figure 3-2: A. Scan of 1M Na_2SO_4 (blank).
B. Multiple fast scan CV for the cadmium system.

the average for the multicycle approach is about 10% smaller than the average for the single-cycle approach. This results from the fact that, in multicycle work, the analyte in the vicinity of the HMDE is depleted after the first several cycles to a point where an electrochemical "steady state" is achieved. As a result, the polarograms obtained for the multicycle process show rounded peaks with a slight increase in peak separation, as can be seen from Figure 3-3. In addition, it is important to remember that the theoretical equations are based on the single-cycle process where, among other conditions, it is assumed that initially the analyte is in one of its two oxidation states or in static equilibrium.

3.3.2 Redox behavior at low sweep rate

The same samples of cadmium sulfate in sodium sulfate were analyzed using single-cycle CV at the low sweep rates of 0.2V/sec, 0.1V/sec and 0.05V/sec.

At these low scan rates where the potential sweep rate does not compete with the kinetic process (23), the electrochemical redox process of cadmium appears perfectly reversible. Figure 3-4 shows that, at all the low sweep rates used, the peak separation obtained is approximately 30mV.

However, a closer look at the polarograms in

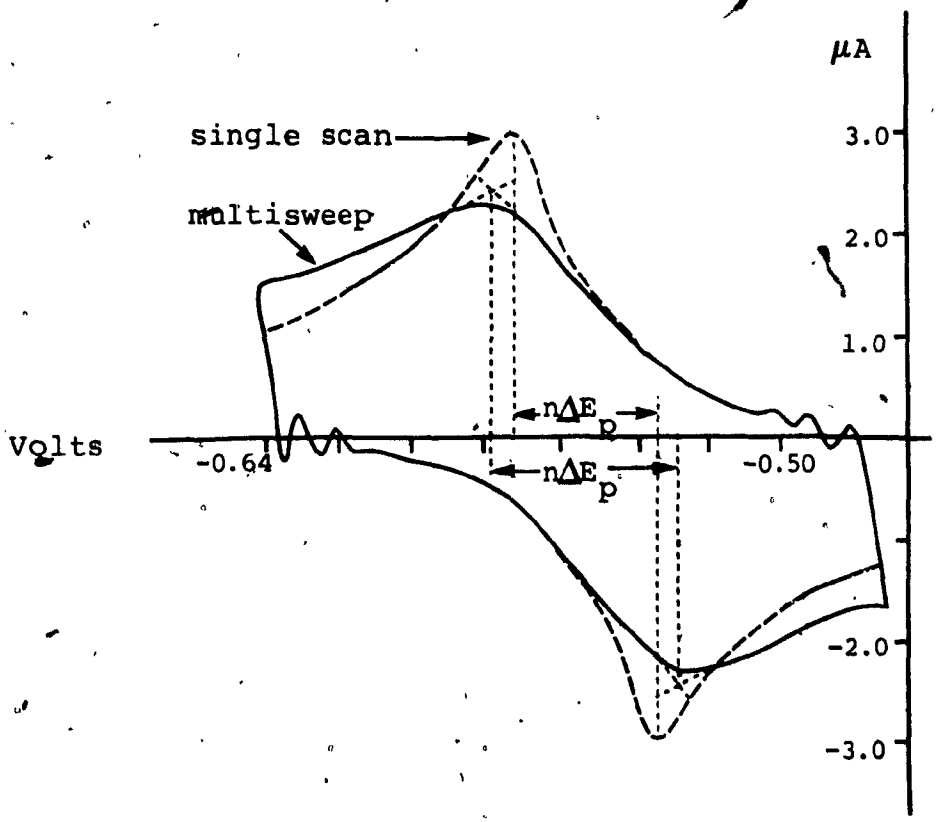

Figure 3-3: A comparison of single and multisweep, rapid scan CV for the cadmium system.

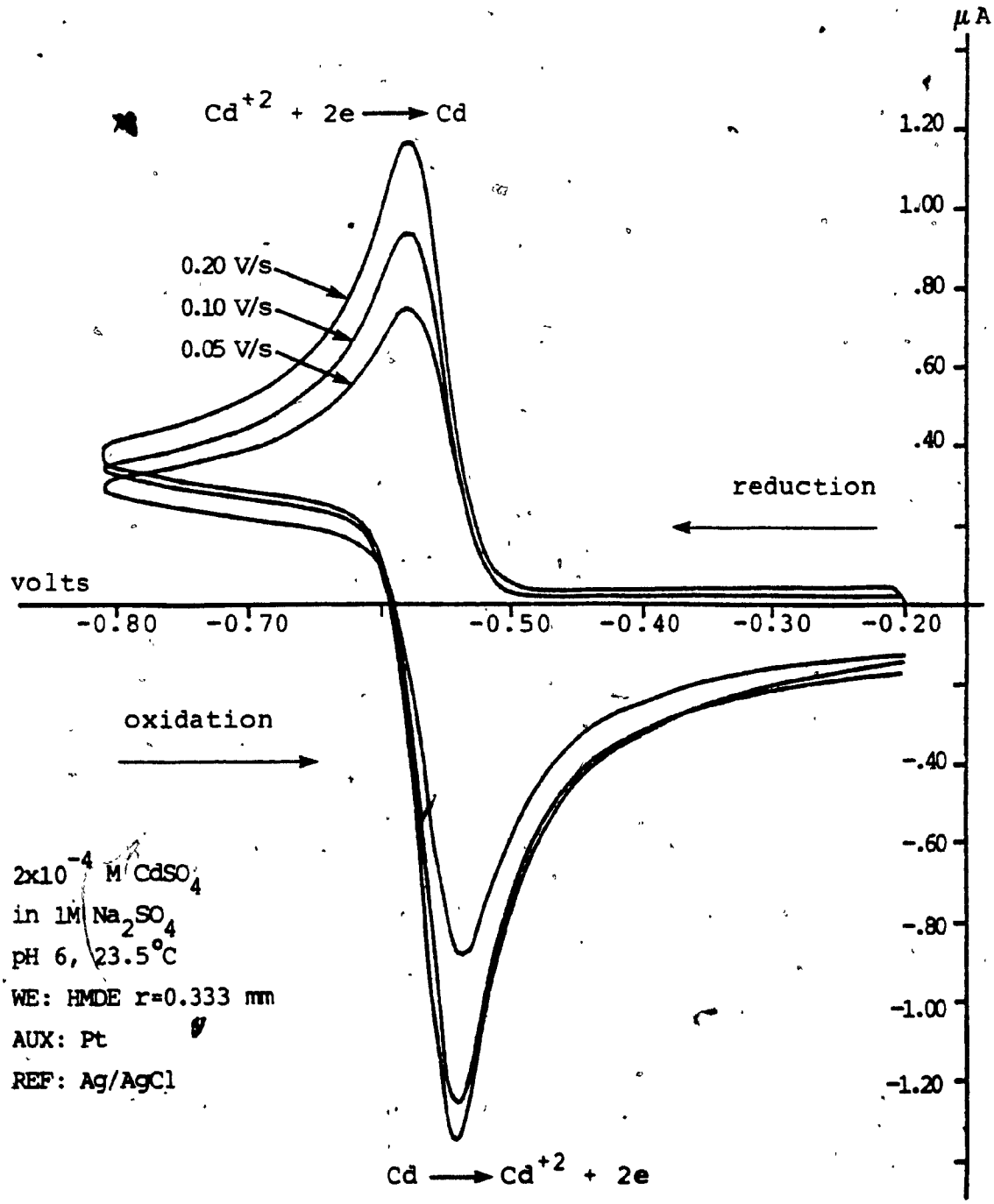

Figure 3-4: A Comparison of Single Cycles CV for Cadmium at Low Scan-rates; 0.05, 0.10, and 0.20 volt/sec.

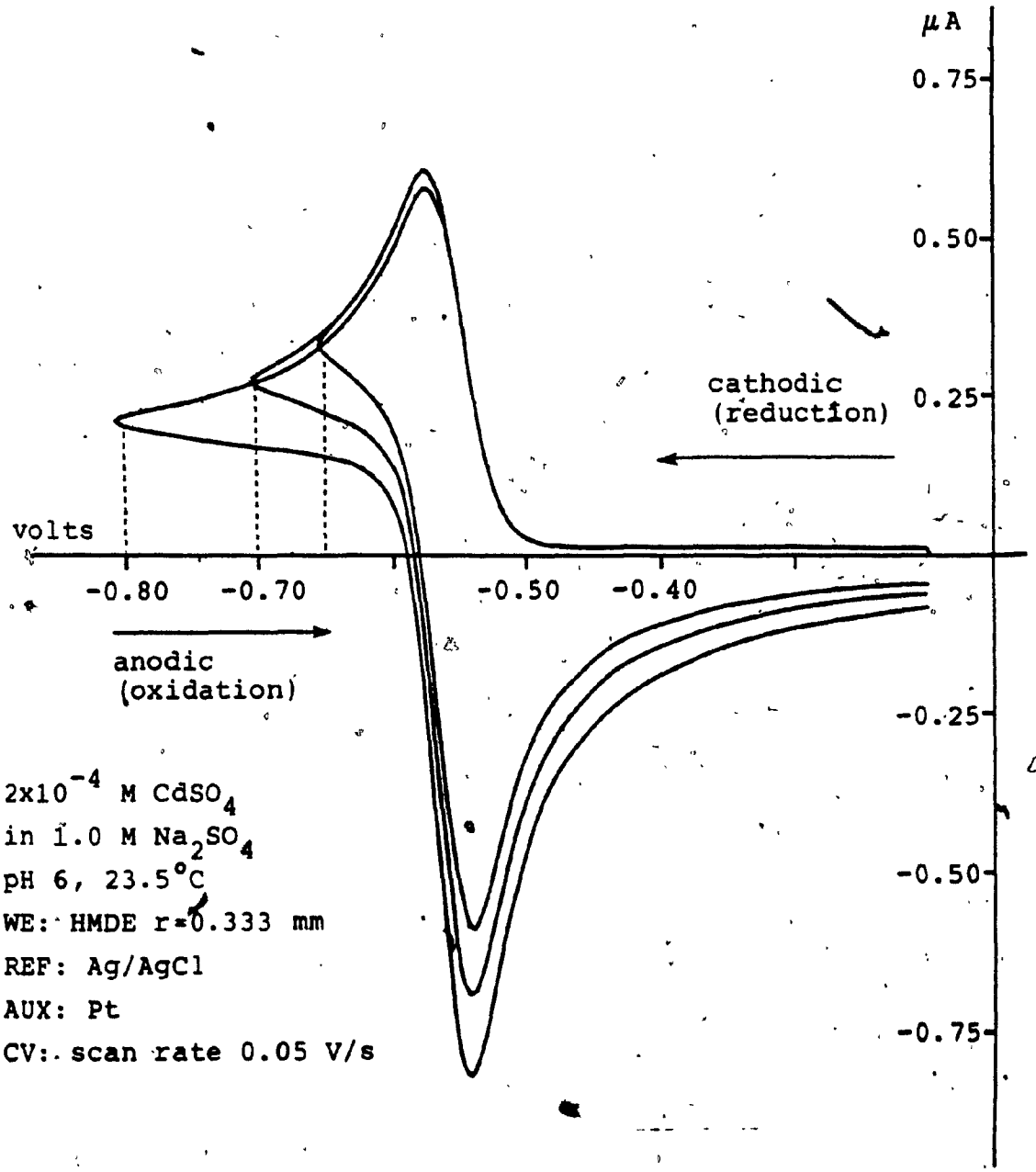

Figure 3-5: The Effect of Switching Potential on the Anodic Peak.

Figure 3-4 reveals that the anodic (oxidation) peaks are significantly larger than the corresponding cathodic peaks. This is common with highly reversible systems, since the reduction process continues rapidly even past the cathodic peak. This produces an excess of reduced substance (also, amalgam formation (26)). As a result, at the anodic position of the scan, the electrode system produces a current which is proportional to this concentration gradient. This effect introduces another important factor in CV, namely the switching potential E_{sw}.

The influence of E_{sw} on the anodic peak is demonstrated in Figure 3-5 where, at a given sweep rate, the switching potential governs the dimensions of the peak. In processes where the kinetic study utilizes the anodic-cathodic peak as a function of rate of reaction, E_{sw} is an important parameter, as will be seen in Chapter 5. However, in this experimental phase, as long as the switching potential is not less than 60mV past the cathodic peak, it will not influence the peak separation (Figure 3-5) or the pertinent kinetic results (27-28).

3.4 Results and Discussion: Zinc

The standard rate of reaction for zinc was evaluted using single-cycle CV. Preliminary sample sweeps indicated that optimum results would be obtained using potential sweep values of 10 to 200 mV/sec. The

location of the anodic and cathodic peaks dictated an initial potential of -0.8 volts and a triangular wave amplitude of 300mV. All potentials were measured versus Ag/AgCl (saturated KCl) at 24°C.

Results for reduction of $3X10^{-4}M$ Zn^{+2} in 1M KCl at different sweep rates within the range are summarized in Table 3-4. From duplicate samples, a total of 48 polarograms were evaluated (Appendix A-4), and the final value for the standard rate constant obtained was:

Zn^{+2} (24°C) $K_s = (4.05 \pm 0.22)X10^{-3}$ cm/sec.

This value is in excellent agreement with results obtained by other methods [e.g., $K_s = 4X10^{-3}$ cm/sec. (29,30)].

The quasi-irreversible behavior of zinc is also manifested in the nature and shape of its polarograms. A typical i-E curve for zinc is shown in Figure 3-6. Here, unlike the case of the highly reversible situation for cadmium, there is a significant difference between the anodic and cathodic segments. In the reduction phase (cathodic), the reluctance of Zn^{+2} to accept electrons is manifested in a shallow slope and rounded peak with an ill-defined maximum. The slow rate of reduction also causes a slow rate of ion depletion in the vicinity of the WE. As a result the current fails to drop sharply past the cathodic peak.

Table 3-4: Standard rate (Ks) determination for the reduction of zinc using single cycle CV.

scan rate volt/sec.	$n\Delta Ep$ mV	Ψ	Ks cm./sec.x10^{-3}
0.01	90	0.79	3.[illegible]
0.02	99	0.60	4.0
0.03	106	0.49	4.0
0.04	110	0.46	4.2
0.05	115	0.40	4.1
0.06	117	0.38	4.3
0.07	121	0.35	4.3
0.08	129	0.30	4.0
0.09	131	0.30	4.2
0.10	133	0.29	4.2
0.15	148	0.22	4.0
0.20	158	0.19	3.8

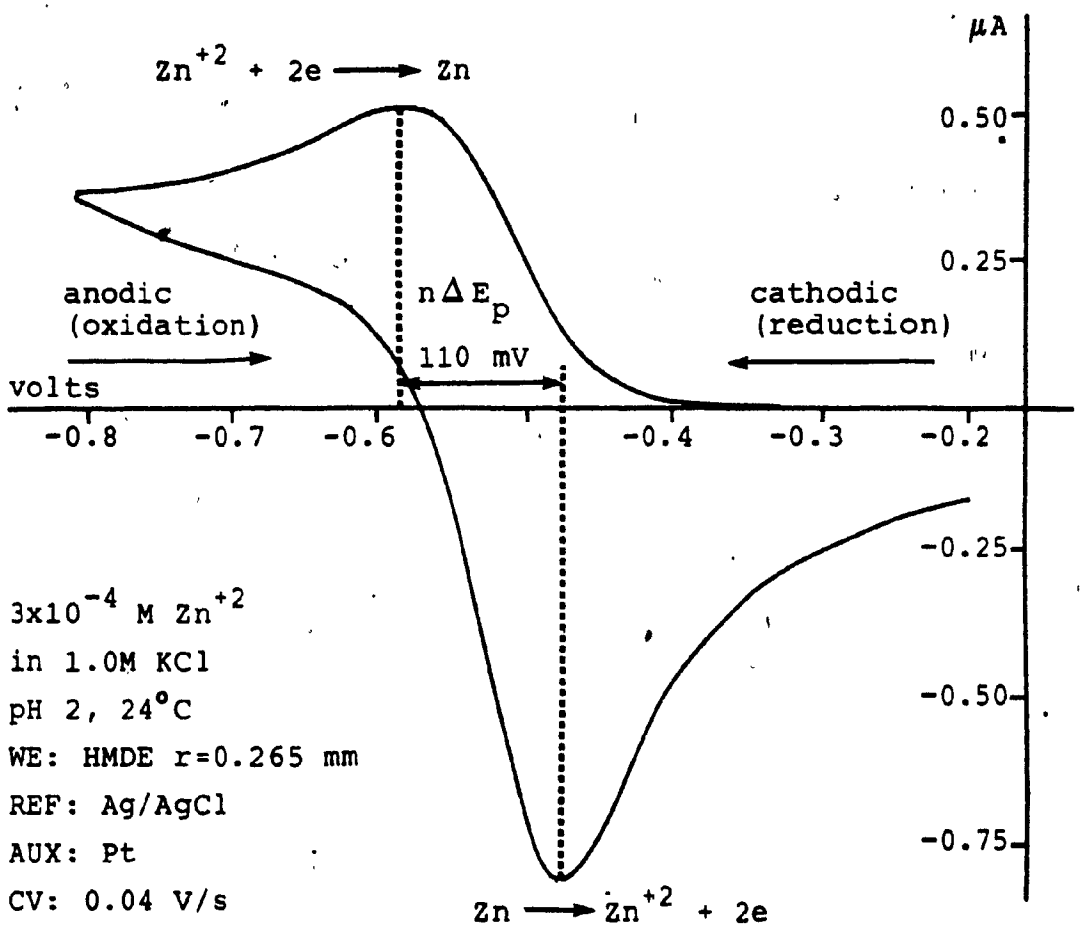

Figure 3-6: Redox Behavior of Zinc by CV.

3.5 Conclusion

The results obtained from this experimental phase suggest that the Metrohm polarographic instruments are indeed suitable for CV analysis. The system showed excellent reproducibility of results, having random variations of less than 5%. These small variations are possibly due to fluctuation in the size of the HMDE, which in this experiment were set manually and therefore open to human error. One could obtain a higher drop-size reproducibility by the use of commercially available electro-mechanical HMDE drives.

From the analytical point of view, this section has demonstrated the relative ease and simplicity of Nicholson's technique for the determination of standard rate constants for simple redox systems. The merits of this technique can be further stressed when used for fast estimations, and pertinent parameters such as α, γ and D_o are not available. In such cases, Equation 3-3 can be used with striking results. For example, the estimation equation was used on the cadmium and zinc samples. Using the mid-range voltage sweeps (70V/sec for cadmium and 80mV/sec. for zinc) yielded:

K_s = 0.15cm/sec for Cd

K_s = 4.9×10^{-3} cm/sec for Zn

It should be noted that these values are within $\pm$25% of the results obtained by the more precise approach.

Finally, it is perhaps appropriate to mention here that it is possible to extrapolate Nicholson's working curve to facilitate more difficult cases (31). Other workers have developed a technique which does not depend on a working curve and can be used on a wider range of peak separations (32).

CHAPTER 4

THE VERSATILITY OF CYCLIC VOLTAMMETRY

4.1 Introduction and Theory

Cyclic voltammetry has been claimed to be the simplest and most useful electrochemical technique for providing a quick, overall picture of an electrode reaction (12). Pertinent literature shows, however, that not all the information available from this technique is used or reported. Generally, when CV is used, the results are presented in terms of i-E curves, peak separations and/or computed kinetic parameters. But data such as $E_{1/2}$ and peak currents are determined by other techniques (e.g., D.C. polarography). This gives rise to ambiguity, since these entitites can be, and usually are, extracted from CV polarograms for kinetic computations.

Although the results obtained by other techniques are useful for the general description of a process, it is perhaps wise to obtain and present as much data as possible from the CV technique.

This is important for two reasons. First, one can describe an entire electrochemical process occurring within a given set of experimental conditions. Second,

use of techniques other than CV will become unnecessary in many cases. The versatility of CV will be demonstrated in this chapter using polarograms obtained from several chromium-polypyridyl complexes. From polarograms obtained under conditions in which these complexes display multiple reversible oxidation states, data such as peak separation, $E_{1/2}$ and peak current-to-concentration ratios will be extracted and interpreted.

The polarographic half-wave potential for reversible processes may be determined using three different computational techniques. The first two methods are as described in Chapter 2 as follows:

$$E_{1/2} = E_p + \frac{0.029}{n} \text{ volts} \qquad (4\text{-}1)$$

$$\text{and } E_{1/2} = E_{p/2} - \frac{0.028}{n} \text{ volts} \qquad (4\text{-}2)$$

where E_p = the potential at which the peak amount i_p is maximum

$E_{p/2}$ = the potential when $i = i_p/2$.

The third method utilizes Nicholson's (28) empirical approach, where $E_{1/2}$ is estimated to occur at a point 85.17% up the cathodic wave. These three techniques are summarized graphically in Figure 4-1.

The accurate measurement of peak current is of great importance in CV, since the ratio of the anodic and cathodic peak currents is significant in the deter-

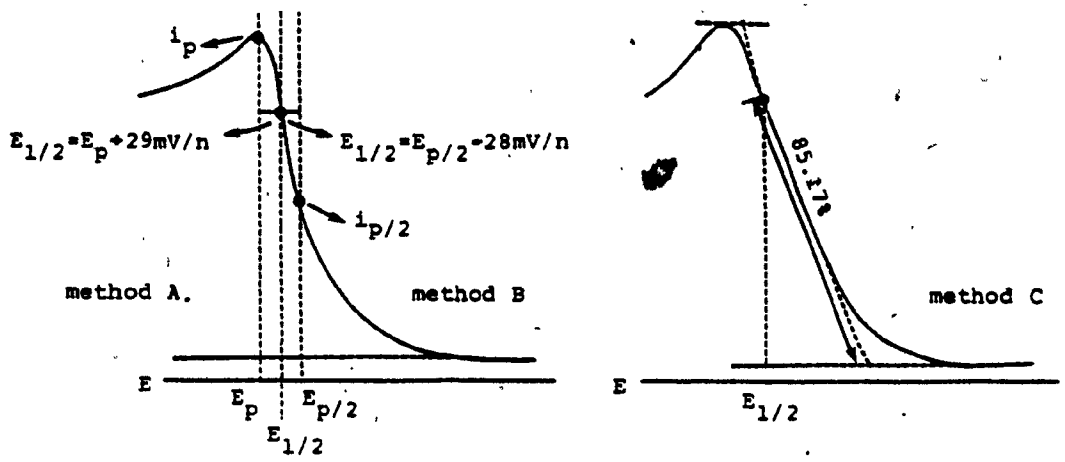

Figure 4-1: The three methods used for evaluating $E_{1/2}$ by CV.

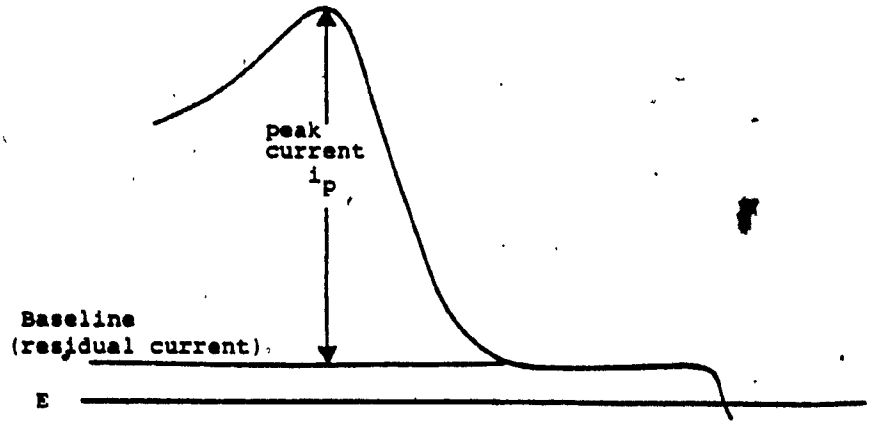

Figure 4-2: Measurement of Peak Current (i_p).

mination of reaction rates, as will be noted in Chapter 5. Numerous techniques have been developed for these evaluations (33,34,35,36). However, for simple i_p/concentration evaluation one could obtain i_p values as in D.C. polarography. Hence, the current is measured from a base line governed by the residual current, as can be seen in Figure 4-2.

4.2 Experimental

4.2.1 Preparation of analyte and supporting electrolyte

The following complexes were received from Dr. N. Serpone, Concordia University.

1. $[Cr(2,2'\text{-bipyridine})_3](ClO_4)_3 \cdot \frac{1}{2}H_2O$

   abbreviated $Cr(bipy)_3^{+3}$

2. $[Cr(2,2',2''\text{-terpyridine})_2](ClO_4)_3 \cdot \frac{1}{2}H_2O$

   abbreviated $Cr(terpy)_2^{+3}$

3. $[Cr(4,4'\text{-dimethyl-}2,2'\text{-bipyridine})_3](ClO_4)_3 \cdot H_2O$

   abbreviated $Cr(me_2\text{-bipy})_3^{+3}$

4. $[Cr(4,4'\text{-diphenyl-}2,2'\text{-bipyridine})_3](ClO_4)_3 \cdot 2H_2O$

   abbreviated $Cr(ph_2\text{-bipy})_3^{+3}$

With the exception of drying at 50°C, these com-

plexes were used as received.

The electrolyte solution was composed of 0.1M tetraethylamonium-tetrafluoroborate ($TEABF_4$) in spectrograde acetonitrile. This supporting electrolyte provided a potential window or working range of +0.5 to -2.5 volts versus Ag/AgCl (saturated KCl) reference.

The drying and preparation procedures for the supporting electrolyte and sample solutions are described in Appendix B-1 and B-2.

4.2.2 Apparatus and experimental parameters

All measurements were obtained with the three electrode cell as described in the previous chapters, consisting of:

WE: HMDE (radius 0.333mm)

AUX: Pt (platinum microelectrode)

REF: Ag/AgCl (saturated KCl)

In order to protect the non-aqueous sample solution from possible water contamination, a special double junction reference electrode was used. This electrode (EA-437) provided a buffer zone of supporting electrolyte between the aqueous KCl and the sample solution. Hence, the electrochemical description of the reference electrode is actually:

Ag/AgCl-saturated KCl/0.1M $TEABF_4$-acetontrile.

Preliminary measurements indicated no potential

difference between the standard and the double-junction reference electrodes.

To further eliminate possible water contamination, an acetonitrile trap was added to the normal washing system on the deoxygenating line. Prepurified nitrogen was used for 30 min. for the deaeration of each sample and subsequent blanketing of samples under analysis.

All measurements were made at 24±1°C using single-cycle CV at 0.1V/sec with a potential range of 0.0 to -2.2 volts. Pertinent instrumental settings are listed in Appendix B-3.

4.3 Results and Discussion

4.3.1 Redox behaviour of Cr-polypyridyl complexes in acetonitrile

Previous voltammetric studies of complexes of chromium with polypyridyle ligands in acetonitrile have shown that, in all cases, chromium forms reversible five-membered redox chains with the metal in formal oxidation states of +III, +II, +I, 0 and -I. A detailed examination of the above by D.C. and AC polarography and controlled potential electrolysis (37, 38) indicated that in the first three redox couples for each complex (III—II, II—I, I—0) the ligands help to stabilize the addition of electrons to the molecular

orbitals, which are primarily metal-centered. By contrast for the last couple (0⟶-I), the metal helps to stabilize the addition of an electron to a ligand-centered molecular orbital.

Preliminary CV runs on the four given complexes indicated that while the first three electron transitions could be easily observed, the fourth transition (0⟶-I) was usually obscured by a large cathodic wave. This wave is caused by the reduction of excess ligand in the solution, and is considerably enhanced by the presence of proton donors, such as water (39, 40, 41). The residual amounts of water could have been removed (42) from the acetonitrile, and the excess ligand extracted from the sample solution. However, due to limited availability of chromium samples and the more general aim of this experimental phase, it was decided to concentrate mainly on the first three redox transitions.

The polarograms in Figures 4-3 to 4-7 show the i-E CV curves for the blank (0.1M $TEABF_4$ in acetonitrile), $Cr(bipy)_3$, $Cr(terpy)_2$, $Cr(Me_2bipy)_3$ and $Cr(ph_2\text{-}bipy)_3$. In addition, Figure 4-8 shows a differential pulse polarogram (DPP) (Appendix B-4) of $Cr(bipy)_3$ at the HMDE. Visual inspection of these polarograms suggested that indeed all the complexes undergo three equivalent transitions. A more precise

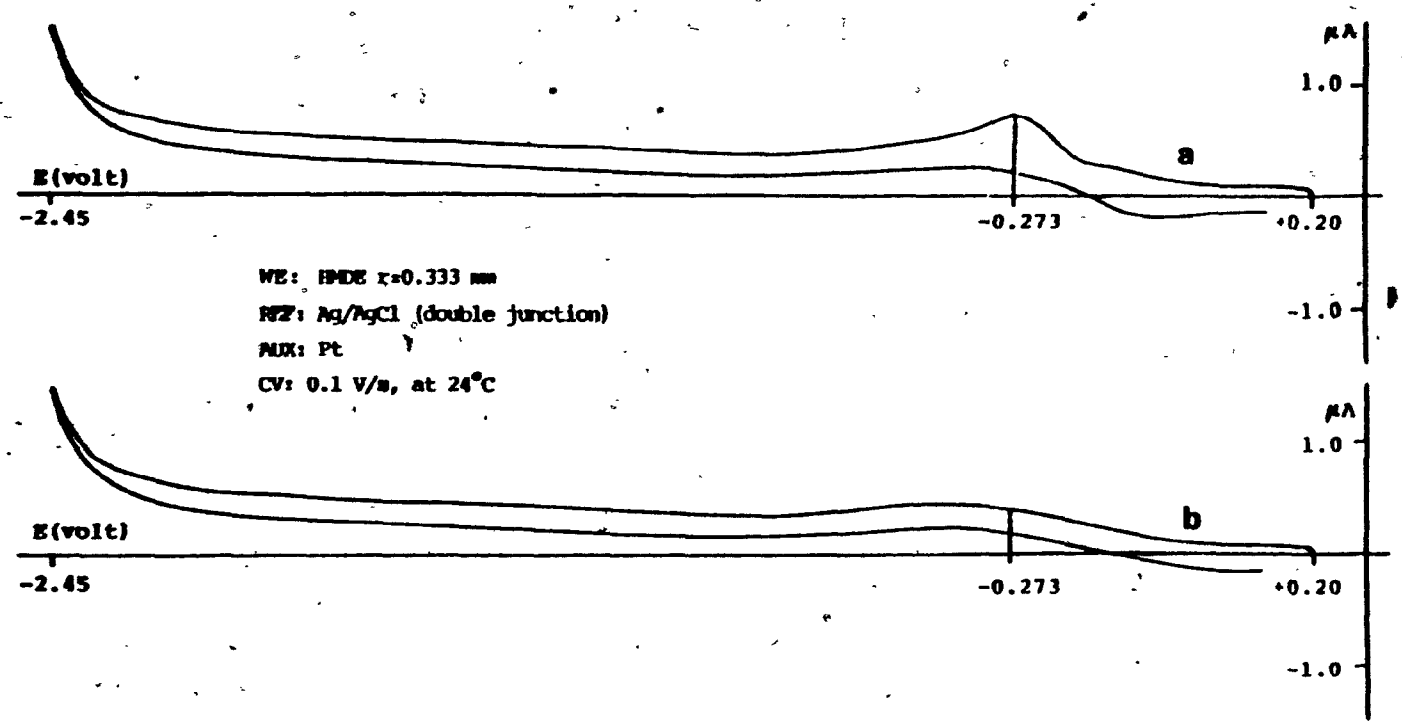

Figure 4-3: CV polarogram of the supporting electrolyte (blank);
0.1M $TEABF_4$ in acetonitrile
a. before degasing and electrolysis
b. after degasing and electrolysis

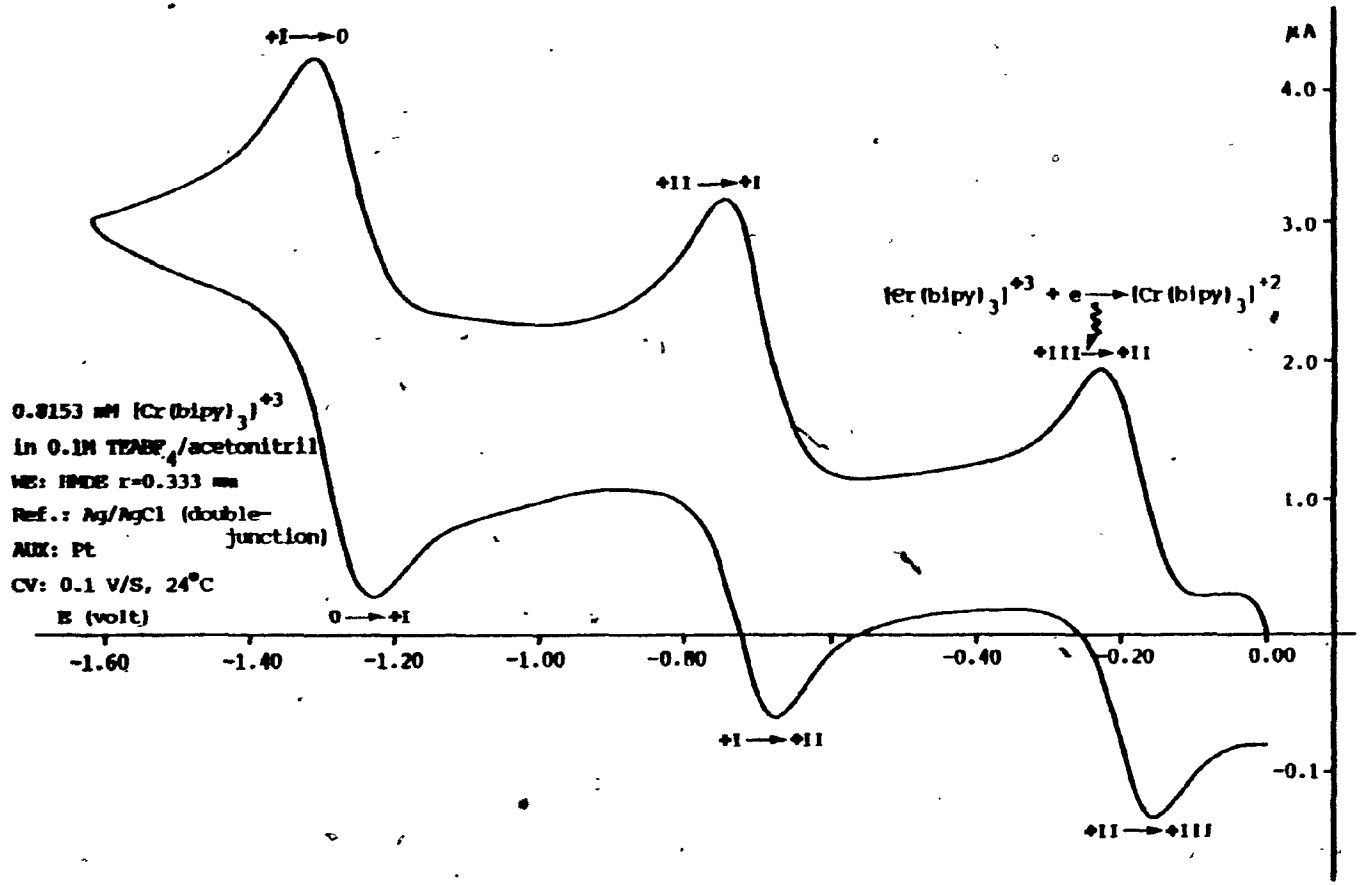

Figure 4-4: CV polarogram of $Cr(bipy)_3$ in acetonitrile; redox behavior.

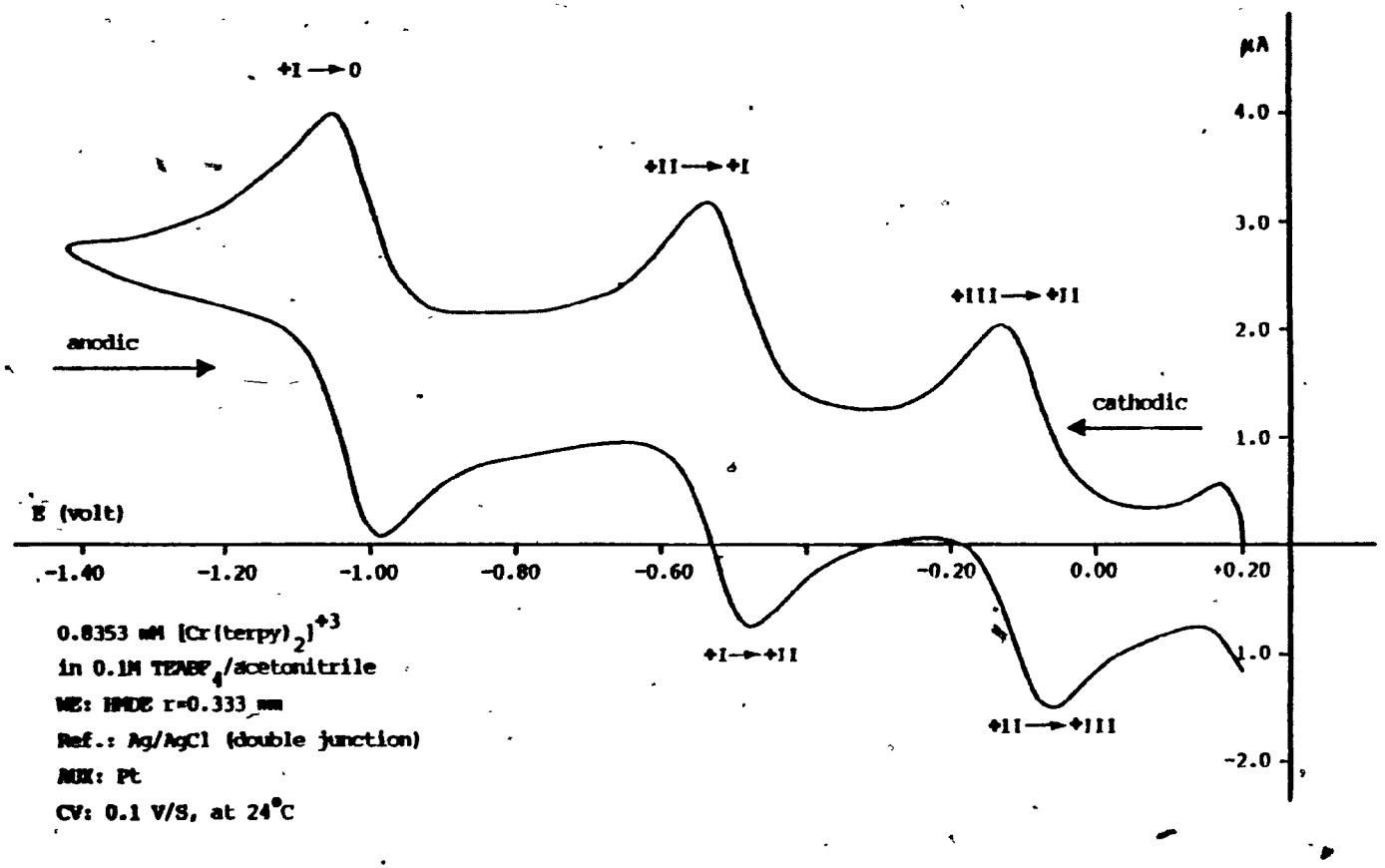

Figure 4-5: CV polarogram of $Cr(terpy)_2$ in acetonitrile; redox behavior.

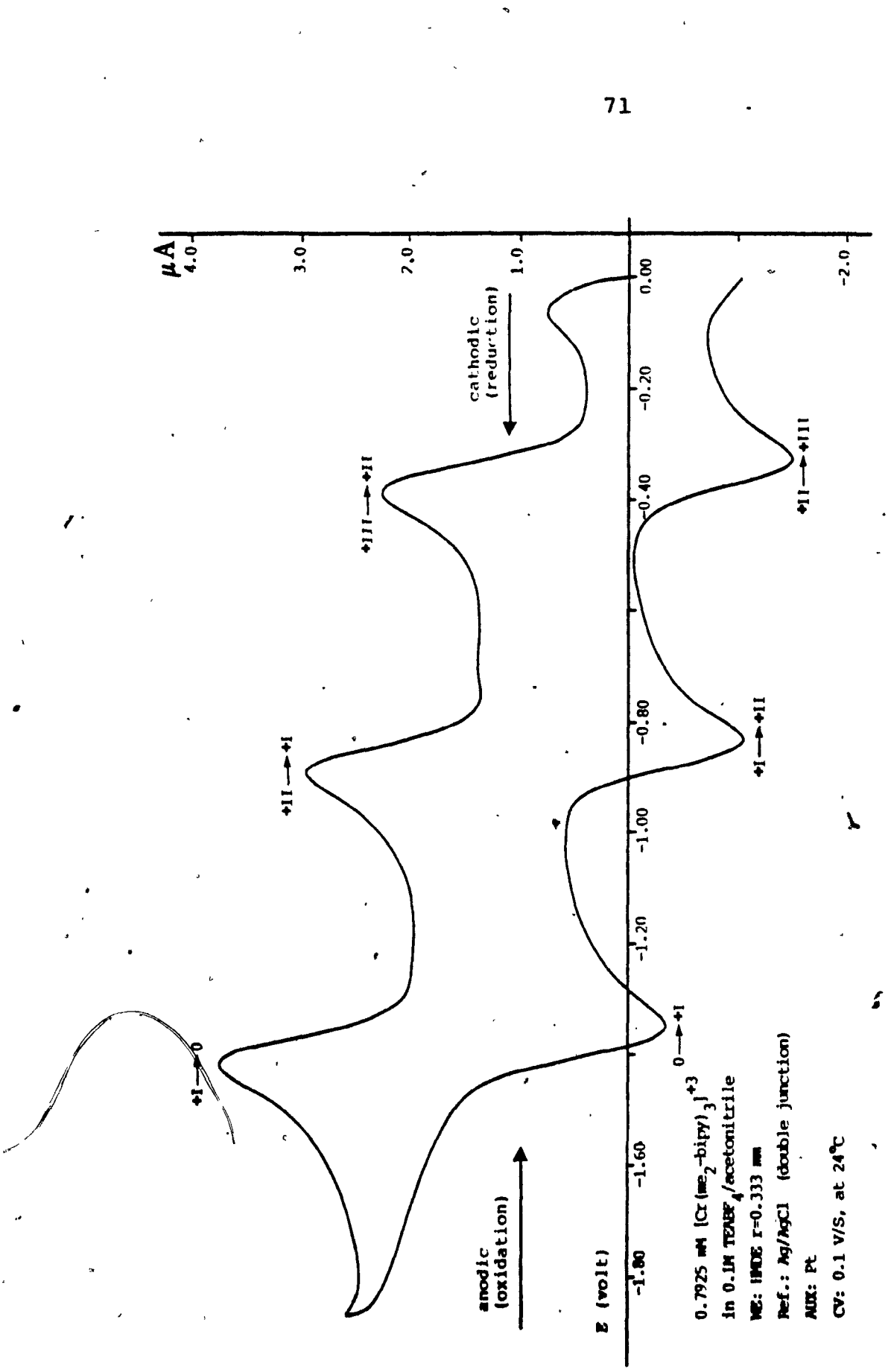

Figure 4-6: CV polarogram of $Cr(me_2\text{-}bipy)_3$ in acetonitrile; redox behavior.

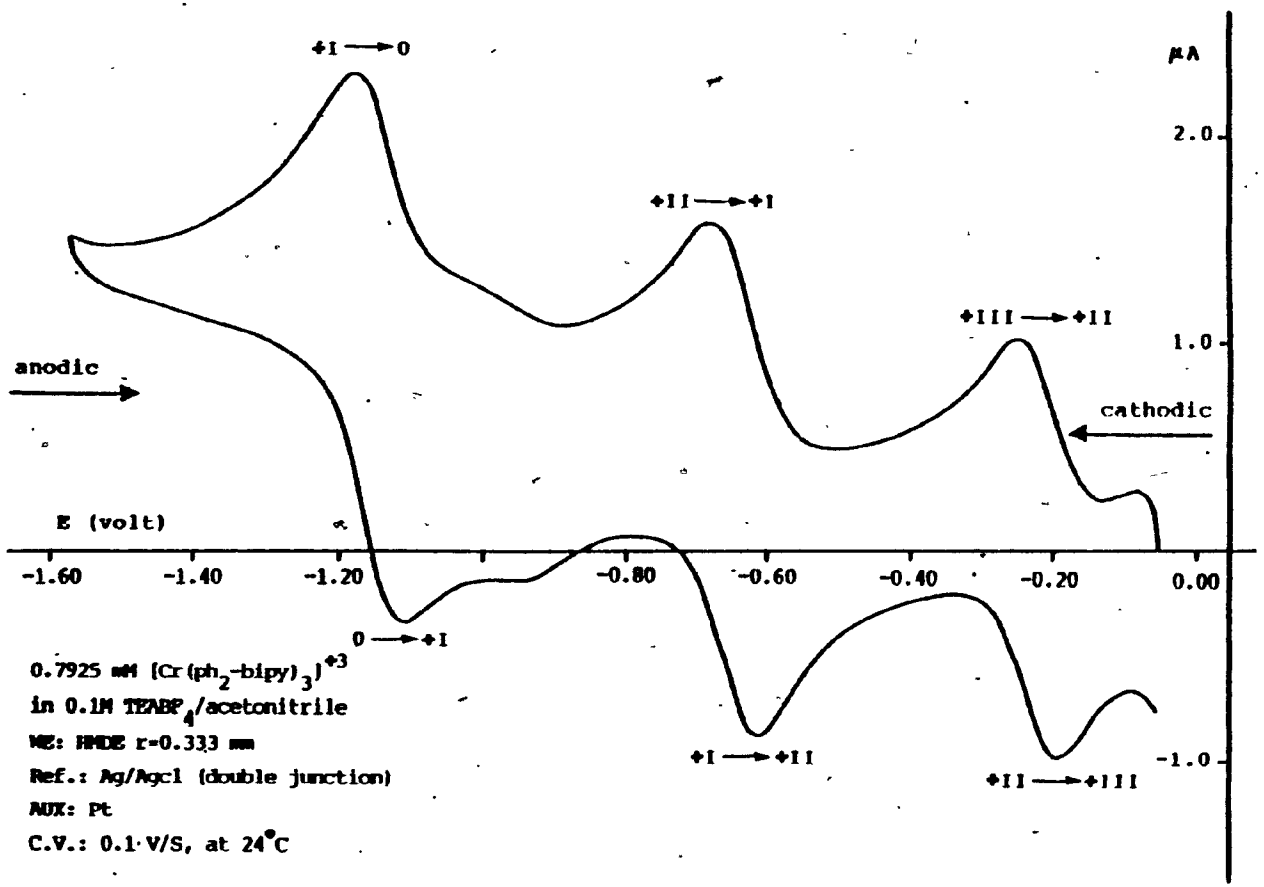

Figure 4-7: CV polarogram of $Cr(ph_2\text{-bipy})_3$ in acetonitrile; redox behavior.

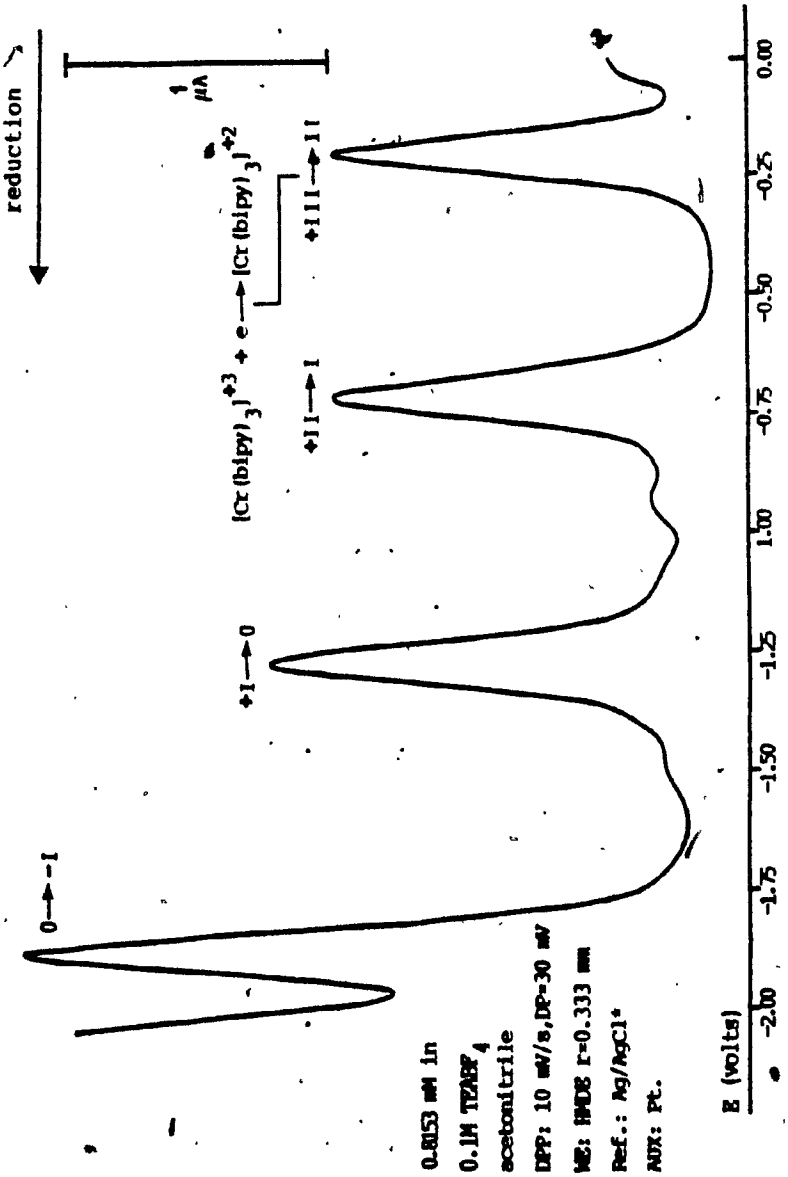

Figure 4-8: DPP polarogram of $[Cr(bipy)_3]^{+3}$ in acetonitrile; four reduction states.

description of the redox behaviour is summarized in Table 4-1. The tabulated values represent averages of at least 10 measurements obtained from two or three sample solutions of each of the chromium samples. The bulk of the data is tabulated in Appendix B-5.

As was described in Chapter 2, the degree of reversibility can be determined from the anodic-cathodic peak separations and from the rising slope of the cathodic wave. For the ideal reversible case

$\Delta E_p \simeq 60/n$ mV and

$|Ep - E_{p/2}| \simeq 57/n$ mV.

Table 4-1 lists two different values of ΔEp obtained as shown in Figure 4-9. The true value of the peak separation is probably an average of these two. The symmetry of the peaks and the values obtained for ΔEp and $E_p - E_{p/2}$ for each transition leads to the conclusion that all the complexes under study have indeed three reversible oxidation states, and each transition involves one electron (n=1). This conclusion is supported by the equivalent values obtained for i_p/c.

Peak current-to-concentration ratio is an important parameter in voltammetry, since it is an indicator of sensitivity as well as of quantity. The fact that no technique other than CV need be used may be best demonstrated by a comparison of the CV values

complex couple (redox)	No of runs	natural ΔEp (mV)	biased ΔEp (mV)	Ep-Ep/2 (mV)*	$i_{p/C}$ * (μA/mM)
$Cr(bipy)_3$					
III→II→III	12	83.0	57.5	58.7	2.03
II →I →II **	12	71.0	51.0	62.0	2.21
I →0 →I	12	76.0	53.0	62.0	2.21
$Cr(terpy)_2$					
III→II→III	13	69.0	47.0	59.0	2.39
II →I →II	13	63.0	47.0	62.0	2.12
I →0 →I	13	66.0	44.0	60.0	2.10
$Cr(me_2\text{-}bipy)_3$					
III→II→III	24	66.0	43.0	60.3	1.94
II →I →II	24	61.0	43.0	58.6	1.75
I →0 →I	24	64.0	42.0	57.6	1.93
$Cr(ph_2\text{-}bipy)_3$					
III→II→III	11	60.0	42.0	53.2	1.53
II →I →II	11	63.0	43.0	61.5	1.55
I →0 →I	11	65.0	42.0	59.5	1.66

Table 4-1: CV data pertinent to the evaluation of the degree of reversibility and equivalency for 3 electron transitions in four different chromium complexes.

* computed only from reduction peaks
** Roman numerals represent oxidation state

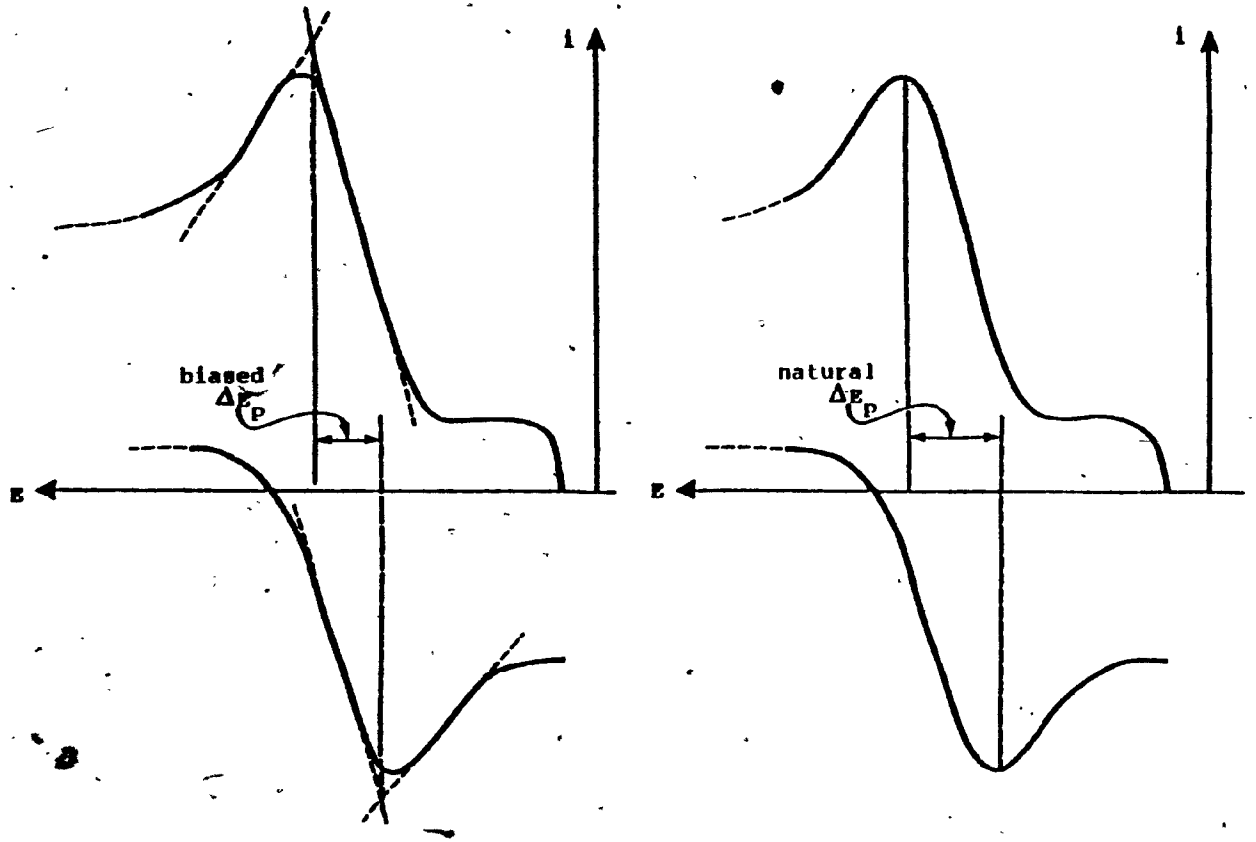

Figure 4-9: Two methods for determining peak separation.

of i_p/c with values obtained by other techniques. Table 4-2 lists a comparison of results obtained for $Cr(bipy)_3$ and $Cr(terpy)_2$ by D.C. and AC polarography (37) and by DPP and CV. The tabulated values indicate that, other than in the degree of sensitivity, there is no significant difference between the methods. It should be noted here that the magnitude of the peaks for DPP and CV could be easily increased by increasing the size of the HMDE and/or by increasing the sensitivity of the voltammetric instrument.

4.3.2 Polarographic half-wave by cyclic voltammetry

The polarographic half-wave potentials were extracted from the CV polarograms obtained for the four chromium complexes using the following methods:

Method A: $E_{1/2} = E_p + 0.029/n$ volts

Method B: $E_{1/2} = E_{p/2} - 0.028/n$ volts

Method C: $E_{1/2}$ = a point 85.17% up the cathodic wave.

The results obtained by these methods were subject to rigorous statistical treatment both between samples and between methods. The reproducibility of results within a method was examined by the use of the Q-test within a sample and the analysis of variance (Anova) F-test between samples. A summary of the final averages is tabulated in Table 4-3.

complex couple (reduction)	POLAROGRAPHY DC [a] $i_{d/c}$*	AC [a] $i_{d/c}$*	DPP [b] $i_{d/c}$*	CV [b] $i_{d/c}$*
$Cr(bipy)_3$				
III→II	3.35	3.45	1.84	2.03
II→I	3.60	3.40	1.84	2.21
I→O	3.20	3.50	2.02	2.21
$Cr(terpy)_2$				
III→II	3.15	3.30	1.81	2.39
II→I	3.40	3.40	1.89	2.12
I→O	3.35	3.30	1.79	2.10

Table 4-2: Comparison of (peak) current-to-concentration ratios obtained by different techniques.

a. data from Hughe & Macero (Inorg. Chem., 15, 2040(1976)).

b. results obtained in this experiment;
CV: 0.1 V/S, HMDE Vs. Ag/AgCl
DPP: 10 mV/S, 30 mV pulse, HMDE Vs. Ag/AgCl

* all units are in μA/mM

complex couple (reduction)	$E_{1/2}$* as determined by methods: A	B	C
$Cr(bipy)_3$			
III ⟶ II	-0.200 ±0.003	-0.199 ±0.003	-0.198 ±0.001
II ⟶ I	-0.720 ±0.002	-0.714 ±0.003	-0.717 ±0.003
I ⟶ 0	-1.282 ±0.002	-1.278 ±0.002	-1.280 ±0.001
$Cr(terpy)_2$			
III ⟶ II	-0.104 ±0.002	-0.102 ±0.002	-0.103 ±0.002
II ⟶ I	-0.511 ±0.004	-0.506 ±0.005	-0.509 ±0.004
I ⟶ 0	-1.028 ±0.002	-1.026 ±0.003	-1.028 ±0.002
0 ⟶ -I	-1.963 ±0.005	-1.952 ±0.005	-1.956 ±0.005
$Cr(me_2\text{-}bipy)_3$			
III ⟶ II	-0.366 ±0.003	-0.361 ±0.003	-0.362 ±0.002
II ⟶ I	-0.868 ±0.003	-0.866 ±0.002	-0.867 ±0.002
I ⟶ 0	-1.388 ±0.003	-1.388 ±0.002	-1.390 ±0.003
0 ⟶ -I	-1.997 ±0.006	-1.987 ±0.004	-1.987 ±0.004
$Cr(ph_2\text{-}bipy)_3$			
III ⟶ II	-0.219 ±0.003	-0.223 ±0.003	-0.221 ±0.003
II ⟶ I	-0.657 ±0.003	-0.653 ±0.002	-0.654 ±0.002
I ⟶ 0	-1.171 ±0.004	-1.169 ±0.003	-1.170 ±0.004
0 ⟶ -I	-1.726 ±0.008	-1.713 ±0.005	-1.719 ±0.003

Table 4-3: Half-wave potentials ($E_{1/2}$) for chromium complexes in acetonitrile as determined by 3 different methods from CV polarograms.

* volts ± standard deviation, Vs. Ag/AgCl at 24°C

A striking feature of the data in Table 4-3 is the fact that in 90% of the cases, the values obtained by Methods A and B are the upper and lower limits respectively, while the values for Method C are contained within this range. The logical explanation of this phenomenon is based on the nature of the methods. Both Methods A and B were derived theoretically and are based on the ideal reversible case where $|E_p - E_{p/2}| = 57/n$ mV. As such, they are slope dependent. Any departure from the ideal reversible process will affect the cathodic slope, and hence cause a divergence between the two methods. On the other hand, Method C, which was derived empirically, is not affected by changes in slope. Rather, it seems to define the pivot point around which the slope is changing as governed by the degree of reversibility.

Logically, one would expect the values obtained by Method C to be the average of those obtained by Methods A and B. This, however, is not the case. Method A evaluates $E_{1/2}$ utilizing the peak potential (i.e., the potential at which the current is maximum). This maximum, however, is not always well-defined. The peaks are often round at the maximum and, in the cases where other electrochemical processes occur in the vicinity, the peaks are distorted to a point where they appear in the shape of a plateau. This is clearly seen

in Figure 4-10, where the reduction 0→-I of $Cr(ph_2\text{-bipy})_3$ is influenced by the reduction of the free ligands. Hence, the exact determination of E_p is difficult and subject to large experimental (measurement) errors.

The performance of the three methods was also compared statistically within samples. From 11 sample solutions, 60 polarograms were recorded, showing a total of 196 peaks. This permitted the comparison of 37 groups with an average of 6 peaks per group. The equivalency of the 3 methods was determined by subjecting the individual averages and standard deviations to the F-test at the 95% ($F_{0.05}$) significance level (Appendix B-6).

The computed statistical results show that in 38% of the cases the values obtained by Method A are not equivalent to these of Methods B and C, while the latter two are equivalent and covarying in 87% of the cases. The equivalency of Methods B and C is also apparent from the data in Table 4-3 (between samples). Both methods produce covarying results whose difference never exceeds 5 mV. This is expected, since Method B is affected mostly by the degree of reversibility of the chemical process and very little by the shape of the maximum region of the peak.

Of the three methods, Method C seems to be the

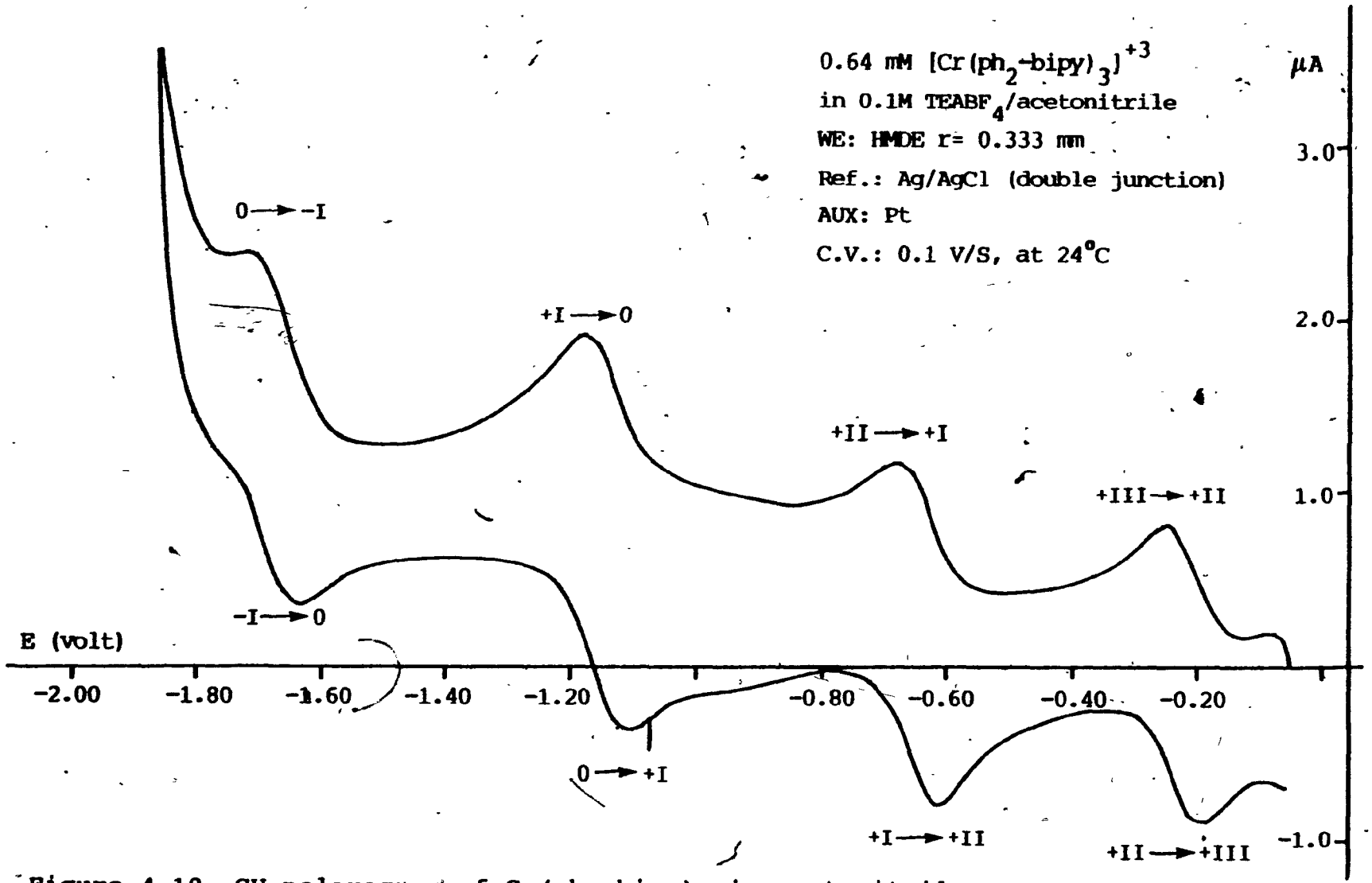

Figure 4-10: CV polarogram of $Cr(ph_2\text{-bipy})_3$ in acetonitrile; four redox transitions (see Table 4-5).

most suitable and reliable. It has shown the best record of reproducibility, with an average standard deviation of less than 3 mV, which is well within the experimental error of ±5 mV. In addition, as described before, it is to a considerable extent independent of peak shape and degree of reversibility.

The results for $E_{1/2}$ as obtained by Method C are in good agreement with literature values obtained by using D.C. polarography. Table 4-4 shows a comparison between techniques for $Cr(bipy)_3$ and $Cr(terpy)_2$.

4.4 Conclusions

Although conclusions are drawn only for a specific group of chemical processes having similar characteristics, this chapter demonstrates that CV has the capability of providing all the data needed for the interpretation of a given electrochemical process.

When solid working electrodes are used, due to their nature, the correlation of peak potential to the classical $E_{1/2}$ is infrequent (12, 43, 44, 45). In such cases, however, the half peak potential should be recorded and reported, since $E_{p/2}$ could easily replace $E_{1/2}$ as a qualitative parameter. Thus, if CV is to become a commonly used reliable tool, results should be presented as shown in Table 4-5 for $Cr(ph_2bipy)_3$. All the data shown in this table were extracted from the

complex couple (reduction)	C.V. $E_{1/2}$ [a]	D.C. POLAROGRAPHY $E_{1/2}$ [b]	$E_{1/2}$ [c]	$E_{1/2}$ [d]
$Cr(bipy)_3$				
III ⟶ II	-0.198	-0.209	-0.210	N.A.*
II ⟶ I	-0.717	-0.715	-0.725	N.A.
I ⟶ 0	-1.280	-1.280	-1.280	N.A.
$Cr(terpy)_2$				
III ⟶ II	-0.103	-0.110	-0.110	-0.118
II ⟶ I	-0.509	-0.516	-0.510	-0.519
I ⟶ 0	-1.028	-1.030	-1.030	-1.027
0 ⟶ -I	-1.952	-1.950	N.A.	-1.950

Table 4-4: Comparison of half-wave potentials ($E_{1/2}$); CV Vs. DC polarography.

a. Obtained in this experiment using method C, volts Vs. Ag/AgCl at 24°C.

b. Results obtained by Hughes & Macero (Inorg. Chem., 15, 2040(1976).

c. Same as b, under conditions of excess ligand.

d. Results obtained by Rao et al. (Inorg. Chim. Acta, 18, 127(1976).

* Not available

reduction	i_p (μA)	$(i_p)/C^*$ (μA/mM)	slope (mV)	ΔE_p (mV)	E_p (volts)	$E_{p/2}$ (volts)	$E_{1/2}^{**}$ (volts)
III ⟶ II	0.915	1.43	100	58	-0.249	-0.198	-0.224
II ⟶ I	0.970	1.51	100	60	-0.691	-0.626	-0.655
I ⟶ 0	1.085	1.69	100	60	-1.197	-1.139	-1.168
0 ⟶ -I	1.360	2.12	100	73	-1.750	-1.680	-1.715

Table 4-5: Data extracted from one CV polarogram of $Cr(ph_2\text{-bipy})_3$ (see figure 4-10)

* 0.64mM $Cr(ph_2\text{-bipy})_3$ in 0.1M $TEABF_4$/acetonitrile

** 0.100V/sec., HMDE Vs. Ag/AgCl at 24°C

polarogram in Figure 4-10.

Technically, the instrumental system presented two problems, both caused by the supporting electrolyte. Due to the viscous nature of acetonitrile, it was difficult to suspend the mercury drop (HMDE) for the duration of the experiment. This problem was solved by using relatively small mercury droplets, and by adjusting the WE capillary so that the droplet was suspended just beneath the surface of the solution. The best solution for such problems is perhaps the U-shaped capillary tube described by Kolthoff (46) on which the mercury droplet sits rather than hangs.

The second problem involved the double-junction reference electrode. The frit in the inner junction (i.e., at the interface between the aqueous KCl and the $TEABF_4$ acetonitrile) kept precipitating salts, probably potassium tetrafluoroborate. As a result, the reference potential began to fluctuate. This problem is not uncommon when working with non-aqueous electrolytes (46). Once discovered, this difficulty was easily solved by periodic wiping of the inner junction frit.

CHAPTER 5

THE RATE OF REACTION OF $Cr(bipy)_3$ AND $Cr(me_2\text{-}bipy)_3$ IN AQUEOUS SOLUTIONS

5.1 Introduction and Theory

As was seen in Chapter 4, in an aprotic solvent such as acetronitrile, the tris bipyridine chromium complexes are reduced in four, well-defined, one-electron steps. The electrochemistry of these ions in water is however not so simple due to catalytic ligand exhanges at the electrode (WE) surface.

5.1.1 Aqueous behavior of $[Cr(bipy)_3]^{+3}$

From i-E curves obtained using a commutator polarographic technique (square wave), Vlcek (47) reported three polarographic waves ($E_{1/2}$ vs. SCE of -0.36, -0.73, and -1.38 volts) for the $[Cr(bipy)_2]^{+3}$ ion in aqueous 0.5M NaCl supporting electrolyte. Vlcek reported no evidence of dissociation of the complex during any stage of the reduction process and concluded that each of the polarographic waves corresponded to a reversible one-electron transfer leading finally to $[Cr(bipy)_3]^{o}$.

In a more extensive study using conventional polarographic techniques, Baker et al. (48) and Tucker

et al. (49) obtained four polarographic waves with $E_{1/2}$ potentials that were substantially different from those obtained by Vlcek. From the behavior of the first two polarographic waves with regard to pH and temperature, Baker suggested the mechanisms shown below:

$$[Cr(bipy)_3]^{+3} + e^- \rightleftharpoons [Cr(bipy)_3]^{+2}$$

$$E_{1/2} = -0.49V \qquad (5\text{-}1)$$

$$[Cr(bipy)_3]^{+2} + 2H_2O \underset{K_2}{\overset{K_1}{\rightleftharpoons}}$$

$$[Cr(bipy)_2\ (H_2O)_2]^{+2} + bipy \qquad (5\text{-}2)$$

$$[Cr(bipy)_3]^{+3} + [Cr(bipy)_2(H_2O)_2]^{+2} \underset{K_4}{\overset{K_3}{\rightleftharpoons}}$$

$$[Cr(bipy)_3]^{+2} + [Cr(bipy)_2(H_2O)_2]^{+3} \qquad (5\text{-}3)$$

$$[Cr(bipy)_2(H_2O)_2]^{+3} + e^- \rightleftharpoons$$

$$[Cr(bipy)_2(H_2O)_2]^{+2} \qquad E_{1/2} = -0.72V \qquad (5\text{-}4)$$

$$[Cr(bipy)_2(H_2O)_2]^{+2} + bipy \underset{K_1}{\overset{K_2}{\rightleftharpoons}}$$

$$[Cr(bipy)_3]^{+2} + 2H_2O \qquad (5\text{-}5)$$

The $[Cr(bipy)_3]^{+3}$ undergoes catalytic ligand exchange at the dme surface to $[Cr(bipy)_2(H_2O)_2]^{+3}$,

which is reduced at a potential more cathodic than the original tris complex. The ligand exchange process was also confirmed by controlled-potential electrolysis and cyclic voltammetric techniques.

The reactions in Equations 5-1 and 5-2 are by themselves reversible. The ligand exchange in Equation 5-2 does not affect the electron transfer in Equation 5-1. But when, in the CV electrochemical process, $[Cr(bipy)_2(H_2O)_2]^{+2}$ is formed in the presence of $[Cr(bipy)_2]^{+3}$, the diaquo complex is very rapidly removed in the reaction described in Equation 5-3. Under these conditions Equation 5-2 appears irreversible. Thus, Equation 5-1 and 5-2 described an electron exchange followed by an irreversible chemical reaction. The rate of dissociation of the complex (K_1 in Equation 5-2) can be evaluated as hereafter described.

5.1.2 Methodology

In their classical paper on stationary electrode kinetics, Nicholson and Shain (21), described a technique for the evaluation of rates of reaction for irreversible chemical processes which are preceded by a reversible electron transfer. The electrochemical process can be described by the following equations:

$$O + ne \rightleftharpoons R \qquad (5\text{-}6)$$

$$R \xrightarrow{K_f} Z \qquad (5\text{-}7)$$

Their technique permits the evaluation of K_f in Equation 5-7 from the anodic/cathodic peak height ratios obtained from the reversible reaction (Equation 5-6) by the use of cyclic voltammetry. From a large number of theoretical polarograms, Nicholson and Shain derived a working curve of i_a/i_c versus $K_f\tau$ (Figure 5-0), where τ is the elapsed time between the potential at which the scan is reversed (E_{sw}) and the $E_{1/2}$ of the cathodic wave. From this relationship one can see that τ is essentially controlling i_a. A large τ will permit Equation 5-7 to eliminate a large amount of reduced species. As a result, the oxidation part of the cycle will yield a smaller anodic peak (i_a). The variation of i_a with τ will therefore permit K_f to remain a constant and in effect eliminate the scan rate and the switching potential as variables in the computation of the kinetic parameter.

The only difficulty with this technique lies in the evaluation of i_a/i_c. While i_c can be easily measured from a well-defined base line (the residual current), the anodic peak i_a is quite difficult to measure since the polarograms do not show a base line

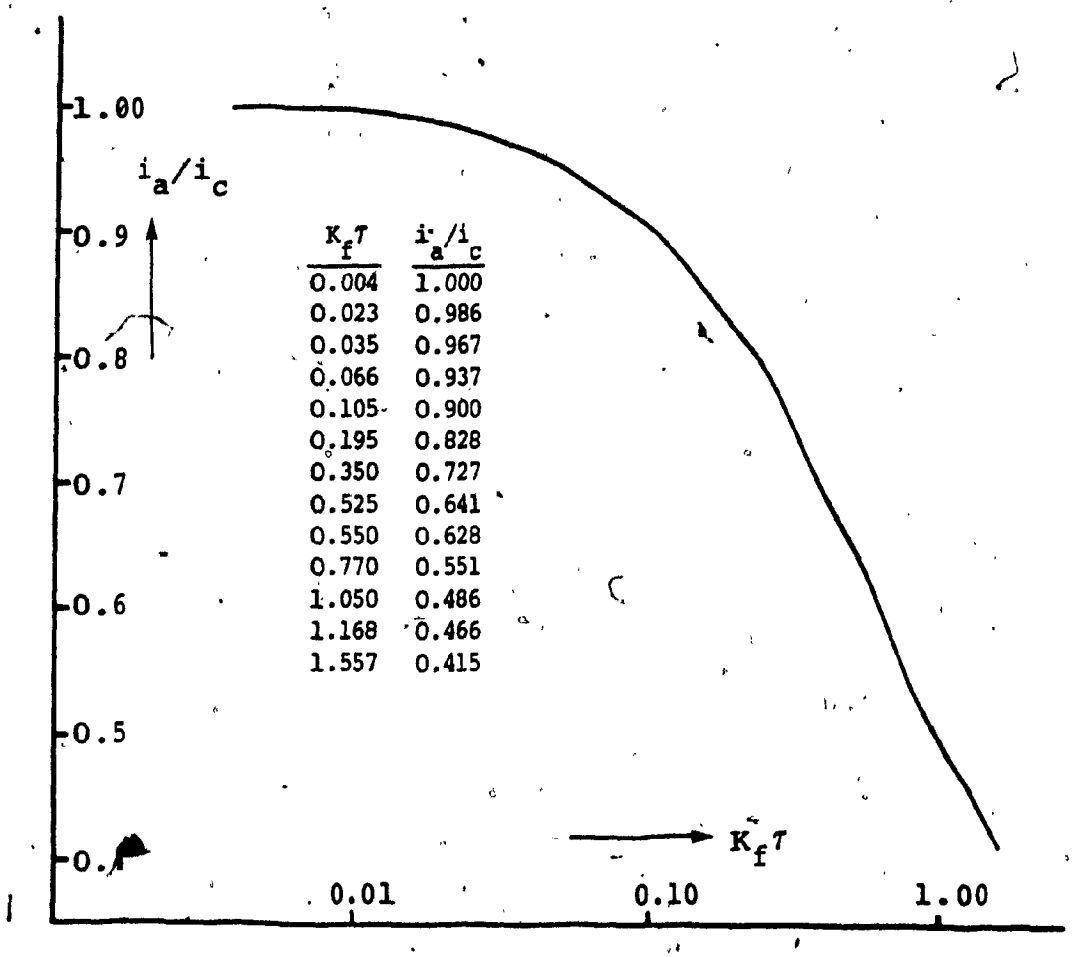

$K_f\tau$	i_a/i_c
0.004	1.000
0.023	0.986
0.035	0.967
0.066	0.937
0.105	0.900
0.195	0.828
0.350	0.727
0.525	0.641
0.550	0.628
0.770	0.551
1.050	0.486
1.168	0.466
1.557	0.415

Figure 5-0: Nicholson's working curve i_a/i_c Vs. $K_f\tau$ (Anal. Chem., 36, 706 (1964)).

at all for the oxidation portion of the scan. In order to obtain a clear (horizontal) base line, one would have to scan well past the cathodic peak. However, due to the nature of the chemical process, this will allow Equation 5-7 to dominate, resulting in an excellent base line but a poor anodic peak. To solve this problem, Nicholson (28) has developed a semiempirical procedure which permits calculation of the ratio i_a/i_c from a single-cycle polarogram. The technique involves the utilization of three easy-to-measure quantities. These are the cathodic peak (i_c), the apparent anodic peak (i_{aa}) and the current at the switching potential (i_{sw}). As can be seen from Figure 5-1, the latter two quantities are also measured from the cathodic base line. Using these measurable parameters, the true peak ratio was found to be:

$$\frac{i_a}{i_c} = \frac{i_{aa}}{i_c} + \frac{0.485 i_{sw}}{i_c} + 0.086 \qquad (5\text{-}8)$$

This relationship essentially allocates a portion of the switching current to the anodic current and hence estimates where the anodic base line would have been.

The elapsed time can be easily evaluated, since $E_{1/2}$ can be computed by either Method B or C as described in Chapter 4. Therefore, in theory, one could

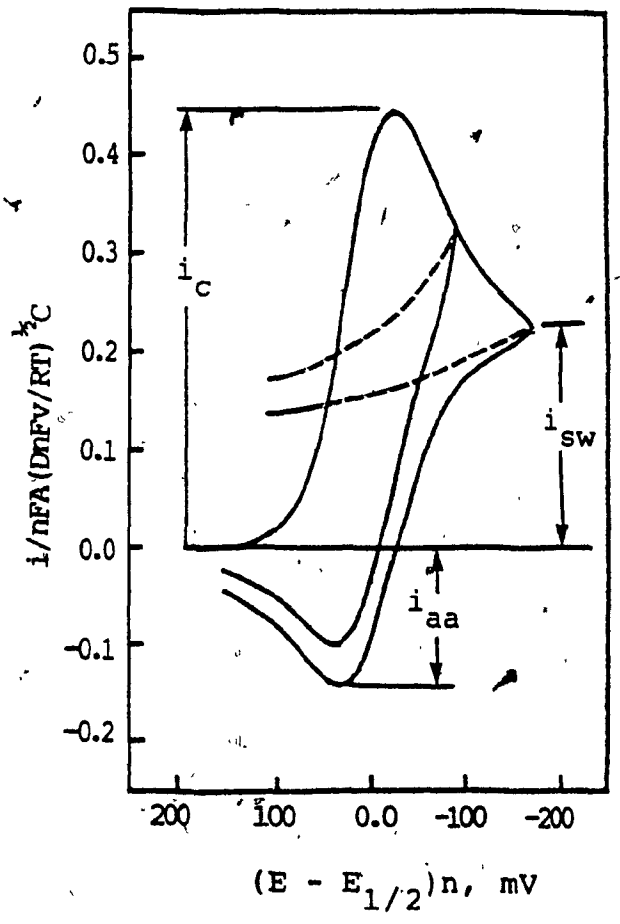

Figure 5-1: Nicholson's easy-to-measure parameters from CV polarograms.

evaluate the kinetic parameter K_f from a single-cycle polarogram.

A striking feature of this technique is that the ratio of peak heights is independent of such experimental parameters as diffusion coefficients and electrode size and surface area (50, 51).

5.2 Experimental

5.2.1 Preparation of analyte and supporting electrolyte

The sample solutions in duplicates for both $Cr(bipy)_3$ and $Cr(me_2\text{-}bipy)_3$ were prepared as indicated in Appendix C-1 to yield:

$5.5X10^{-5}$ M complex in 0.1M potassium chloride.

The concentrations and the supporting electrolyte were chosen in order to facilitate the comparison of results with literature values under similar conditions (for $Cr(bipy)_3$).

5.2.2 Apparatus and experimental parameters

All measurements were obtained with the three electrode cell as described in the previous chapters, consisting of:

WE: HMDE (radius 0.423, 0.384, 0.333, and 0.265mm)

AUX: Pt (platinum microelectrode)

Ref: standard calomel, SCE (saturated KCl) and Ag/AgCl (saturated KCl).

All measurements were taken at an ambient temperature of 24±1°C or, when needed, at elevated temperatures of up to 35°C, controlled by passing hot water through the built-in glass jacket of the cell.

5.3 Results and Discussion

5.3.1 Preliminary results and complications: $Cr(bipy)_3$

Initial runs on the $Cr(bipy)_3$ samples were carried out at 25°C with an unadjusted pH of 5.2, and all potentials were measured versus the Ag/AgCl (saturated KCl) reference electrode. The resulting polarograms suggested the presence of multiple complicating factors, of which the most outstanding was a large residual current (capacitance). When measured from the zero-current line (start), the residual current was often half the size of the reduction peak, as can be seen from Figure 5-2. A visual comparison of the polarogram in Figure 5-2 with that of the ideal case in Figure 5-1 suggested that straightforward measurements of i_c, i_{aa} and i_{sw} are quite impossible.

In addition, the cathodic peak gave a maximum at -0.44 volts versus Ag/AgCl with a computed $E_{1/2}$ of -0.410 volts. Adding -0.04 volts to the $E_{1/2}$ value (in order to compensate for the difference between the Ag/AgCl and the SCE reference electrodes) yielded a value which was still 40 mV more positive than that

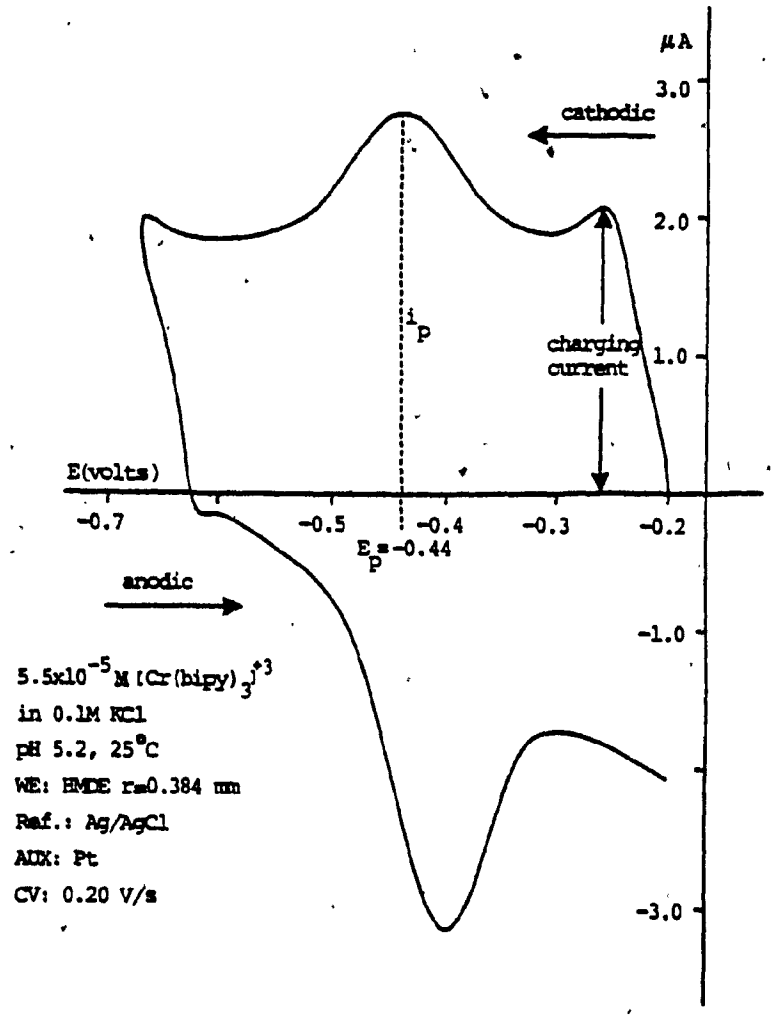

Figure 5-2: CV polarogram of aqueous $Cr(bipy)_3$.

reported in the literature ($E_{1/2}$ = -0.49V). Furthermore, at lower than 0.2 V/sec. scan rates, the cathodic wave became rounded and ill-defined.

Another puzzling phenomenon was the size of the anodic peak. While, according to theory, it was supposed to be much smaller than its cathodic counterpart, in reality (Figure 5-2) it was equal or larger. In addition, the anodic peak did not always occur at the same potential. It was at times broad and occurred at the same potential as the cathodic peak, which again, from the theoretical point of view, is impossible.

All of the above observations suggested that the process involved more than one electrochemical reaction. Since the time lapses between scans at the HMDE somewhat resemble those in polarographic stripping techniques (52,53), suspected impurities such as lead (Pb) were removed by electrolysis from both the mercury and the supporting electrolyte (Appendix C-2). This, however, did not improve the results, suggesting that the problem lay within the complex sample. That this was probably the case became more apparent when the scan was extended to -1.20 volts. Both anodic-first and cathodic-first scans in Figures 5-3 and 5-4 show the two expected reduction waves; $+3 \rightarrow +2$ for $[Cr(bipy)_3]^{+3}$ and $[Cr(bipy_2(H_2O)_2]^{+3}$. However, the oxidation portion of the scans presented

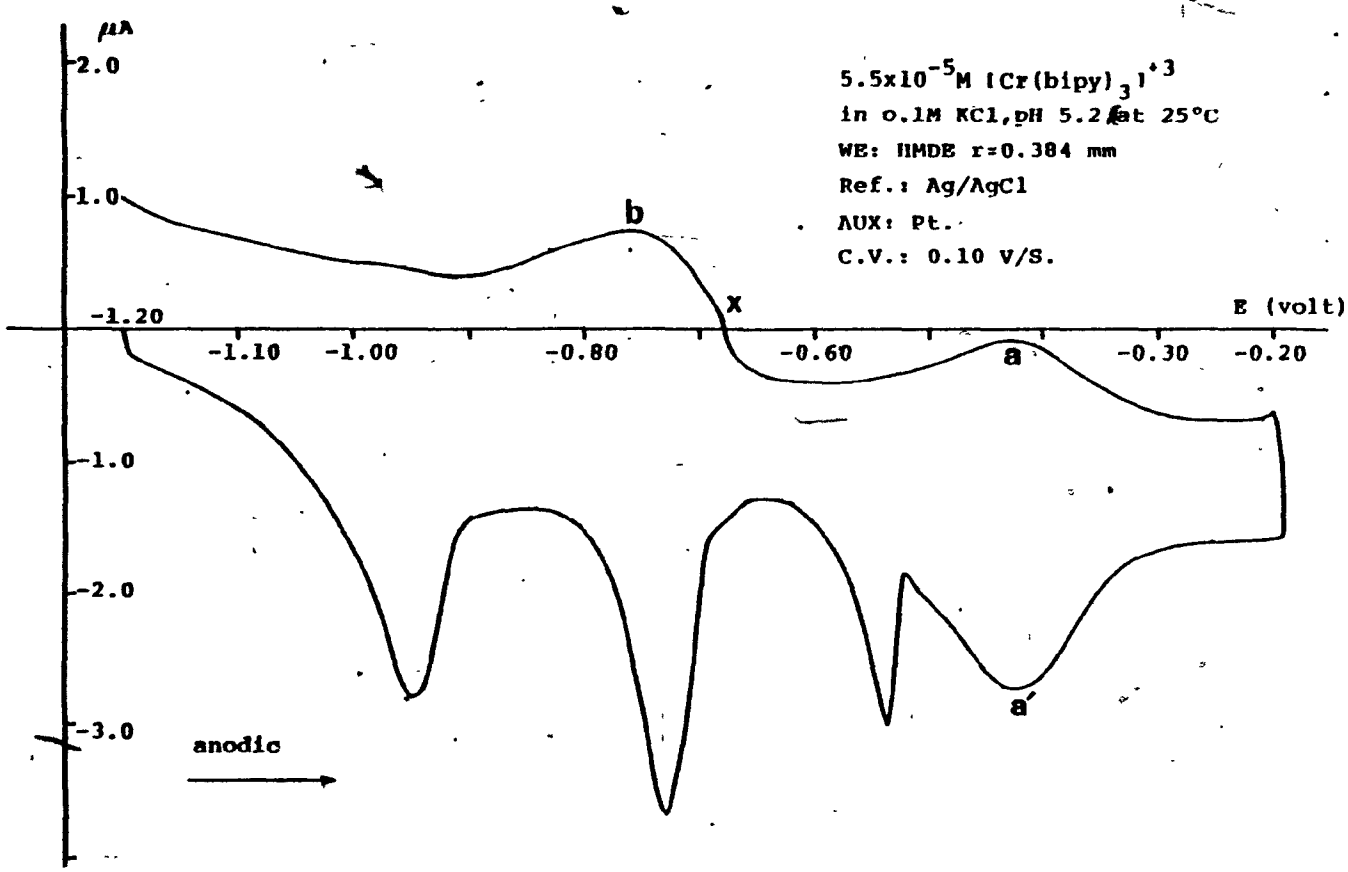

Figure 5-3; CV polarogram of $Cr(bipy)_3$; extended range, starting anodically
a&a': redox according to equation 5-1.
b : reduction of the diaquo complex (equation 5-4).

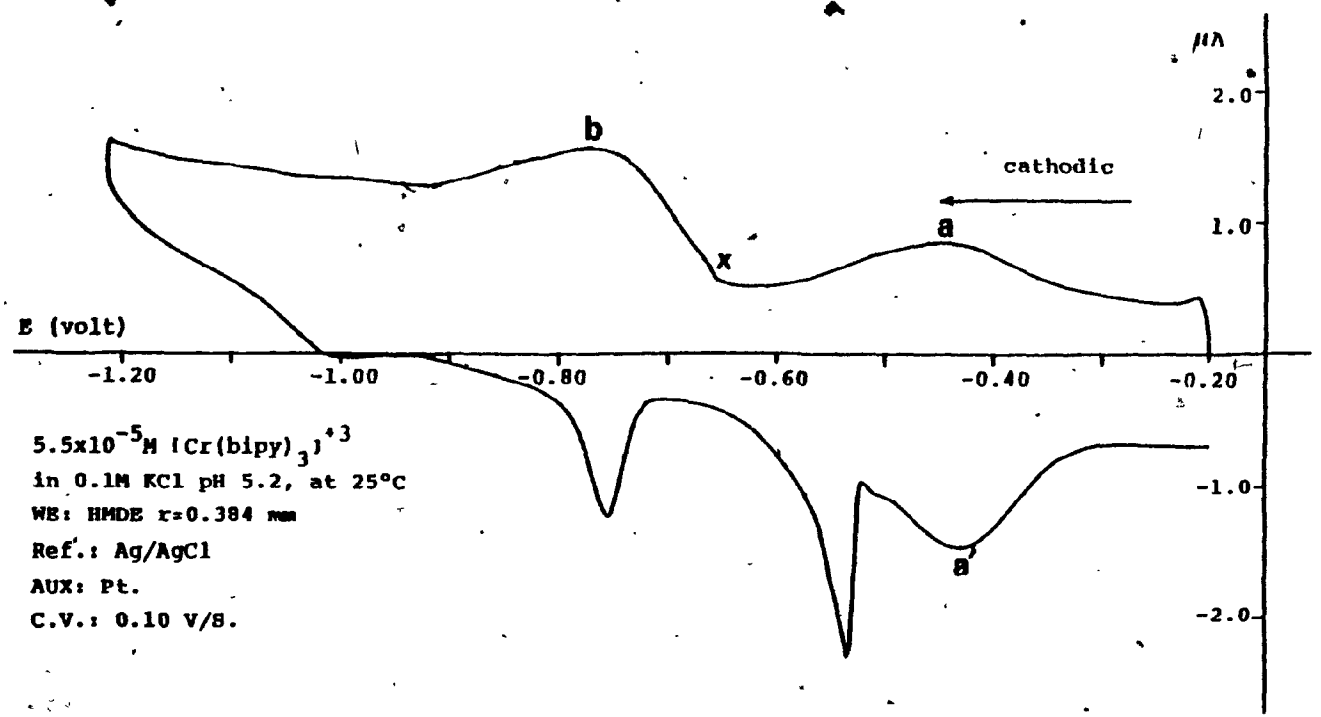

Figure 5-4: CV polarogram of $Cr(bipy)_3$; extended range, starting cathodically
a&a': redox according to equation 5-1.
b : reduction of the diaquo complex (equation 5-4).

several large anodic peaks which did not correspond to any obvious reduction or chemical process. In addition, the reduction peak for $[Cr(bipy)_2(H_2O)_2]^{+3}$ was quite broad, indicating that it was the result of several peaks. This became more apparent when multicycle CV was used. The polarogram in Figure 5-5 shows that the cathodic peak is actually composed of three peaks, of which the most relevant is the small peak circled in the polarogram. This peak seemed to be shifting with both the scan rate and the switching potential (E_{sw}). For example, Figure 5-6 shows it appearing at as low as -0.615 volts (designated X). The sharply rising slope of this peak and its general shape and size suggested that it might be caused by the fast reduction of an intermediate species or that it was due to charge delocalizing on the chromium in the catalytic reaction (Equation 5-2). Figure 5-6 also shows that the anodic peak (peak A) for the reoxidation of $[Cr(bipy)_3]^{+2}$ is also composed of more than one peak. This isomerization-like behavior could be caused by two similar species (i.e., the product of the primary reaction in Equation 5-1 and the product of the catalytic reactions in Equations 5-2 or 5-5.)

All of the foregoing indicated that the solution (as prepared) contained more than one system at equilibrium and that the primary reaction (Equation

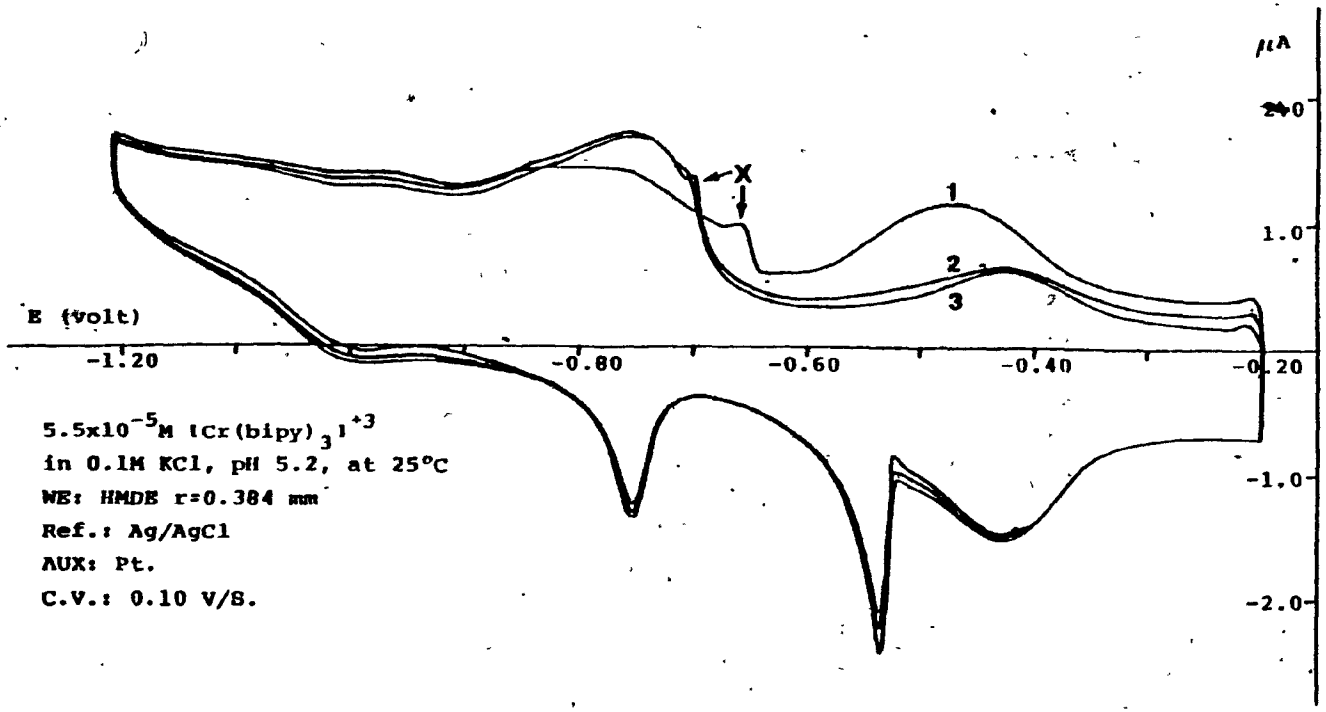

Figure 5-5: Three cycles CV polarogram of aqueous $Cr(bipy)_3$.
X. indication that the reduction peak of the diaquo comlex (equation 5-4) is a composition of several peaks.

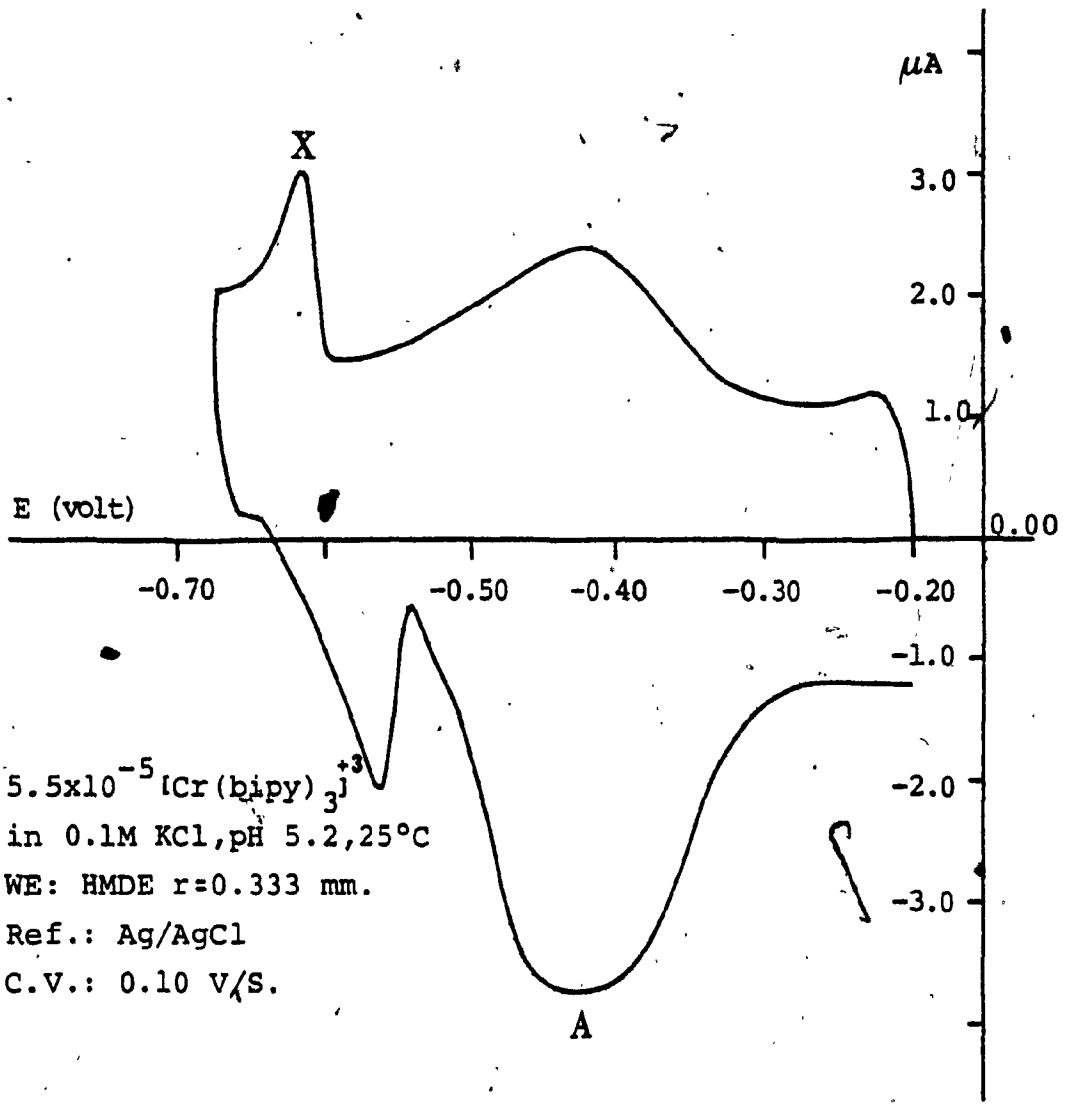

Figure 5-6: CV polarogram of aqueous $Cr(bipy)_3$. The anodic (oxidation) peak 'A' suggests the presence of more then one peak, and peak 'X' indicates the the existance of an intermediate species.

5-1) is probably further complicated by the presence of excess ligand (as was described in Chapter 4) and by other subspecies (54), such as $[Cr(bipy)(H_2O)_4]^{+2}$ and $[Cr(H_2O)_6]^{+2}$.

5.3.2 Preanalysis sample treatment

It became obvious from Section 5.3.1 that in order to proceed with the determination of the rate of reaction K_f, two major complicating factors had to be eliminated or at least greatly minimized. These were the size of the charging (residual) current and the presence of intermediate species at the outset.

The effect of charging current was greatly reduced by decreasing the size of the working electrode (smaller Hg droplet). This action was decided upon after it was observed that the size of this electrode has a greater effect on the charging current than on the faradaic current.

The second problem was solved by the use of prolonged electrolysis at the HMDE. The technique involved multicycle scanning between 0 and +0.3 volts vs. SCE while passing N_2 through the solution (as stirring). The positive potential scanning induced most of the analyte to form the primary species $[Cr(bipy)_3]^{+3}$. This process, however, took about 40 minutes, and the accidental fall of the HMDE made it neces-

sary to start over again. Figure 5-7 shows the metamorphic transition at a point 15 minutes into the process. The original cathodic peak has split into two distinct peaks. The peak at -0.33V will eventually shift more anodically and finally disappear, while the peak at -0.49V will grow and shift to -0.51V to yield the final product.

Attempts were made to reduce the duration of the above process by using electrolysis at a platinum (Pt) gauze electrode. However, this proved to be ineffective, probably due to differences in catalytic effect between platinum and mercury.

5.3.3 Results: $Cr(bipy)_3$

Although the electrolyzed sample gave large and well-defined peaks, the residual currents were not completely minimized, and their effect was noted both at the beginning of the cycle and at the switching point (E_{sw}). As a result, the potential at which the scan was reversed had little or no effect on the anodic peak, as is clearly seen in Figure 5-8. This made it impossible to use the technique described in Section 5.1.2 to estimate the true i_a/i_c ratio, since only i_{sw} varies with τ and this is not sufficient to maintain K_f constant. Hence a different method had to be developed.

It was observed that the residual current at the

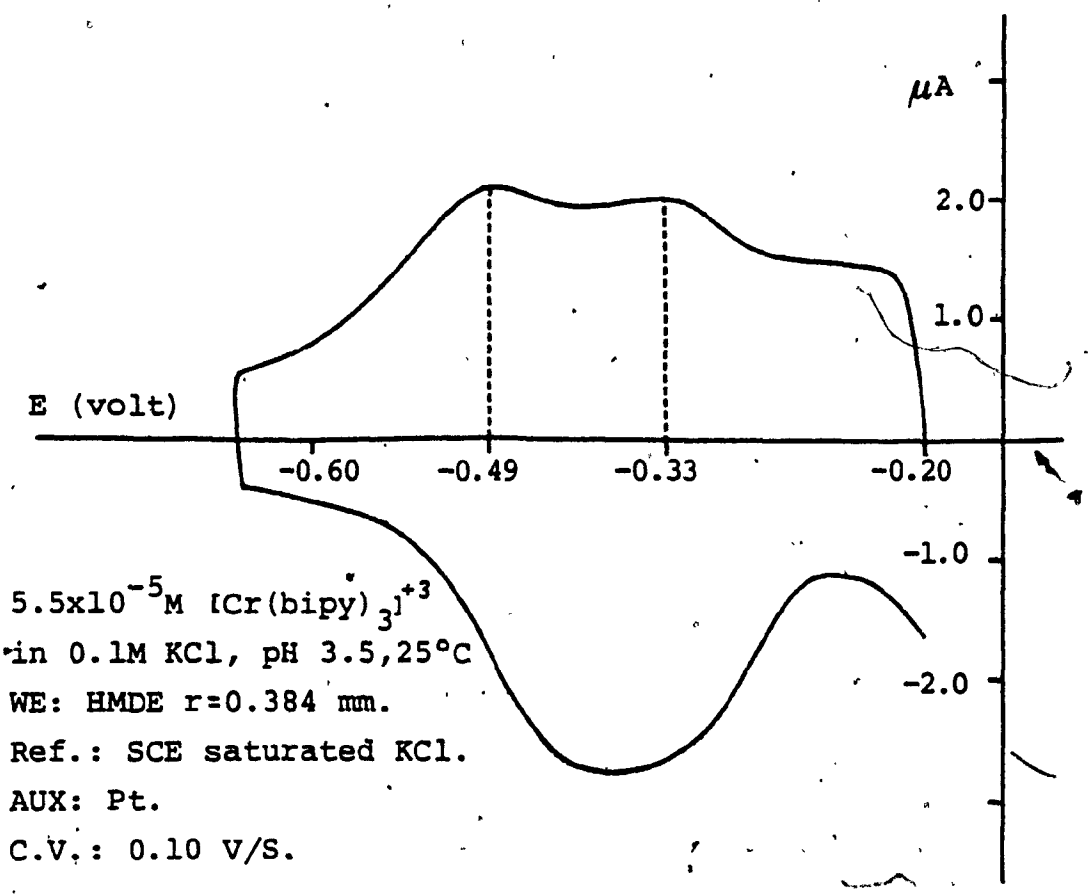

Figure 5-7: Aqueous Cr(bipy)$_3$; cathodic (reduction) peak splitting after 15 min. of electrolysis.

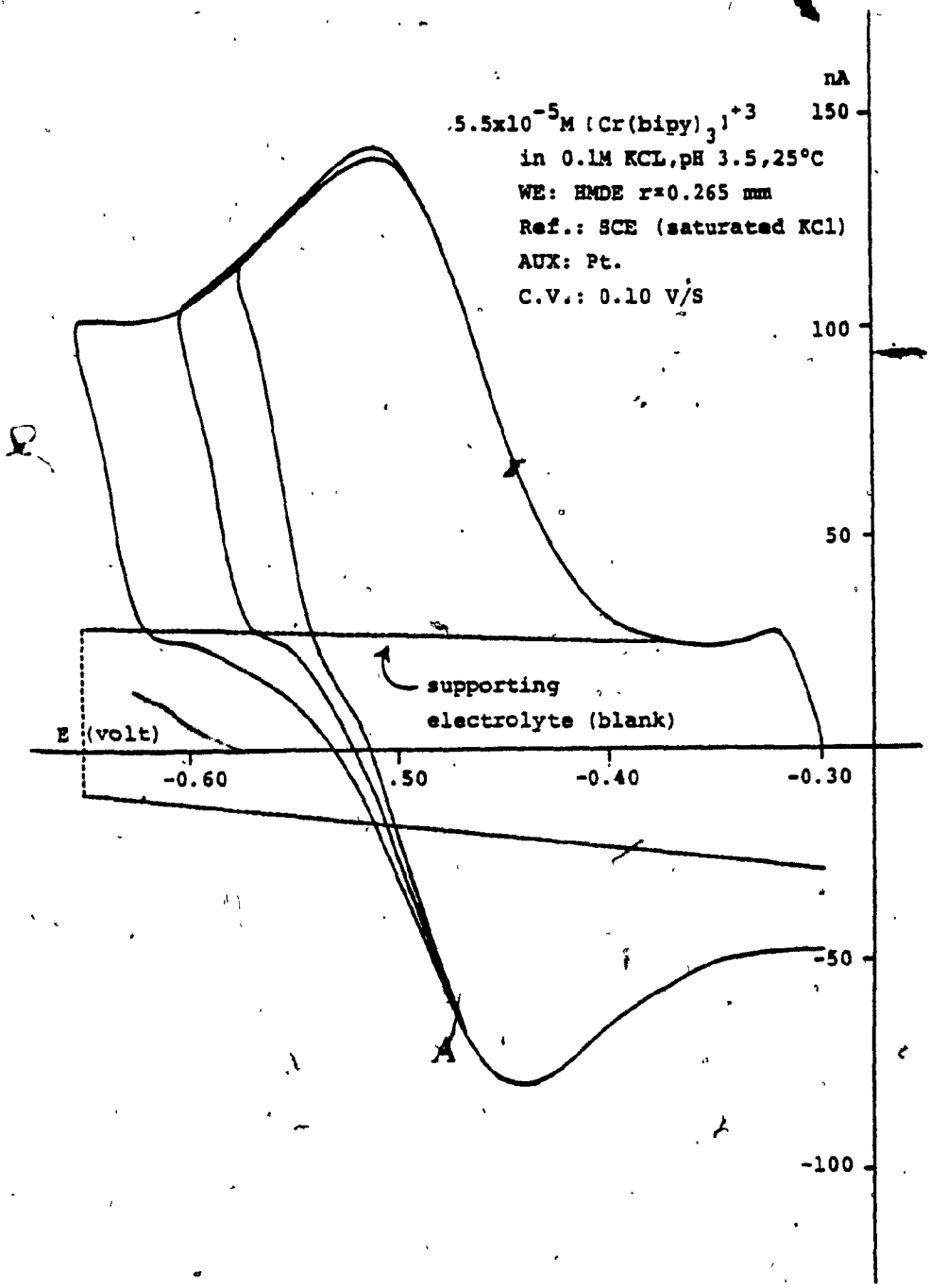

Figure 5-8: Aqueous $Cr(bipy)_3$; composition of three polarograms having different switching potentials. From this polarogram it can be seen that E_{switch} does not affect the anodic peak 'A'.

start of the scan was mainly due to the supporting electrolyte (Figure 5-8). However, due to the nature of the electrochemical evaluation (one Hg drop suspended for an hour), it was hardly possible to obtain scans for both the supporting electrolyte and the analyte solution at the same HMDE. Consequently, a large number of scans were recorded for the supporting electrolyte (blank) at different potential scan rates. This permitted the construction of theoretical blank models (Appendix C-3), which were then superimposed on the sample runs and provided the base line for the measurements of the cathodic peaks. For reasons described in detail in Appendix C-4, the anodic peaks (true values) were measured from a point at which the current reaches equilibrium when the cycle is stopped at the switching potential. Figure 5-9 demonstrates the technique by which all the polarograms were evaluated to yield the true values of i_a and i_c and hence their ratio.

Finally, the analyte solutions were acidified and adjusted to pH 3.5. This was done in order to prevent sample deterioration, so that the samples could be analyzed over several weeks.

The results obtained from duplicate samples of $Cr(bipy)_3$ at 23° and 25°C are summarized in Table 5-1. The K_f values tabulated at each scan rate are averages

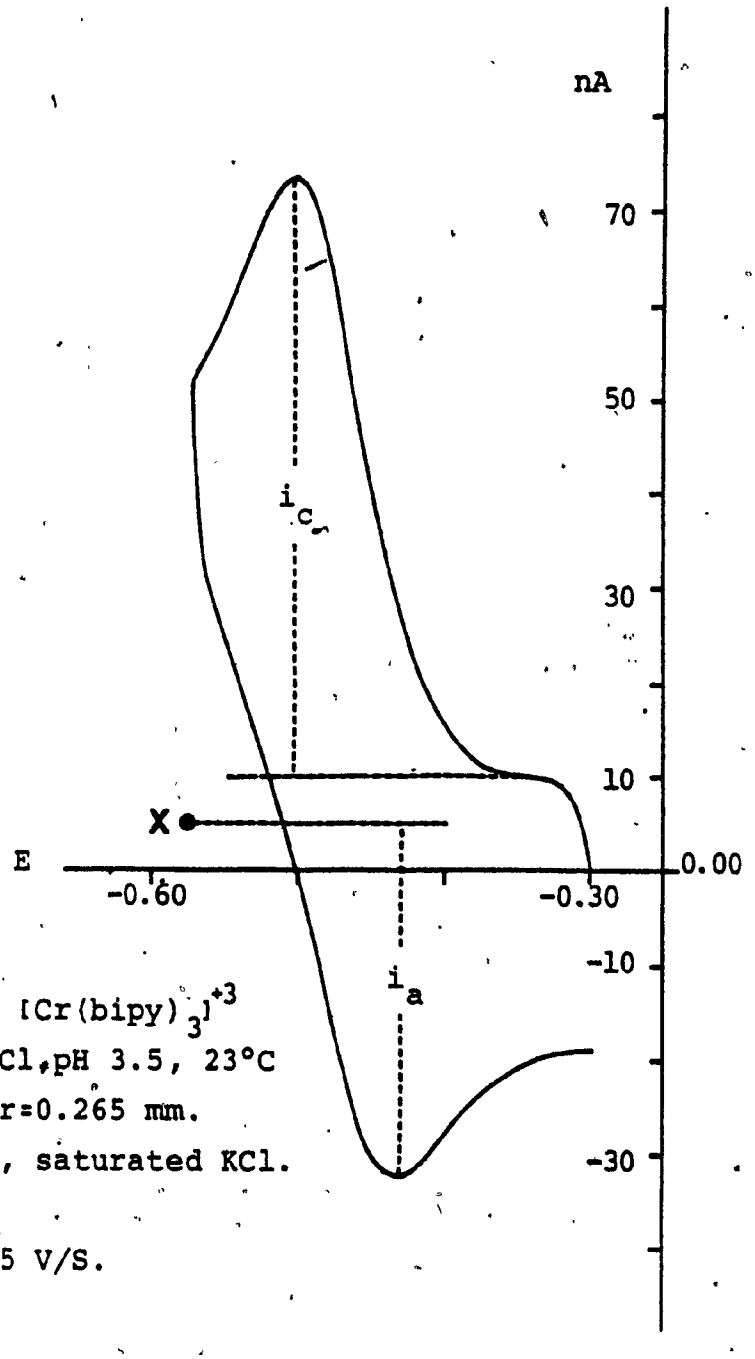

Figure 5-9: Peak magnitude determinations. Reduction peak (i_c) is measured from the residual current. Oxidation peak (i_a) is measured from a point of current equilibrium (X) at half cycle.

	scan rate (V/S)	E_{start} (V.)	E_{switch} (V.)	cathodic peak (V.)	$E^{*}_{1/2}$ (V.)	i_a/i_c	$K_f\tau$	τ (sec.)	$K_f \pm \sigma$ ($sec.^{-1}$)
a	0.040	-0.300	-0.575	-0.503	-0.478_a	0.574	0.700 ±0.046	2.49	0.282 ±0.017
	0.050	-0.300	-0.575	-0.502	-0.476	0.617	0.579 ±0.028	1.97	0.295 ±0.014
	0.070	-0.300	-0.580	-0.500	-0.475	0.673	0.448 ±0.023	1.50	0.298 ±0.015
	0.090	-0.300	-0.600	-0.524	-0.495	0.740	0.328 ±0.044	1.16	0.293 ±0.035
	0.100	-0.300	-0.580	-0.508	-0.487	0.745	0.321 ±0.012	1.04	0.310 ±0.012
b	0.060	-0.300	-0.575	-0.502	-0.475_b	0.632	0.542 ±0.037	1.67	0.324 ±0.022
	0.070	-0.300	-0.577	-0.502	-0.475	0.647	0.507 ±0.025	1.44	0.352 ±0.018
	0.100	-0.300	-0.595	-0.520	-0.497	0.721	0.359 ±0.046	1.03	0.348 ±0.348

Table 5-1: Computed rate of reaction (K_f) using different scan rates for $Cr(bipy)_3$ at 23 and 25°C

a. determined at 23°C

b. determined at 25°C

* measured Vs. SCE saturated KCl

obtained from a minimum of four determinations. The bulk of the data is tabulated in Appendix C-5. Averaging all the rates of reaction (K_f) at all the scan rates yielded the final values for $Cr(bipy)_3$:

$K_f = 0.293 \pm 0.022$ sec^{-1} at 23°C

$K_f = 0.343 \pm 0.028$ sec^{-1} at 25°C

The relatively high values for the standard deviations are due to the fact that the reproducibility of the polarographic (CV) determinations was within ±10%, a range which has also been reported by other workers (48). In addition, no attempts were made to reject high or low values, since in principle one should be able to estimate K_f from a single polarogram--for example, from the polarogram in Figure 5-9, i_a/i_c = 0.613. From this ratio one obtains from the working curve $K_f \tau = 0.594$. The elapsed time is then

$$\tau = \frac{E_{1/2} - E_{sw}}{\text{SCAN RATE}} = \frac{-0.475V-(-0.575V)}{0.05V/Sec} = 2.00 \text{ sec.}$$

$$\text{Hence } K_f = \frac{K_f \tau}{\tau} = \frac{0.594}{2.000} = 0.297 \text{ sec.}^{-1}$$

The results obtained at 25°C, pH 3.5, are in reasonable agreement with reported results, K_f = 0.38 sec.$^{-1}$, obtained by other polarographic techniques and by direct chemical methods (48,56). The 10% difference between the results obtained in this experiment and the reported values could be attributed to differences in

pH. The pH, however, was not specified in the literature.

On the other hand, the value of 0.293 sec^{-1} obtained at 23°C and pH 3.5 was in total disagreement with 0.108 sec^{-1} at pH 5 reported by Soignet and Hargis (54) and obtained by the same CV technique. Such a large difference in K_f values could not be attributed to differences in pH (48). A close examination of the data presented by Soignet revealed the reason for at least part of the observed difference in K_f. In his computation he estimates $E_{1/2}$ by simply multiplying the peak potential by 0.8517 (85.17%). This kind of "short-cut" yields a correct value only when the slope of the cathodic peak begins to rise at zero volts; in all other cases this would lead to a divergence in obtained values. This is especially significant when one wishes to compare two or more similar species with cathodic peaks at different potential as Soignet and Hargis did (54,56) and as this experimental work will essay for $Cr(bipy)_3$ and $Cr(me_2\text{-}bipy)_3$.

The balance of the difference in the K_f values is probably due to the different treatment given to the residual currents. The effects of capacitance currents are not mentioned in their paper, but neither do they show pictures of pertinent polarograms.

5.3.4 Results: $Cr(me_2\text{-}bipy)_3$

The aqueous behaviour of $Cr(me_2\text{-}bipy)_3$ is similar to that of $Cr(bipy)_3$ as described in Section 5.1.1. Hence the reactions of interest are

$$[Cr(me_2\text{-}bipy)_3]^{+3} + e^- \rightleftharpoons [Cr(me_2\text{-}bipy)_3]^{+2} \quad (5\text{-}9)$$

$$[Cr(me_2\text{-}bipy)_3]^{+2} + 2H_2O \overset{K_f}{\rightleftharpoons}$$

$$[Cr(me_2\text{-}bipy)_2(H_2O)_2]^{+2} + bipy \quad (5\text{-}10)$$

Here again, the aim is to determine the rate of reaction/dissociation (K_f) in an electrochemical process where a reversible electron transfer is followed by an irreversible chemical process.

All the determinations were obtained at room temperature (25°C) and, for comparison purposes, all analyte solutions were adjusted to pH 3.5. Potentials were measured versus SCE.

The results obtained from duplicate samples at various scan rates are summarized in Table 5-2. The tabulated K_f values represent an average of a minimum of four determinations. The bulk of the data is listed in Appendix C-6. Averaging the K_f values obtained at all scan rates yielded, for $5.5X10^{-5}$ M $Cr(me_2\text{-}bipy)_3$ in 0.1M KCl:

$K_f = 0.353 \pm 0.032$ sec^{-1} at 25° C

scan rate (V/S)	E_{start} (V.)	E_{switch} (V.)	cathodic peak (V.)	$E^{*}_{1/2}$ (V.)	i_a/i_c	$K_f\tau$	τ (sec.)	$K_f \pm \sigma$ ($sec.^{-1}$)
0.040	-0.450	-0.745	-0.665	-0.645	0.533	0.846 ±0.040	2.50	0.339 ±0.015
0.060	-0.450	-0.745	-0.670	-0.642	0.599	0.637 ±0.048	1.80	0.355 ±0.027
0.080	-0.450 -0.500	-0.755	-0.677	-0.652	0.673	0.452 ±0.061	1.30	0.349 ±0.046
0.100	-0.450 -0.500	-0.755 -0.760	-0.680	-0.653	0.708	0.379 ±0.018	1.05	0.363 ±0.023

Table 5-2: Computed rate of reaction (K_f) using different scan rates for $Cr(me_2\text{-bipy})_3$ at 25°C

* measured Vs. SCE saturated KCl

This is in excellent agreement with the results obtained for $Cr(bipy)_3$.

The rate of reaction, K_f, was also determined at a variety of temperatures as summarized in Table 5-3. All the presented values were determined at 0.1 V/sec and are an average of 4 determinations. An Arrhenius plot of these rate constants was performed ($\log K_f$ vs. $\frac{1}{T}$) and the least-squares line through the points showed a correlation coefficient of 0.986. From the slope of the plot an activation energy, E_a, of 18.4 Kcal was calculated using the relation:

$$\log K = \log A - \frac{E_a}{2.303RT}$$

where: log A = plot intercept

R = gas constant

T = temperature in ^oK

The energy of activation obtained here (18.4 Kcal) is somewhat lower than reported values for similar complexes, where the range is 20 to 26 Kcal (48, 54, 56, 57). However, this kind of comparison is not very meaningful since, like K_f, E_a varies with pH and other experimental parameters, such as excess ligand, in this determination.

Finally, Figure 5-10 demonstrates the transitions in the polarographic (CV) peaks as a function of temperature. It should be noted that, in these cases, K_f is affected not only by changes in the i_a/i_c ratios

Temp.	scan rate (V/S)	E_{start} (V.)	E_{switch} (V.)	cathodic peak (V.)	$E_{1/2}^{*}$ (V.)	i_a/i_c	$K_f \tau$	τ (sec.)	$K_f \pm \sigma$ ($sec.^{-1}$)
22°C	0.100	-0.500	-0.760	-0.683	-0.655	0.781	0.264	1.05	0.251 ±0.004
25°C	(see Table 5-2 for pertinent data at this temperature)				-0.653				0.353 ±0.032
29°C	0.100	-0.500	-0.750	-0.675	-0.650	0.593	0.644	1.02	0.638 ±0.035
32.5°C	0.100	-0.500	-0.745	-0.674	-0.650	0.578	0.689	0.95	0.723 ±0.056
35°C	0.100	-0.500	-0.735	-0.657	-0.633	0.500	0.976	1.02	0.957 ±0.016

Table 5-3: Variation of K_f with temperature; 5.5×10^{-5}M $[Cr(me_2\text{-bipy})_3]^{+3}$ in 0.1M KCl.
* measured Vs. SCE saturated KCl

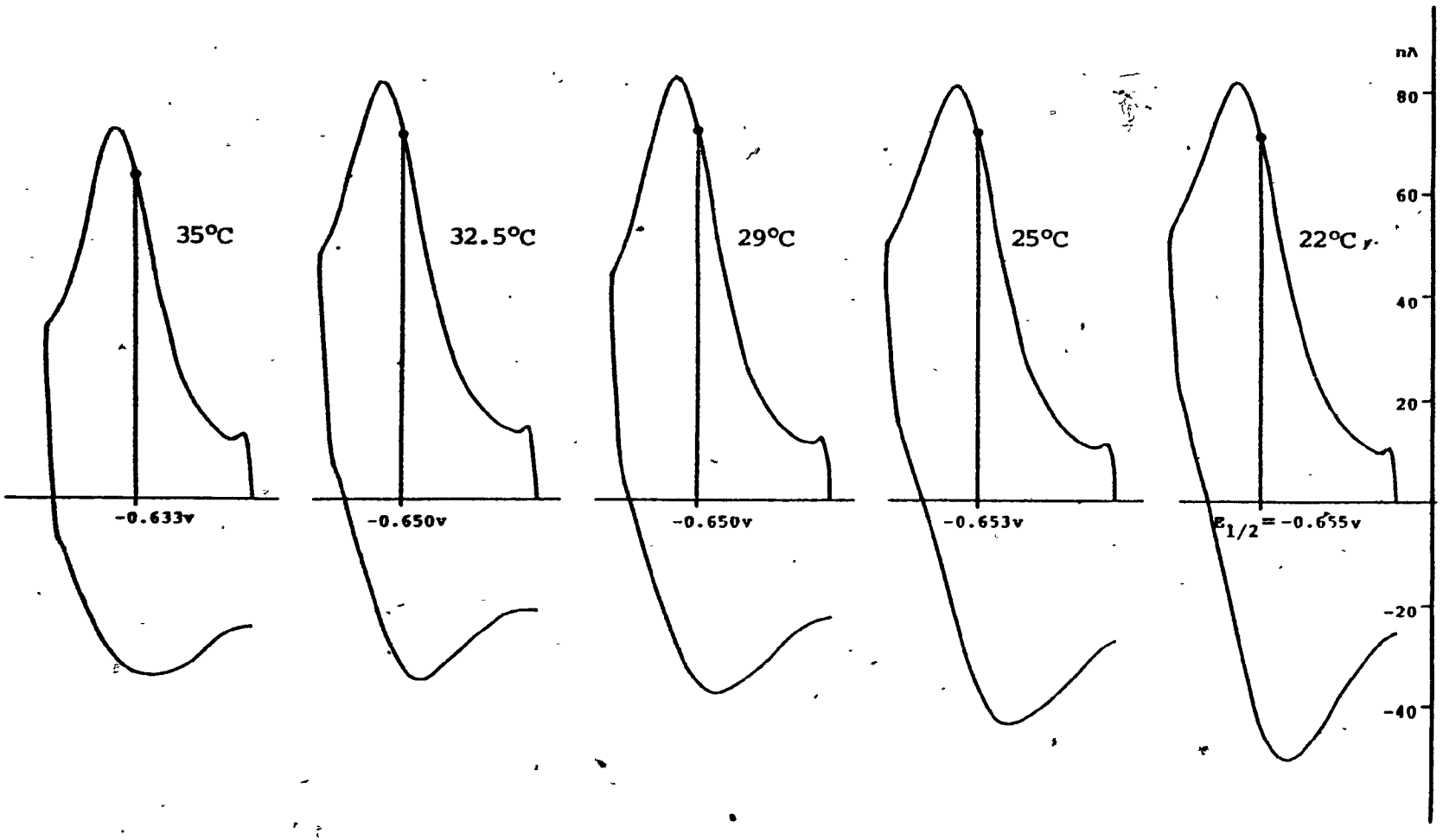

Figure 5-10: CV polarograms of aqueous $[Cr(me_2\text{-bipy})_3]^{+3}$; redox behavior as a function of temperature.

but also by the anodic shift of $E_{1/2}$ with the increase in temperature, as can be seen in Table 5-3.

5.4 Conclusions

The CV technique described in this chapter is commonly used for fast estimations of reaction rates. However, this chapter demonstrates the importance of fully understanding the technique. Parameters such as residual currents and half-wave potentials should be taken into account and properly evaluated.

The semiempirical method developed in this experiment for the true evaluation of i_a/i_c has proven to be reasonably reliable, as can be deduced from the fact that the results (K_f) at the various scan rates did not diverge.

The merits of CV as a general tool were again demonstrated since, in addition to estimating K_f, it also gave a clear picture of the overall electrochemical process and indicated possible trouble spots such as peaks due to intermediate reactions. Moreover, taking into account the complexity of the evaluating method and the fact that the determinations were carried out over several weeks (using the same samples), the technique produced excellent results. Reproducibility of results, both within and between samples, was always within $\pm$10%. This gave an overall average of $\pm$7%, which is equal or

better than reported literature values (48, 54).

CHAPTER 6

GENERAL CONCLUSIONS, INSTRUMENT EVALUATION, AND SUGGESTIONS FOR FUTURE RESEARCH

6.1 Conclusions

Throughout all the experimental phases, the cyclic voltammetry technique has proven to be a powerful tool in the study of electrode kinetics. From the simple rate evaluation of Cd and Zn to the complex behaviour of aqueous chromium complexes, data was always easily reproducible. Furthermore, the work carried out here indicates that in many instances CV could be self-sufficient and provide all the needed electrochemical data for a given species.

The results obtained in Chapter 3 and particularly these of Chapter 4 were the foundation for the work in Chapter 5. These preliminary approaches provided proper methods for the evaluation of the pertinent parameters, such as half-wave potential and current behaviour at switching potential. Consequently, the semiempirical method developed in Chapter 5 has proven to be reliable; it produced K_f values for $Cr(bipy)_3$ (Table 5-1) which were in good

agreement with the literature results.

Based on the above, the results listed in Table 5-2 for the original work on the rate of reaction (K_f) of aqueous $Cr(me_2\text{-bipy})_3$ can be considered as highly reliable.

6.2 Instrument Evaluation

Both the polarograph and the signal generator used in these experiments demonstrated a high degree of linearity, good signal-to-noise ratio and good reproducibility. The small variations in current magnitude (i.e., peak heights) that were observed were due mainly to the variations in the size of the HMDE. This, however, did not influence the results, since the computations were based on peak current ratios. In cases where absolute peak values are needed, the problem can be easily rectified by using automatic, electronically controlled hanging mercury drop electrodes which are commercially available (Metrohm).

6.3 Suggestions for Instrumental Modifications and Improvements

The problems arising from charging currents were reported to be reduced to a negligible level in more advanced CV instruments (58, 59, 60). These systems employ small-amplitude square-wave pulses or an AC wave superimposed on the CV potential ramp and are

synchronized by digital computers to yield optimum results. In such cases Nicholson's simple technique for peak ratio evaluation can and should be used. Hence, it would be very profitable to integrate the various pulse techniques of the multifunction polarograph (E-506) with the CV technique. This could yield a CV instrument with a sensitivity comparable to DPP, both in terms of minimization of residual current effects and of peak definitions.

The existing controls for scan-rate on the function generator (E-612) are graduated so that only multiples of 0.001, 0.01, 0.1, 1.0 and 10 V/sec. can be set accurately. Consequently, one cannot set a scan-rate of 0.15 V/sec or 1.5 V/sec etc. without external calibration. This problem can and should be rectified by the addition of a potentiometer and/or larger dials with subdivision graduations.

Finally, as is the case with most commercially available function generators, the Metrohm E-612 has only two controls that govern the triangular potential wave; one sets the start and finish potential and the other controls the amplitude. It would be an asset to have two separate controls for start and finish. This would facilitate the study of complex reaction mechanisms, since, for example, one could start a CV scan at a potential past a particular reduction value

and then continue cathodically. However, on the returning anodic portion of the sweep, one could set the finish point so that the oxidation process for the above reduction could be recorded.

6.4 Suggestion for Future Research Work

From the conclusions drawn in this thesis, as well as from the work of other researchers, the scope and range of application of CV is obvious. The following suggestions are based only on observations and data collected by the author using CV and other techniques.

6.4.1 Charging current in cyclic voltammetry

Unlike other polarographic techniques, the effects of charging current (i_c) in CV are compounded. To start with, as can be seen from Equation 2-5, i_c is proportional to the scan rate. Hence, in all rapid sweep techniques, the magnitude of i_c is not insignificant. In addition, in CV work, one is confronted with three versions of i_c. The first occurs at the beginning of the sweep and is similar to that for all other voltammetric techniques. The second occurs at the point of potential switch-over (E_{sw}). Finally, the discharge occurs at the end of the cycle. Due to the cyclic nature of the potential sweep, total charge is equal to total discharge. This, however,

does not shed much light on the behaviour of i_c at E_{sw}. Consequently, most workers by-pass the problem of i_c by creating empirical methods or by the use of sophisticated equipment. Hence, the author suggests a mathematical investigation of the relationships between the charging currents, how they are influenced by E_{sw}, and their effect on the location of the baseline for the returning portion of the sweep.

6.4.2 Comparison of techniques: CV vs. Kalousek

Kalousek polarography (61) is a variation of square-wave and pulse techniques. Here the recorded current results in part from the oxidation of the reduced species produced at the working electrode. Thus, the technique enables investigation of reversibility to be carried out in one sweep (non-cyclic). In addition, it is possible to determine the rate constants of electron transfers, the number of transferred electrons and, to some extent, the life periods of intermediate species generated at the electrodes (62-67).

A comparison between CV and Kalousek would basically evaluate the advantages and disadvantages of the rapid-sweep and slow-sweep techniques used in electrochemical kinetics studies.

6.4.3 +IV oxidation state of chromium-polypyridyl complexes

The preliminary investigation of the non-aqueous behaviour of chromium complexes (Chapter 4) also included some anodic (oxidation) scans. In these runs several electrolyte solutions and a variety of electrodes were tried in order to establish the best combination that would allow scans to greater than +2.0 volts. The solutions that were examined were acetonitrile and DMSO with either $TEABF_4$ or TEAP depolarizer. The working electrodes that were tried were platinum, carbon paste and glassy carbon. The best results were obtained using 0.1M TEAP in acetonitrile with a platinum auxillary, platinum working electrode and Ag/AgCl (double junction) reference. This combination provided a positive scan range of +2.65 volts.

The polarograms in Figure 6-1 show a run of the supporting electrolyte and a scan of 1.694 mM $Cr(terpy)_2^{+3}$. The anodic peak at +2.28 volts (denoted X) might be due to $Cr(terpy)_2^{+4}$. Although there is a hint of a cathodic peak for this transition, the reversibility of this reaction is not clear. Dr. N. Serpone of Concordia University also suggested that the anodic peak might be due to deterioration of excess perchlorate. The author feels that further investigation of this scan range could yield some interesting and important results.

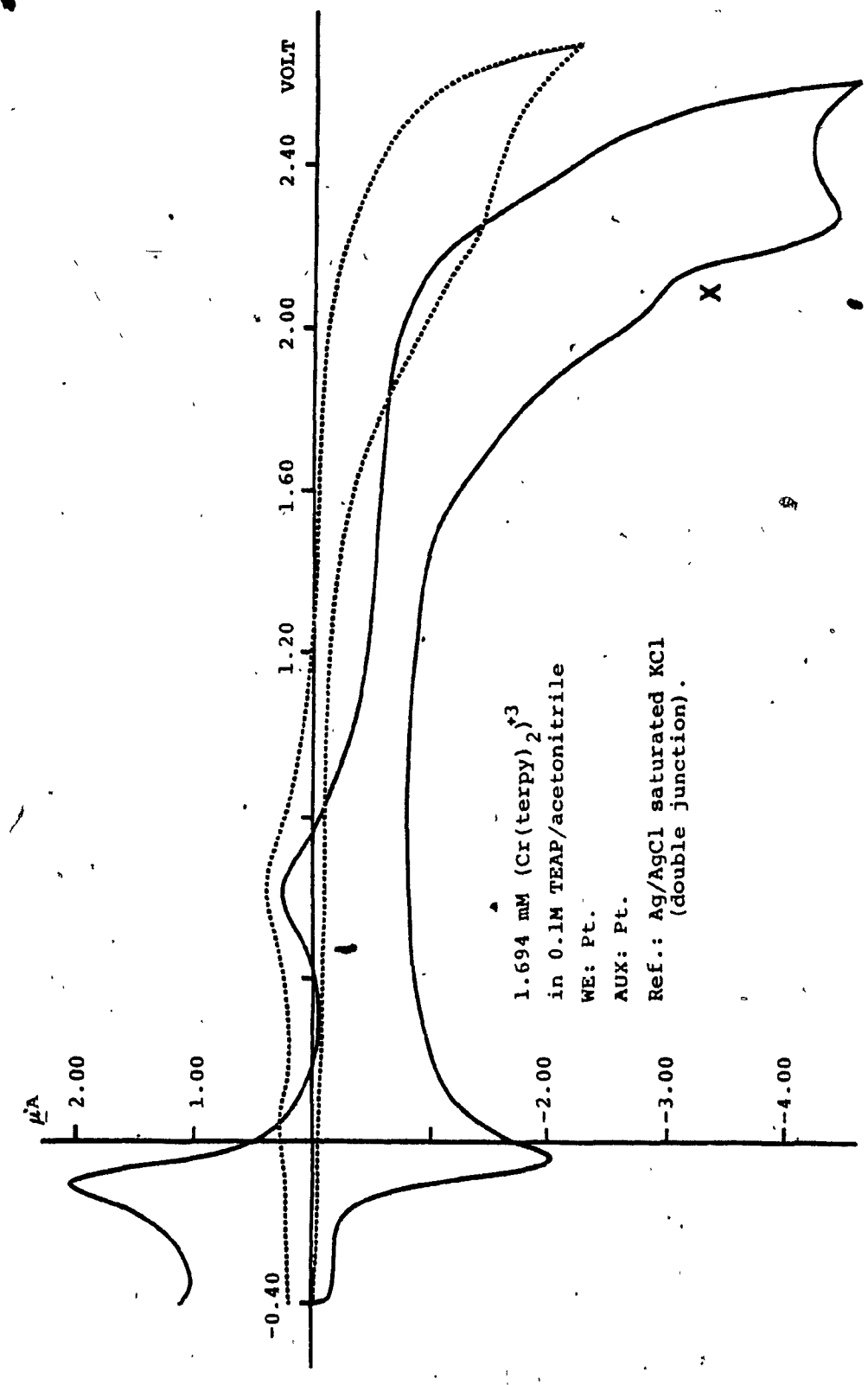

Figure 6-1: Anodic scan of $(Cr(terpy)_2)^{3}$; possible +IV oxidation state.

REFERENCES

1. Davison, W., J. Electroanal. Chem., 87, 395 (1978).
2. Batley, G. E., & Florence, T. M., J. Electroanal. Chem., 55, 23 (1978).
3. Cheng, H. Y., Schnk, J., Huff, R., & Adams, R. N., J. Electroanal. Chem., 100, 23 (1979).
4. Lane, R. F., Hubbard, A. T., & Blaha, C. D., Bioelectrochem. and Bioenergetics, 5, 504 (1978).
5. Adams, R. N., Electrochemistry at Solid Electrods, Chapter 5, Marcel Dekker, Inc., N. Y. (1969).
6. Andrieux, C. P., Blocman, C., Dumas-Bouchiat, J. M., M'Halla, F., & Saveant, J. M., J. Electroanal. Chem., 113(1), 19 (1980).
7. Ibid, 113(1), 1 (1980).
8. Heyrovsky, J., Principles of Polarography, Academic Press, N. Y. (1965).
9. Dick, J. G., Analytical Chemistry, McGraw-Hill Inc., N. Y. (1973).
10. Meites, L., Polarographic Techniques, Interscience, N. Y. (1967).
11. Delahay, P., New Instrumental Methods in Electrochemistry, Interscience, N. Y. (1954).
12. Adams, R. N., Electrochemistry at Solid Electrods,

Marcel Dekker Inc., N. Y. (1969).

13. Heyrovsky, J., Chem. Listy, 16, 256 (1922).
14. Ilkovic, D., J. Chim. Phys., 35, 129 (1938).
15. Flato, J. B., Anal. Chem., 44(1), 75A (1972).
16. Barker, G. C., & Gardner, A. W., Z. Anal. Chem., 173, 9 (1960).
17. Randle, J. B., Trans. Faraday Soc., 44, 327 (1948).
18. Sevcik, A., Collection Czech. Chem. Comm., 13, 349 (1948).
19. Matsuda, H., & Ayabe, Y., Z. Elektrochem., 59, 494 (1955).
20. Mueller, T., & Adams, R. N., Anal. Chim. Acta, 35, 482 (1961).
21. Nicholson, R. S., & Shain, I., Anal. Chem., 36, 706 (1964).
22. Nicholson, R. S., & Shain, I., Anal. Chem., 37, 178 (1965).
23. Nicholson, R. S., Anal. Chem., 37(11), 1351 (1965).
24. Okinaka, Y., Talanta, Vol. 11, 203 (1964).
25. Tanaka, N., & Tamamushi, R., Electrochem. Acta, 9, 963 (1965).
26. Floyd, H., Electrochem. Acta, 9, 963 (1964).
27. Matsuda, H., Z. Electrochem., 61, 489 (1957).
28. Nicholson, R. S., & Shain, I., Anal. Chem., 38, 1406 (1960).
29. Barker, G. C., Anal. Chem. Acta, 18, 118, (1958).

30. Heyrovsky, J., & Kuta, J., Principles of Polarography, Academic Press, N. Y. (1966), p. 216.

31. Diaz, A. F., & Kanazawa, K. K., J. Electroanal. Chem., 103, 233 (1979).

32. Klingler, R. J., & Kochi, J. K., J. Phys. Chem., 85, 1731 (1981).

33. Olmstead, M. L., & Nicholson, R. S., Anal. Chem., 38, 150 (1966).

34. Hawley, D., & Adams, R. N., J. Electroanal. Chem., 10, 376 (1965).

35. Nelson, R., Seo, E. T., Leedy, D., & Adams, R. N., Z. Anal. Chem., 224, 184 (1967).

36. Schwarz, W. M., & Shain, I., J. Phys. Chem., 70, 845 (1966).

37. Hughes, M. C., & Macero, D. J., Inorg. Chem., 15, 2040 (1976).

38. Rao, J. M., Hughes, M. C., & Macero, D. J., Inorganica Chimica Acta, 28, 237 (1976).

39. Millefiori, S., J. Hetrocycl. Chem., 7, 149 (1970).

40. Tabner, B. J., & Yandle, J. R., J. Chem. Soc., A, 381 (1968).

41. Given, P. H., & Peover, M. E., J. Chem. Soc., 385 (1960).

42. Coetzee, J. F., Cunningham, G. P., McGuire, D. K., & Padmanabhan, G. R., Anal. Chem., 34, 1139 (1962).

43. Ferrett, D. J., Trans. Faraday Soc., 52, 390

(1955).

44. Marple, T. L., & Rogers, L. B., Anal. Chem., 25, 1351 (1953).

45. Tsukamoto, T., Proc 1st Inter. Polarog. Congr., Prague, 1951, pp. 524-541.

46. Larson, R. C., Anal. Chim. Acta, 25, 371 (1961).

47. Vlcek, A. A., Nature, 189, 393 (1961).

48. Baker, B. R., & Mehta, D., Inorg. Chem., 4, 848 (1965).

49. Tucker, B. V., Fitzgerald, J. M., Hargis, L. G., & Rogers, L. B., J. Electroanal. Chem., 13, 400 (1967).

50. Spell, E. J., Anal. Chem., 51(13), 2287 (1979).

51. Olmstead, M. L., Anal. Chem., 41, 862 (1969).

52. Vydra, F., Stulik, K., & Julakova, E., Electrochemical Stripping Analysis, J. Wiley & Sons, N.Y. 1976.

53. Copelad, T. R., & Skogerboe, E., Anal. Chem., 46 (14), 1257 (1974).

54. Soignet, D. M., & Hargis, L. G., Inorg. Chem., 11 (10), 2349 (1972).

55. Candlin, J. P., Halpern, J., & Trimm, D. L., J. Am. Chem. Soc., 85, 1019 (1964).

56. Basolo, F., Hayes, J. C., & Neumann, H. M., J. Am. Chem. Soc., 75, 5102 (1953).

57. Wilkins, R. G., & Ellis, P., J. Am. Chem. Soc., 299

(1959).

58. Blutstein, H., & Bond, A. M., Anal. Chem., 46, 1934 (1974).

59. McDonald, D. D., J. Electrochem. Soc., 125, 1443 (1978).

60. Creason, S. C., Loyd, R. J., & Smith, D. E., Anal. Chem., 44, 1159 (1972).

61. Kalousek, M., Collection Chem. Comm. (Czech.), 13, 105 (1948).

62. Koutecky, J., Chem. Listy, 49, 1454 (1955).

63. Kinard, W. F., Philp, R. H., & Propst, R. C., Anal. Chem., 39, 1556 (1967).

64. Matsuda, H., Z. Electrochem., 62, 977 (1958).

65. Ruzic, I., J. Electroanal. Chem., 39, 111 (1972).

66. Opekar, F., J. Electroanal. Chem., 85, 207 (1977).

67. Weber, J., Chem. Listy, 52, 1888 (1958).

68. Seto, S., Master's Thesis, Concordia University (1981).

69. Schwarz, W. M., & Shain, I., J. Phys. Chem. 70, 845 (1966).

APPENDIX A

A-1 Preparation of Supporting Electrolye and Analyte Solutions; Cadmium and Zinc

Since this thesis is not concerned with analytical limits of detection or with the effects of concentration gradiants, the preparation of analyte solutions was a straightforward task (i.e. accurately measured, without standarization).

Sodium sulfate (Fisher Scientific A. G.)

1M Na_2SO_4: 142.02 g Na_2SO_4 dissolved and diluted to one liter in glass distilled H_2O

Potassium chloride (Fisher Scientific A. G.)

1M KCl: 74.56 g KCl/1000 ml H_2O (glass distilled)

$2X10^{-4}M$ Cd^{+2}/1M Na_2SO_4

0.0104 g $CdSO_4$ (M.W. = 208.46)/250m. 1M $NaSo_4$

$3X10^{-4}M$ Zn^{+2}/1M KCl

2 ml of 1000 ppm Zn^{+2} solution diluted to 10 ml using 1M KCl

A-2 Working Curve of $n\Delta E_p$ vs Ψ

The working curve shown in Figure 3-1 was constructed as per Nicholson's (58) tabulated values listed below. For practical purposes however, the Ψ values were obtained by the use of a curve fitting computer program.

$n\Delta E_p$	Ψ
20.00	61
7.00	63
6.00	64
5.00	65
4.00	66
3.00	68
2.00	72
1.00	84
0.75	92
0.50	105
0.35	121
0.25	141
0.10	212

A-3 Standard Rate of Reaction (K_s) Data for the Reduction of Cadmium

The K_s values obtained by single-cycle CV for both samples of cadmium are recorded in Table

A-1. Values for peak separation were measured from the screen of the storage oscilloscope (pictures are not available). The corresponding values were then determined from the working curve in A-2, and K_s was computed using Equation 3-4.

In the case of multicycle CV, peak separations were measured from polarograms recorded on polaroid film. The computed K_s values from this technique are listed in Table A-2.

A-4 Standard Rate of Reaction (K_s) Data for the Reduction of Zinc

The results for zinc are listed in Table A-3. The tabulated values at each scan rate represent an average of results obtained from two determinations (polarograms).

SCAN RATE (V/s)	$n\Delta E_p$ (mV)	Ψ	K_s (cm/sec)	
40	90	0.800	0.24	
40	90	0.800	0.24	
40	91	0.770	0.23	
40	91.5	0.760	0.23	
60	96	0.655	0.24	
60	98	0.620	0.23	
60	96	0.655	0.24	
60	99	0.600	0.22	
80	108	0.465	0.20	SAMPLE 1
80	108	0.465	0.20	
80	108	0.465	0.20	
80	109	0.455	0.20	
100	114	0.405	0.20	
100	112	0.425	0.20	
100	113	0.415	0.20	
100	114	0.405	0.20	
40	91	0.770	0.23	
40	91	0.770	0.23	
40	91.5	0.760	0.23	
40	91	0.770	0.23	
60	97	0.635	0.24	
60	98	0.620	0.23	
60	98	0.620	0.23	
60	98	0.620	0.23	
80	106	0.485	0.21	SAMPLE 2
80	105	0.500	0.22	
80	106	0.485	0.21	
80	106	0.485	0.21	
100	114	0.405	0.19	
100	116	0.390	0.19	
100	114	0.405	0.19	
100	115	0.400	0.19	

TABLE A-1: Computed K_s Values for the Reduction of Cd^{+2} at 23°C Using Single-Cycle CV

FRAME	SCAN RATE (V/s)	$n\Delta E_p$ (mV)	Ψ	K_s (cm/sec)	
1	40	94	0.700	0.21	
2	60	100	0.580	0.22	SAMPLE 1
3	80	106	0.485	0.21	
4	100	126	0.325	0.16	
1	40	92	0.750	0.23	
2	60	96	0.655	0.24	SAMPLE 2
3	80	112	0.425	0.18	
4	100	120	0.360	0.17	

TABLE A-2: Computed K_s Values for the Reduction of Cd^{+2} at 23°C Using Multicycle CV.

SCAN RATE (mV/5)	$n\Delta E_p$ (mV)	Ψ	$K_s x10^{-3}$ (cm/sec)	
10	89.5	0.810	3.8	
20	100.0	0.585	3.8	
30	104.0	0.515	4.1	
40	109.0	0.455	4.2	
50	114.0	0.405	4.2	
60	116.3	0.385	4.4	SAMPLE 1
70	121.3	0.350	4.3	
80	128.8	0.305	4.0	
90	131.3	0.295	4.1	
100	133.8	0.285	4.2	
150	148.8	0.223	4.0	
200	157.5	0.185	3.8	
10	91.3	0.760	3.5	
20	98.8	0.470	4.1	
30	107.5	0.470	3.8	
40	110.0	0.455	4.2	
50	116.3	0.385	4.0	
60	117.5	0.375	4.3	SAMPLE 2
70	121.3	0.350	4.3	
80	130.0	0.300	3.9	
90	130.0	0.300	4.2	
100	132.5	0.287	4.2	
150	147.5	0.225	4.0	
200	157.5	0.185	3.8	

TABLE A-3: Computed K_s Values for the Reduction of Zn^{+2} at 24°C pH 2, Using single cycle CV.

APPENDIX B

B-1 Preparation of Supporting Electrolye: 0.1M Tetraethyleamonium-tetrafluoroborate in Acetonitrile

Acetonitril; Eastman spectrograde (99.+%). $TEABF_4$; Alfa products, M.W. = 217.06g/M.

Other than being kept dry by the use of zeolyte (molecular sieve), the acetonitrile was used as received. Prior to use, the zeolyte was dried at 80° to 90° C under vacuum for 48 hours. The zeolyte treatment was found to be very useful, since it absorbed all the moisture (H_2O) without adding any electrochemical interferences.

$TEABF_4$ was also used as received. Initial sample preparation indicated that recrystallization was unnecessary. However again, in order to eliminate water problems, the crystals were dried for 24 hours at 50° C under vacuum prior to use.

The 0.1M $TEABF_4$/acetonitrile was prepared in 5 aliquots by dissolving 4.341 g $TEABF_4$ and diluting to 200 ml.

B-2 Chromium Complexes: Preparation of Analyte Solutions

Prior to use, all complexes were dried at 70° C in vacuum. Due to rapid deterioration of sample solutions, the analytes were prepared in small quantities according to need. Hence, the preparation of analytes (sample solution) was a straightforward process.

$Cr(bipy)_3$

$[Cr(2,2'\text{-bipyridine})_3](ClO_4)_3 \cdot \frac{1}{2}H_2O$

M.W. = 827.840 g/M

Sample 1: (0.01355 g complex in 20 ml 0.1M $TEABF_4$/acetonitrile) = 0.8153 mM $Cr(bipy)_3^{+3}$;

Sample 2: (0.01350 g complex in 20 ml 0.1M $TEABF_4$/acetonitrile) = 0.8153 mM $Cr(bipy)_3^{+3}$.

Sample 3: (0.01360 g complex in 20 ml 0.1M $TEABF_4$/acetonitrile) = 0.8214 mM $Cr(bipy)_3^{+3}$.

$Cr(terpy)_2$

$[Cr(2,2',2''\text{-terpyridine})_2](ClO_4)_3 \cdot 2\frac{1}{2}H_2O$

M.W. = 861.9298 g/M

Sample 1: (0.0180 g complex in 25 ml 0.1M $TEABF_4$/ acetonitrile) = 0.8353 mM $Cr(terpy)_2^{+3}$.

Sample 2: (0.91802 g complex in 25 ml 0.1M $TEABF_4$/ acetonitrile) = 0.8353 mM $Cr(terpy)_{2+3}$

Sample 3: (0.0155 g complex in 25 ml 0.1M $TEABF_4$/ acetonitrile) = 0.7193 mM $Cr(terpy)_2^{+3}$

$\underline{Cr(me_2\text{-}bipy)_3}$

$[Cr(4,4'\text{-dimethyl-}2,2'\text{-bipyridine})_3](ClO_4)_3 \cdot H_2O$

M.W. = 921.084 g/M

Sample 1: (0.0146 g complex in 20 ml 0.1M $TEABF_4$/ acetonitrile) = 0.7925 mM $Cr(me_2\text{-}bipy)_3^{+3}$

Sample 2: (0.14603 g complex)/20 ml

= 0.7926 mM $Cr(me_2bipy)_3^{+3}$

Sample 3: (0.01430 g complex/20 ml

= 0.7708 mM $Cr(me_2\text{-}bipy)_3^{+3}$

$\underline{Cr(ph_2\text{-}bipy)_3}$

$[Cr(4,4'diphenyl-2,2'-bipyridine)_3](ClO_4)_3 \cdot 2H_2O$

M.W. = 1311.524 g/M

Sample 1: (0.02050 g complex in 25 ml 0.1M $TEABF_4$/ acetonitrile) = 0.6250 mM $Cr(ph_2\text{-bipy})_3^{+3}$

Sample 2: (0.0210 g complex/25 ml = 0.6404 mM $Cr(ph_2\text{-bipy}_3)^{+3}$

B-3 Instrumental Settings for the Analysis of Chromium Complexes in Acetonitrile

$Cr(bipy)_3$

Sample 1

E612 (function generator):	E506 (polarography):
U(E start) = 0.000 volts	Mode = D.C.
ΔU(E switch) = 1.600 volts	U = 0.00 volts
Scan; isosceles triangle	ΔU = 2.00 volts
Scan rate = 0.10 volt/sec	mm/t_{drop} = 2, t_{drop} = 6 sec.
	Sens. = $1.5X10^{-8}$ Amp./mm

X-Y Recorder: X = 0.1 V/cm

Y = 0.1 V/cm = 0.255 μA/cm*

*The values for the current axis (Y) were

obtained by measuring the deflection in mm. or cm. along the Y-axis of the oscilloscope or X-Y recorder resulting from rotating the current compensation potentiometer on the E506 a fixed number of units and is given by the following:

$$i(\text{Y-axis}) = \frac{[I_{comp.}(\text{dev.})][F_{pot.}(\text{mm/dev.})][\text{Sens.(A/mm)}]}{[\text{deflection (mm)}]}$$

where $F_{pot.}$ = potentiometer factor = 1.056 mm/dev.

Sample 2

Same as Sample 1, but with an expanded voltage axis, i.e.

X-Y Recorder: X = 0.05 V/cm

Y = 0.1 V/ch = 0.255 μA/cm.

Sample 3

E612:	E506:
U = 0.00 V	D.C.
ΔU = -2.05 V	U = 0.00 V, ΔU = -2.5 V
Scan: isosceles triangle	mm/t_{drop} = 2, t_{drop} = 6 s
Scan rate: 0.10 V/S	A/mm = $4X10^{-8}$ A/mm

X-Y Recorder: X = 0.1 V/cm

Y = 0.1 V/cm = 0.684 μA/cm

<u>Cr(terpy)$_2$</u>

Sample 1

E612:

U = +0.20 V

ΔU = -1.40 V

Scan = isosceles triangle

Scan rate = 0.10 V/S

X-Y Recorder: X = 0.1 V/cm

Y = 0.1 & 0.05 V/cm = 0.426 & 0.340 μA/cm

E506:

D.C.

U = 0.00 V, ΔU = -2.00

mm/t_{drop} = 2, t_{drop} = 6_s

A/mm = 2.5 & $4X10^{-8}$ A/mm

Sample 2

E612:

U = +0.15 V

ΔU = -1.40 V

Scan: isosceles triangle

Scan rate: 0.10 V/sec

X-Y Recorder: X = 0.1 V/cm

Y = 0.05 V/cm = 0.3408 μA/cm

E506:

D.C.

U = 0.00 V, ΔU = -2.00

mm/t_{drop} = 2, t_{drop} = 6_s

A/mm = $4X10^{-8}$ A/mm

Sample 3

E612:

U = +0.095 V

ΔU = -2.05 V

Scan = isosceles triangle

Scan rate = 0.10 V/sec

X-Y Recorder: X = 0.1 V/cm

Y = 0.1 V/cm = 4.255 μA/cm

E506;

D.C.

U = 0.00 V, ΔU = -2.00

mm/t_{drop} = 2, t_{drop} = 6_s

A/mm = $2.5X10^{-8}$ A/mm

$\underline{Cr(me_2\text{-}bipy)_3}$

Sample 1

E612:	E506:
U = 0.00 V	D.C.
ΔU = -1.85 V	U = 0.00 V, ΔU = -2.00
Scan = isosceles triangle	mm/t_{drop} = 2, t_{drop} = 6s
Scan rate = 0.1 V/sec	A/mm = $1.5X10^{-8}$ A/mm

X-Y Recorder: X = 0.05 V/cm

Y = 0.1 V/cm = 0.255 μA/cm

Sample 2

E612:	E506:
U = 0.00 V	D.C.
ΔU = -1.90 V	U = 0.00 V, ΔU = -2.00
Scan = isosceles triangle	mm/t_{drop} = 2, t_{drop} = 6s
Scan rate = 0.10 V/S	A/mm = $1.5X10^{-8}$ A/mm

X-Y Recorder: X = 0.1 V/cm

Y = 0.1 V/cm = 0.4255 μA/cm

Sample 3

E612:	E506:
U = -0.10 V	D.C.
ΔU = -1.90 V & -2.10	U = 0.00 V, ΔU = -2.00
Scan = isosceles triangle	mm/t_{drop} = 2, t_{drop} = 6s
Scan rate = 0.10 V/sec	A/mm = $2.5X10^{-8}$ A/mm

X-Y Recorder: X = 0.1 V/cm

Y = 0.1 V/cm = 0.4255 μA/cm

$\underline{Cr(PH_2\text{-bipy})_3}$

Sample 1

E612:

U = -0.05 V

ΔU = -1.90 V

Scan = isosceles triangle

Scan rate = 0.10 V/S

E506:

D.C.

U = 0.00 V, ΔU = -2.00

$mm/t_{drop} = 2$ $t_{drop} = 6_s$

$A/mm = 1X10^{-8}$ & $1.5X10^{-8}$ A/mm

X-Y Recorder: X = 0.1 V/cm

Y = 0.1 V/cm = 0.1702 & 0.2553 μA/cm

Sample 2

E612:

U = 0.00 V

ΔU = -1.6 V

Scan = isosceles triangle

Scan rate = 0.10 V/S

E506:

D.C.

U = 0.00 V, ΔU = -2.00

$mm/t_{drop} = 2$, $t_{drop} = 6_s$

$A/mm = 1X10^{-8}$ A/mm

$2.5X10^{-8}$ A/mm

$4X10^{-8}$ A/mm

X-Y Recorder: X = 0.05 & 0.1 V/cm

Y = 0.10 & 0.05 V/cm

Potentials for all samples (from all complexes) were measured vs. Ag/AgCl (double junc-

tion) at the HMDE of radius 0.333 mm.

B-4 D.P.P.: Instrumental Settings for $Cr(bipy)_3$ & $Cr(terpy)_2$

E506:

Mode: P (differential pulse) WE: HMDE R = 0.333 mm

U = 0.0 V REF: Ag/AgCl (double junction)

ΔU = -2.00 V

t_{drop} = 0.4 sec AUX: Pt.

mm/t = 0.5

D.P. (pulse amplitude) 20 & 30 mV

Scan rate 10 mV/sec

B-5 Results for the Reduction of Chromium Complexes in Acetonitrile

In the following tables, Roman numerals represent oxidation states. The data listed were acquired using instrumental settings as described in Appendix B-3 and B-4 for concentrations described in B-2.

The half-wave potential in the DPP mode for $Cr(bipy)_3$ and $Cr(me_2\text{-}bipy)_3$ listed in Tables B-4 and B-11 was computed using

$$E_{1/2} = E_p - 0.028 \text{ mV}.$$

Table B-1: $Cr(bipy)_3$; CV data obtained from sample 1

Trans. and Run No.	E_p (V)	$\frac{E_p}{2}$ (V)	Slope x (mV)	ΔE_p (mV) (natural)	ΔE_p (mV) (biased)	i_p (cm)	i_p (μA)	$\frac{i_p}{c}$	$E_{\frac{1}{2}}$ a	$E_{\frac{1}{2}}$ b	$E_{\frac{1}{2}}$ c
III → II											
1	-0.237	-0.177	105	95	65	6.55	1.67	2.04	-0.209	-0.205	-0.205
2	-0.235	-0.178	105	95	60	6.60	1.68	2.05	-0.207	-0.206	-0.202
3	-0.235	-0.177	102	85	60	6.57	1.67	2.04	-0.207	-0.205	-0.200
4	-0.235	-0.177	100	85	60	6.55	1.67	2.04	-0.207	-0.205	-0.200
II → I											
1	-0.750	-0.688	105	75	60	6.75	1.72	2.10	-0.722	-0.716	-0.720
2	-0.745	-0.680	110	70	50	6.85	1.75	2.14	-0.717	-0.708	-0.715
3	-0.745	-0.688	108	70	50	6.20	1.58	1.93	-0.717	-0.716	-0.720
4	-0.750	-0.690	100	70	55	6.20	1.58	1.93	-0.722	-0.718	-0.720
I → 0											
1	-1.322	-1.260	110	85	60	6.80	1.73	2.11	-1.294	-1.288	-1.290
2	-1.320	-1.255	105	80	55	6.75	1.72	2.10	-1.292	-1.283	-1.288
3	-1.315	-1.255	110	85	60	6.95	1.77	2.16	-1.287	-1.283	-1.285
4	-1.318	-1.258	105	90	60	7.00	1.79	2.19	-1.290	-1.286	-1.288

Table B-2: $Cr(bipy)_3$; CV data from sample 2

Trans. and Run No.	E_p (V)	$\frac{E_p}{2}$ (V)	Slope x (mV)	ΔEp (mV) (natural)	ΔE_p (mV) (biased)	i_p (cm)	i_p (μA)	$\frac{i_p}{C}$	$E_{\frac{1}{2}}$ a.	$E_{\frac{1}{2}}$ b	$E_{\frac{1}{2}}$ c
III → II											
1	-0.228	-0.173	95	75	55	6.40	1.63	2.00	-0.200	-0.201	-0.198
2	-0.223	-0.170	95	70	55	6.60	1.68	2.06	-0.194	-0.198	-0.195
3	-0.229	-0.170	98	90	60	6.85	1.75	2.15	-0.200	-0.198	-0.199
4	-0.228	-0.173	100	98	60	4.15	1.77	2.17	-0.199	-0.201	-0.198
II → I											
1	-0.745	-0.685	100	70	50	7.90	2.01	2.47	-0.716	-0.713	-0.715
2	-0.745	-0.684	102	70	45	8.05	2.05	2.51	-0.716	-0.712	-0.713
3	-0.743	-0.684	105	105	55	6.60	1.68	2.06	-0.714	-0.712	-0.709
4	-0.737	-0.667	120	70	40	4.50	1.91	2.34	-0.708	-0.695	-0.702
I → 0											
1	-1.309	-1.250	102	75	52	7.65	1.95	2.40	-1.280	-1.278	-1.280
2	-1.308	-1.250	102	78	50	7.35	1.88	2.31	-1.279	-1.278	-1.280
3	-1.310	-1.252	98	83	57	7.00	1.79	2.20	-1.281	-1.280	-1.280
4	-1.314	-1.249	110	73	47	4.00	1.70	2.09	-1.285	-1.277	-1.281

Table B-3: $Cr(bipy)_3$; CV data from sample 3

Trans. and Run No.	E_p (V)	$\frac{E_p}{2}$ (V)	Slope x (mV)	ΔE_p (mV) (natural)	ΔE_p (mV) (biased)	i_p (cm)	i_p (μA)	$\frac{i_p}{C}$	$E_{\frac{1}{2}}$ a	$E_{\frac{1}{2}}$ b	$E_{\frac{1}{2}}$ c
III → II											
1	-0.232	-0.168	105	75	50	2.40	1.63	1.98	-0.203	-0.196	-0.198
2	-0.230	-0.175	100	75	50	2.15	1.46	1.78	-0.201	-0.203	-0.199
3	-0.230	-0.168	105	90	60	2.45	1.67	2.03	-0.201	-0.196	-0.196
4	-0.230	-0.170	100	75	55	2.45	1.67	2.03	-0.201	-0.198	-0.198
II → I											
1	-0.750	-0.688	105	75	50	2.40	1.63	1.98	-0.721	-0.716	-0.717
2	-0.749	-0.687	105	65	50	2.75	1.87	2.28	-0.720	-0.715	-0.715
3	-0.750	-0.687	105	80	60	2.75	1.87	2.28	-0.721	-0.715	-0.717
4	-0.750	-0.686	110	65	50	3.15	2.14	2.60	-0.721	-0.714	-0.714
I → 0											
1	-1.310	-1.248	105	60	40	2.45	1.67	2.03	-1.281	-1.276	-1.280
2	-1.313	-1.247	105	68	45	2.60	1.77	2.15	-1.284	-1.275	-1.278
3	-1.312	-1.250	105	70	55	2.70	1.84	2.24	-1.283	-1.278	-1.280
4	-1.312	-1.250	110	70	60	3.00	2.04	2.48	-1.283	-1.278	-1.280

Table B-4: $Cr(bipy)_3^{3+}$ data from differential pulse polography

Trans. & Run No.	i_p (μA)	$\frac{i_p}{C}$	E_p (V)	$E_{\frac{1}{2}}$ (V)
III → II				
1	1.53	1.88	-0.180	-0.208
2	1.47	1.80	-0.180	-0.208
3	1.11	1.36	-0.180	-0.208
4	1.04	1.28	-0.180	-0.208
II → I				
1	1.53	1.88	-0.687	-0.715
2	1.46	1.79	-0.689	-0.717
3	1.08	1.33	-0.685	-0.713
4	0.88	1.08	-0.685	-0.713
I → 0				
1	1.65	2.02	-1.239	-0.127
2	1.65	2.02	-1.239	-0.127
3	1.15	1.41	-1.232	-0.126
4	0.98	1.20	-1.232	-0.126
0 → -I				
1	2.02	2.48	-1.839	-1.867
2	2.30	2.82	-1.854	-1.889
3	---------- drop fell ----------			
4	1.63	2.00	-1.839	-1.867

Table B-5: $Cr(terpy)_2$; CV data from sample 1

Trans: and Run No.	E_p (V)	$\frac{E_p}{2}$ (V)	Slope x (mV)	ΔEp (mV) (natural)	ΔE_p (mV) (biased)	i_p (cm)	i_p (μA)	$\frac{i_p}{c}$	$E_{\frac{1}{2}}$ a	$E_{\frac{1}{2}}$ b	$E_{\frac{1}{2}}$ c
III → II											
1	-0.133	-0.075	105	70	50	4.90	1.67	2.00	-0.104	-0.103	-0.103
2	-0.130	-0.072	105	65	45	4.70	1.60	1.92	-0.101	-0.100	-0.100
3	-0.133	-0.074	107	65	45	4.10	1.75	2.09	-0.104	-0.102	-0.102
4	-0.135	-0.075	105	68	48	6.80	1.45	1.74	-0.106	-0.103	-0.106
II → I											
1	-0.540	-0.475	105	65	45	5.55	1.91	2.29	-0.511	-0.503	-0.513
2	-0.539	-0.479	105	60	40	5.20	1.77	2.12	-0.510	-0.507	-0.508
3	-0.542	-0.481	110	65	43	4.15	1.77	2.11	-0.514	-0.509	-0.514
4	-0.546	-0.485	105	65	43	7.00	1.49	1.78	-0.517	-0.513	-0.516
I → 0											
1	-1.055	-0.999	98	70	45	5.40	1.84	2.20	-1.026	-1.027	-1.028
2	-1.055	-0.997	98	65	45	5.20	1.77	2.12	-1.027	-1.025	-1.026
3	-1.059	-1.000	105	68	45	4.50	1.91	2.29	-1.030	-1.028	-1.030
4	-1.060	-1.003	100	68	40	6.70	1.43	1.71	-1.031	-1.030	-1.029

Table B-6: $Cr(terpy)_2$; CV data from sample 2

Trans. and Run No.	E_p (V)	$\frac{E_p}{2}$ (V)	Slope x (mV)	ΔE_p (mV) (natural)	ΔE_p (mV) (biased)	i_p (cm)	i_p (μA)	$\frac{i_p}{C}$	$E_{\frac{1}{2}}$ a	$E_{\frac{1}{2}}$ b	$E_{\frac{1}{2}}$ c
III → II											
1	-0.135	-0.075	105	75	50	5.00	1.70	2.04	-0.106	-0.103	-0.104
2	-0.135	-0.074	105	72	47	5.15	1.75	2.09	-0.106	-0.102	-0.105
3	-0.132	-0.070	105	60	45	5.30	1.80	2.15	-0.103	-0.098	-0.104
II → I											
1	-0.542	-0.478	110	70	45	5.80	1.97	2.36	-0.513	-0.506	-0.510
2	-0.540	-0.482	100	60	40	5.60	1.90	2.27	-0.511	-0.510	-0.512
3	-0.545	-0.483	100	60	40	5.40	1.84	2.20	-0.516	-0.511	-0.513
I → 0											
1	-1.055	-1.000	100	70	50	5.75	1.96	2.35	-1.026	-1.028	-1.025
2	-1.057	-1.000	105	70	50	5.50	1.87	2.24	-1.028	-1.028	-1.027
3	-1.057	-1.000	100	65	45	5.50	1.87	2.24	-1.028	-1.028	-1.028

Table B-7: $Cr(terpy)_2$; CV data from sample 3

Trans. and Run No.	E_p (V)	$\frac{E_p}{2}$ (V)	Slope x (mV)	ΔE_p (mV) (natural)	ΔE_p (mV) (biased)	i_p (cm)	i_p (μA)	$\frac{i_p}{C}$	$E_{\frac{1}{2}}$ a	$E_{\frac{1}{2}}$ b	$E_{\frac{1}{2}}$ c
III → II											
1	-0.120	-0.064	100	65	35	4.40	1.87	2.60	-0.091	-0.092	-0.094
2	-0.117	-0.057	105	70	45	5.00	2.13	2.96	-0.088	-0.085	-0.087
3	-0.122	-0.057	105	70	55	5.15	2.19	3.04	-0.093	-0.085	-0.088
4	-0.125	-0.065	105	65	40	4.60	1.96	2.73	-0.097	-0.093	-0.095
5	-0.120	-0.065	100	68	55	5.15	2.19	3.04	-0.091	-0.093	-0.090
6	-0.120	-0.062	100	80	55	4.50	1.91	2.66	-0.091	-0.080	-0.088
II → I											
1	-0.545	-0.484	100	65	42	3.50	1.49	2.07	-0.515	-0.512	-0.512
2	-0.538	-0.470	105	60	40	3.70	1.57	2.18	-0.509	-0.498	-0.505
3	-0.538	-0.475	110	60	40	3.65	1.55	2.15	-0.509	-0.503	-0.502
4	-0.540	-0.479	100	60	40	3.40	1.45	2.02	-0.511	-0.507	-0.511
5	-0.538	-0.478	100	60	40	3.30	1.41	1.96	-0.509	-0.506	-0.509
6	-0.532	-0.468	105	67	43	3.40	1.45	2.02	-0.503	-0.496	-0.500
I → 0											
1	-1.054	-1.000	90	65	40	3.60	1.53	2.13	-1.025	-1.028	-1.025
2	-1.045	-0.985	95	65	40	3.55	1.51	2.10	-1.016	-1.013	-1.020
3	-1.055	-0.995	97	62	40	3.40	1.45	2.02	-1.026	-1.023	-1.023
4	-1.055	-0.995	100	65	48	3.45	1.47	2.04	-1.026	-1.023	-1.025
5	-1.052	-0.992	95	60	40	3.30	1.41	1.96	-1.023	-1.020	-1.020
6	-1.045	-0.985	100	60	40	3.25	1.38	1.92	-1.016	-1.013	-1.015

Table B-7 (con't.)

Trans. and Run No.	E_p (V)	$\frac{E_p}{2}$ (V)	Slope x (mV)	ΔE_p (mV) (natural)	ΔE_p (mV) (biased)	i_p (cm)	i_p (μA)	$\frac{i_p}{C}$	$E_{\frac{1}{2}}$ a	$E_{\frac{1}{2}}$ b	$E_{\frac{1}{2}}$ c
0 → -I											
1	-1.993	-1.928	105	100	40	8.00	3.40	4.73	-1.964	-1.956	-1.955
2	-1.985	-1.925	100	100	50	6.50	2.76	3.84	-1.956	-1.953	-1.950
3	-1.998	-1.930	115	120	65	7.10	3.02	4.20	-1.967	-1.958	-1.962
4	-1.995	-1.925	107	107	60	7.10	3.02	4.20	-1.966	-1.953	-1.960
5	-1.998	-1.923	120	120	55	7.75	3.30	4.59	-1.969	-1.951	-1.957
6	-1.987	-1.913	120	105	60	7.40	3.15	4.38	-1.958	-1.941	-1.949

Table B-8: $Cr(me_2\text{-}bipy)_3$; CV data from sample 1

Trans. and Run No.	E_p (V)	$\frac{E_p}{2}$ (V)	Slope x (mV)	ΔE_p (mV) (natural)	ΔE_p (mV) (biased)	i_p (cm)	i_p (μA)	$\frac{i_p}{C}$	$E_{\frac{1}{2}}$ a	$E_{\frac{1}{2}}$ b	$E_{\frac{1}{2}}$ c
III → II											
1	-0.400	-0.338	105	85	58	6.65	1.70	2.15	-0.371	-0.366	-0.370
2	-0.398	-0.333	105	70	45	5.60	1.43	1.80	-0.369	-0.369	-0.363
3	-0.395	-0.333	105	70	48	5.55	1.42	1.79	-0.366	-0.361	-0.363
4	-0.393	-0.333	100	65	45	7.20	1.84	2.32	-0.364	-0.361	-0.359
5	-0.392	-0.333	95	65	45	5.50	1.40	1.77	-0.363	-0.361	-0.363
6	-0.394	-0.332	102	68	45	6.80	1.74	2.19	-0.365	-0.360	-0.362
II → I											
1	-0.898	-0.839	96	60	47	5.35	1.37	1.73	-0.869	-0.867	-0.868
2	-0.895	-0.836	95	60	42	4.80	1.23	1.55	-0.866	-0.864	-0.868
3	-0.898	-0.839	98	70	45	4.75	1.21	1.33	-0.869	-0.867	-0.867
4	-0.891	-0.839	90	60	40	6.25	1.60	2.02	-0.862	-0.867	-0.864
5	-0.898	-0.840	95	65	42	5.05	1.29	1.63	-0.869	-0.868	-0.868
6	-0.898	-0.838	100	70	47	5.65	1.44	1.82	-0.869	-0.866	-0.867
I → 0											
1	-1.415	-1.360	95	65	45	6.05	1.55	1.96	-1.386	-1.388	-1.390
2	-1.420	-1.358	100	65	45	5.70	1.46	1.84	-1.391	-1.386	-1.390
3	-1.415	-1.358	100	75	40	5.60	1.43	1.81	-1.386	-1.386	-1.385
4	-1.415	-1.360	92	65	43	7.00	1.79	2.26	-1.386	-1.388	-1.389
5	-1.420	-1.361	100	70	40	5.65	1.44	1.82	-1.391	-1.389	-1.390
6	-1.421	-1.362	100	70	45	6.65	1.70	2.14	-1.393	-1.390	-1.393

Table B-9: $Cr(me_2\text{-}bipy)_3$; CV data from sample 2

Trans. and Run No.	E_p (V)	$\frac{E_p}{2}$ (V)	Slope x (mV)	ΔEp (mV) (natural)	ΔE_p (mV) (biased)	i_p (cm)	i_p (μA)	$\frac{i_p}{C}$	$E_{\frac{1}{2}}$ a	$E_{\frac{1}{2}}$ b	$E_{\frac{1}{2}}$ c
III → II											
1	-0.398	-0.338	100	70	42	2.50	1.02	1.29	-0.369	-0.366	-0.363
2	-0.396	-0.333	97	75	45	4.10	1.75	2.21	-0.368	-0.361	-0.362
3	-0.396	-0.334	105	70	47	3.70	1.57	1.98	-0.368	-0.362	-0.363
4	-0.393	-0.333	100	65	40	4.45	1.89	2.38	-0.364	-0.361	-0.363
5	-0.392	-0.333	95	65	40	3.65	1.55	1.96	-0.363	-0.361	-0.363
II → I											
1	-0.898	-0.838	100	65	45	3.15	1.34	1.69	-0.869	-0.866	-0.866
2	-0.898	-0.835	100	65	40	4.40	1.87	2.36	-0.869	-0.863	-0.864
3	-0.900	-0.838	105	68	50	3.65	1.55	1.96	-0.871	-0.866	-0.870
4	-0.898	-0.835	105	70	50	3.70	1.57	1.98	-0.869	-0.863	-0.865
5	-0.900	-0.838	100	65	45	4.25	1.81	2.28	-0.871	-0.866	-0.868
I → 0											
1	-1.418	-1.358	100	75	50	3.00	1.28	1.62	-1.386	-1.386	-1.388
2	-1.418	-1.358	100	65	43	4.25	1.81	2.28	-1.386	-1.386	-1.389
3	-1.420	-1.363	105	70	47	3.80	1.62	2.04	-1.391	-1.391	-1.395
4	-1.416	-1.360	100	65	45	4.40	1.87	2.36	-1.387	-1.388	-1.388
5	-1.418	-1.363	92	65	40	4.00	1.70	2.14	-1.386	-1.391	-1.392

Table B-10: $Cr(me_2\text{-}bipy)_3$; CV data from sample 3

Trans. and Run No.	E_p (V)	$\frac{E_p}{2}$ (V)	Slope x (mV)	ΔE_p (mV) (natural)	ΔE_p (mV) (biased)	i_p (cm)	i_p (μA)	$\frac{i_p}{C}$	$E_{\frac{1}{4}}$ a	$E_{\frac{1}{4}}$ b	$E_{\frac{1}{4}}$ c
III → II											
1	-0.390	-0.333	100	60	35	3.55	1.51	1.96	-0.361	-0.361	-0.362
2	-0.390	-0.332	100	70	45	3.15	1.34	1.74	-0.361	-0.360	-0.363
3	-0.394	-0.332	105	65	44	3.85	1.64	2.13	-0.366	-0.360	-0.362
4	-0.390	-0.332	100	62	40	3.78	1.61	2.09	-0.361	-0.360	-0.360
5	-0.389	-0.332	95	50	40	3.40	1.45	1.88	-0.360	-0.360	-0.360
6	-0.390	-0.332	100	55	30	3.40	1.45	1.88	-0.361	-0.360	-0.361
7	-0.390	-0.333	100	65	45	3.30	1.40	1.82	-0.361	-0.361	-0.362
8	-0.390	-0.331	100	60	40	3.20	1.36	1.76	-0.361	-0.359	-0.358
9	-0.375	-0.315	100	60	40	3.25	1.38	-	-	-	-
10	-0.390	-0.322	105	70	45	3.20	1.36	1.76	-0.361	-0.350	-0.360
11	-0.392	-0.330	100	70	40	3.95	1.68	2.18	-0.363	-0.358	-0.362
12	-0.392	-0.335	100	70	43	3.10	1.32	1.71	-0.363	-0.363	-0.362
13	-0.390	-0.333	98	55	45	3.18	1.35	1.75	-0.361	-0.361	-0.362
II → I											
1	-0.892	-0.835	100	60	40	3.20	1.36	1.76	-0.863	-0.863	-0.863
2	-0.890	-0.835	93	50	35	2.45	1.04	1.35	-0.861	-0.863	-0.860
3	-0.893	-0.836	95	52	40	2.83	1.20	1.56	-0.864	-0.864	-0.863
4	-0.890	-0.835	90	60	45	3.10	1.32	1.71	-0.861	-0.863	-0.862
5	-0.890	-0.834	95	55	40	2.92	1.24	1.61	-0.861	-0.862	-0.860
6	-0.890	-0.835	95	55	40	2.78	1.18	1.53	-0.861	-0.863	-0.865
7	-0.890	-0.834	95	55	40	2.65	1.13	1.47	-0.861	-0.862	-0.862
8	-0.892	-0.832	105	60	40	3.33	1.42	1.84	-0.863	-0.860	-0.860
9	-0.875	-0.820	100	65	45	3.03	1.29	-	-	-	-
10	-0.886	-0.830	90	60	40	2.65	1.13	1.47	-0.857	-0.858	-0.855
11	-0.888	-0.833	90	58	38	2.85	1.21	1.57	-0.859	-0.861	-0.860
12	-0.890	-0.836	90	60	42	2.85	1.21	1.57	-0.861	-0.864	-0.865
13	-0.890	-0.833	100	60	45	3.25	1.38	1.79	-0.861	-0.861	-0.863

Table B-10 (con't.)

Trans. and Run No.	E_p (V)	$\frac{E_p}{2}$ (V)	Slope x (mV)	ΔE_p (mV) (natural)	ΔE_p (mV) (biased)	i_p (cm)	i_p (μA)	$\frac{i_p}{C}$	$E_{\frac{1}{4}}$ a	$E_{\frac{1}{4}}$ b	$E_{\frac{1}{4}}$ c
I → 0											
1	-1.410	-1.355	100	60	35	3.60	1.53	1.98	-1.381	-1.383	-1.385
2	-1.415	-1.360	93	60	35	2.78	1.18	1.53	-1.386	-1.388	-1.385
3	-1.414	-1.360	95	58	40	3.30	1.40	1.82	-1.385	-1.388	-1.387
4	-1.418	-1.357	95	65	40	3.50	1.50	1.95	-1.389	-1.385	-1.386
5	-1.412	-1.351	100	60	35	3.40	1.45	1.88	-1.383	-1.379	-1.381
6	-1.413	-1.354	105	60	43	3.30	1.40	1.82	-1.384	-1.382	-1.382
7	-1.415	-1.355	105	60	40	3.17	1.35	1.75	-1.386	-1.383	-1.390
8	-1.412	-1.350	100	65	37	3.45	1.47	1.91	-1.383	-1.378	-1.380
9	-1.395	-1.338	100	62	45	3.40	1.45	-	-	-	-
10	-1.415	-1.353	100	60	40	3.25	1.38	1.79	-1.386	-1.381	-1.380
11	-1.410	-1.355	90	60	37	3.30	1.40	1.82	-1.381	-1.383	-1.382
12	-1.410	-1.353	95	60	40	3.40	1.45	1.88	-1.381	-1.381	-1.383
13	-1.410	-1.353	95	55	45	3.45	1.47	1.91	-1.381	-1.381	-1.383
0 → -I											
2	-2.030	-1.960	110	135	70	15.05	6.40	8.30	-2.001	-1.988	-1.990
3	-2.030	-1.962	105	132	75	18.85	8.02	10.40	-2.001	-1.990	-1.990
4	-2.035	-1.963	100	135	75	19.90	8.47	10.99	-2.006	-1.991	-1.989
5	----------				NOT AVAILABLE				----------		
6	----------				NOT AVAILABLE				----------		
7	-2.020	-1.953	120	N.A.	N.A.	19.75	8.40	10.90	-1.991	-1.981	-1.982
8	----------				NOT AVAILABLE				----------		
9	----------				NOT AVAILABLE				----------		
10	-2.020	-1.955	100	N.A.	70	20.65	8.78	11.39	-1.991	-1.983	-1.980
11	----------				NOT AVAILABLE				----------		
12	----------				NOT AVAILABLE				----------		
13	-2.023	-1.960	100	N.A.	N.A.	20.60	8.77	11.38	-1.994	-1.988	-1.988

Table B-11: $Cr(me_2\text{-}bipy)_3$; DPP data

Trans. & Run No.	i_p (μA)	$\frac{i_p}{C}$	E_p (V)	$E_{\frac{1}{2}}$ (V)
III → II				
1	2.08	2.74	-0.342	-0.371
2	2.05	2.70	-0.346	-0.374
3	1.85	2.44	-0.342	-0.370
4	2.10	2.76	-0.344	-0.372
II → I				
1	1.78	2.34	-0.837	-0.865
2	1.68	2.21	-0.844	-0.872
3	1.60	2.11	-0.829	-0.857
4	1.70	2.24	-0.838	-0.866
I → 0				
1	1.80	2.37	-1.346	-1.374
2	1.70	2.24	-1.353	-1.381
3	1.63	2.14	-1.320	-1.348
4	1.85	2.43	-1.350	-1.378
0 → -I				
1	5.00	6.58	-1.914	-1.942
2	5.00	6.58	-1.921	-1.949
3	4.63	6.09	-1.880	-1.908
4	4.75	6.25	-1.914	-1.942

Table B-12: $Cr(ph_2\text{-}bipy)_3$; CV data from sample 1

Trans. and Run No.	E_p (V)	$E_{\frac{p}{2}}$ (V)	Slope x (mV)	ΔEp (mV) (natural)	ΔE_p (mV) (biased)	i_p (cm)	i_p (μA)	$\frac{i_p}{C}$	$E_{\frac{1}{4}}$ a	$E_{\frac{1}{4}}$ b	$E_{\frac{1}{4}}$ c
III → II											
1	-0.245	-0.188	100	60	50	5.40	0.919	1.47	-0.216	-0.216	-0.218
2	-0.246	-0.195	110	60	35	5.45	0.928	1.48	-0.217	-0.223	-0.220
3	-0.250	-0.193	110	65	40	5.65	0.962	1.55	-0.221	-0.221	-0.218
4	-0.250	-0.195	110	60	45	4.12	1.052	1.68	-0.221	-0.223	-0.223
5	-0.243	-0.192	107	63	50	4.20	1.072	1.71	-0.214	-0.220	-0.218
II → I											
1	-0.683	-0.623	100	65	40	5.50	0.936	1.50	-0.654	-0.651	-0.653
2	-0.684	-0.624	100	68	40	5.50	0.936	1.50	-0.655	-0.652	-0.653
3	-0.673	-0.612	105	53	35	5.00	0.851	-	-	-	-
4	-0.685	-0.623	100	58	45	3.65	0.932	1.49	-0.656	-0.651	-0.652
5	-0.680	-0.620	100	63	45	3.75	0.957	1.53	-0.651	-0.648	-0.650
I → 0											
1	-1.198	-1.139	105	60	45	5.78	0.984	1.57	-1.169	-1.167	-1.169
2	-1.197	-1.140	100	55	30	5.85	0.996	1.59	-1.168	-1.168	-1.169
3	-1.204	-1.142	100	68	40	5.85	0.995	1.59	-1.175	-1.170	-1.172
4	-1.208	-1.145	110	70	45	4.50	1.149	1.84	-1.179	-1.173	-1.177
5	-1.203	-1.145	105	75	45	4.05	1.034	1.65	-1.174	-1.173	-1.173
0 → -I											
1	-1.763	-1.686	125	85	40	6.60	1.123	1.80	-1.734	-1.714	-1.718
2	-1.760	-1.684	125	80	30	6.45	1.100	1.76	-1.731	-1.712	-1.718
3	-1.764	-1.690	115	85	45	6.10	1.040	1.66	-1.735	-1.718	-1.724
4	-1.780	-1.698	135	90	50	4.85	1.238	-	-	-	-
5	-1.760	-1.688	120	75	50	5.15	1.315	2.10	-1.731	-1.716	-1.723

Table B-13: $Cr(ph_2\text{-}bipy)_3$; CV data from sample 2

Trans. and Run No.	E_p (V)	$\frac{E_p}{2}$ (V)	Slope x (mV)	ΔE_p (mV) (natural)	ΔE_p (mV) (biased)	i_p (cm)	i_p (μA)	$\frac{i_p}{C}$	$E_{\frac{1}{4}}$ a	$E_{\frac{1}{4}}$ b	$E_{\frac{1}{4}}$ c
III → II											
1	-0.246	-0.197	103	54	39	5.80	0.987	1.54	-0.217	-0.225	-0.223
2	-0.251	-0.196	103	57	36	5.75	0.979	1.53	-0.222	-0.224	-0.223
3	-0.250	-0.197	100	60	45	2.75	0.936	1.46	-0.221	-0.225	-0.217
4	-0.247	-0.196	100	60	45	2.80	0.953	1.49	-0.218	-0.224	-0.224
5	-0.249	-0.198	100	58	40	2.15	0.915	1.43	-0.220	-0.226	-0.224
6	-0.252	-0.197	100	65	40	2.18	0.923	1.44	-0.223	-0.225	-0.224
II → I											
1	-0.684	-0.625	98	66	41	6.25	1.064	1.66	-0.655	-0.653	-0.653
2	-0.688	-0.625	103	65	47	6.32	1.076	1.68	-0.659	-0.653	-0.655
3	-0.689	-0.626	95	70	45	3.05	1.038	1.62	-0.660	-0.654	-0.657
4	-0.687	-0.624	100	68	50	2.85	0.970	1.51	-0.658	-0.652	-0.653
5	-0.691	-0.626	100	60	40	2.25	0.970	1.51	-0.662	-0.654	-0.655
6	-0.687	-0.627	95	60	45	2.20	0.936	1.46	-0.658	-0.656	-0.657
I → 0											
1	-1.194	-1.135	103	67	47	6.20	1.055	1.65	-1.165	-1.163	-1.166
2	-1.198	-1.138	103	72	44	6.13	1.043	1.63	-1.167	-1.166	-1.165
3	-1.198	-1.138	100	63	40	3.10	1.055	1.65	-1.167	-1.166	-1.169
4	-1.201	-1.142	90	62	45	3.55	1.209	1.89	-1.172	-1.170	-1.172
5	-1.197	-1.139	100	60	40	2.55	1.085	1.69	-1.168	-1.167	-1.168
6	-1.203	-1.145	95	65	45	2.38	1.013	1.58	-1.174	-1.173	-1.174
0 → -I											
1	NOT AVAILABLE										
2	NOT AVAILABLE										
3	-1.747	-1.682	105	75	50	4.45	1.515	2.37	-1.718	-1.710	-1.716
4	-1.752	-1.678	115	80	50	4.20	1.430	2.23	-1.723	-1.706	-1.715
5	-1.750	-1.680	120	73	45	3.20	1.360	2.12	-1.721	-1.708	-1.715
6	-1.762	-1.685	120	85	50	3.15	1.340	2.09	-1.733	-1.719	-1.719

B-6 Statistical Comparison of the Half-wave Potentials as Obtained by Methods A, B and C

The half-wave potentials listed in Tables B-1 through B-13 were subjected to statistical analysis of variance (ANOVA). The analysis involved the comparison of means obtained by the various methods, both between methods and between samples. The computed "F" values were obtained as shown in the following table.

TABLE B-14: ANOVA

SOURCE OF VARIATION	DEGREE OF FREEDOM	SUM OF SQUARES	MEAN SQUARE	COMPUTED F
TREATMENT	K-1	SSA	$S_1^2 = \frac{SSA}{K-1}$	$F = \frac{S_1^2}{S_2^2}$
ERROR	or $\frac{K(n-1)}{(N-K)}$	SSE	$S_2^2 = \frac{SSE}{N-K}$	
TOTAL		SST		

where SST = total sum of squares = $\sum_{i=1}^{K} \sum_{J=1}^{n_i} X_{iJ}^2 - \frac{T^2}{N}$

SSA = treatment sum of squares = $\sum_{i=1}^{K} \frac{Ti^2}{n_i} - \frac{T^2}{N}$.

SSE = Error sum of squares = SST - SSA

K = Number of groups being compared

n = Number of measurements per group

N = total number of measurements.

The test hypothesis is that all the means are equal at the 0.05 (95%) level of significance.

Table B-15 shows an example of ANOVA results for statistical treatment between methods within a given sample of $Cr(me\text{-}_2bipy)_3$. Similarly, Table B-16 lists results obtained between samples for a given method.

REDUCTION	NO. OF RUNS	HALF WAVE POTENTIALS $E_{1/2}$± FOR METHODS: A	B	C	POP. MEAN $E_{1/2}$±	COMPUTED F	F(95%)
III to II	12	-0.3617±0.0015	-0.3594±0.0031	-0.3612±0.0013	-0.3608±0.0024	3.39	$F_{(2,33)}$=3.29
	12	-----	-0.3594±0.0031	-0.3612±0.0013	-0.3603±0.0026	3.00	$F_{(1,22)}$=4.30
II to I	12	-0.8611±0.0016	-0.8620±0.0017	-0.8615±0.0026	-0.8615±0.0021	0.54	$F_{(2,33)}$=4.30
	12	-----	-0.8620±0.0017	-0.8615±0.0026	-0.8618±0.0023	0.28	$F_{(1,22)}$=4.30
I to 0	12	-1.384±0.0025	-1.3830±0.0030	-1.3840±0.0030	-1.3834±0.0029	0.56	$F_{(2,33)}$=3.29
	12	-----	-1.3830±0.0030	-1.3840±0.0030	-1.3832±0.0030	0.64	$F_{(1,22)}$=4.30
0 to -I	6	-1.997±0.0057	-1.9870±0.0036	-1.9870±0.0036	-1.9900±0.0070	9.29	$F_{(2,15)}$=3.68
	6	-----	-1.9870±0.0036	-1.9870±0.0036	-1.9867±0.0040	0.02	$F_{(1,10)}$=4.96

TABLE B-15: $Cr(me_2\text{-bipy})_3$; "ANOVA" Between Methods

REDUCTION	$E_{1/2}$± FOR; SAMPLE, METHOD & NO. OF RUNS			POP. MEAN	COMPUTED	$F_{(95\%)}$
	1, C, 6	2, C, 5	3, C, 12	$E_{1/2}$±	F	
III to II	-0.363±0.003	-0.363±0.0004	-0.361±0.001	-0.362±0.002	2.51	$F_{(2,20)}$=3.49
II to I	-0.867±0.001	-0.867±0.002	-0.862±0.0003	-0.864±0.004	13.77	$F_{(2,20)}$=3.49
	-0.867±0.001	-0.867±0.002	-----	-0.867±0.002	0.12	$F_{(1,8)}$ =5,12
I to 0	-1.389±0.003	-1.390±0.003	-1.384±0.003	-1.387±0.004	13.18	$F_{(2,20)}$=3.49
	-1.389±0.003	-1.390±0.003	-----	-1.390±0.003	0.28	$F_{(1,9)}$ =5.12

TABLE B-16: $Cr(me_2\text{-bipy})_3$ Method C; "ANOVA" Between Sample

APPENDIX C

C-1 Preparation of Aqueous $[Cr(bipy)_3]^{+3}$ and $[Cr(me_2\text{-}bipy)_3]^{+3}$ Analyte Solutions

Analyte solutions for both $Cr(bipy)_3$ and $Cr(me_2\text{-}bipy)_3$ were prepared to yield $5.5X10^{-5}M$ concentrations by diluting 1000 ppm stock solutions of chromium complexes in 0.1M KCl.

$Cr(bipy)_3$ M.W. = 827.89 g/M

2.30 ml of 1000 ppm diluted to 50.5 ml (KCl)

$$= 4.554X10^{-5} \text{ g/ml} = \frac{4.554X10^{-2} \text{ g/l}}{827.89 \text{ g/M}} = 5.501 \text{ M}$$

$Cr(me_2\text{-}bipy)_3$ M.W. = 921.084 g/M

2.50 ml of 1000 ppm diluted to 49.5 ml (0.1 KCl)

$$= 5.051X10^{-5} \text{ g/ml} = \frac{5.051X10^{-2} \text{ g/l}}{921.084 \text{ g/M}} = 5.48X10^{-5} \text{ M}$$

Adjustment of pH 3.5 was made by acidifying the 0.1M KCl supporting electrolyte with ultra-pure HCl prior to sample dilution.

C-2 Purification of Mercury (for HMDE) and Supporting Electrolyte

The purification by electrolysis was carried out in a cell system built and developed by Seto (68) and is based on the principles of electrochemical stripping. The cell consisted of three electrodes--a mercury pool, a large cylindrical platinum gauze electrode and an Ag/AgCl (saturated KCl) reference. The latter two were contained within beakers with fritted-disc bottoms so that they were physically separated from the solution undergoing purification. When the cell was used for the purification of the supporting electrolyte (0.1M KCl), the electrodes were connected so that the mercury pool was the cathode and the platinum electrode acted as anode. The potential across the electrodes was adjusted to -1.00 V vs Ag/AgCl with an initial current flow of 25 mA. Thus, any metallic impurities in the solution were reduced at and adsorbed by the mercury pool. The process was carried out for 12 hours, and purification was considered complete when the monitoring current meter indicated no current flow (zero Amperes or steady state).

For the purification of mercury, the Hg

needed for the HMDE was used as the mercury pool electrode. However, in this case, the Hg pool was the anode and the platinum gauze acted as the cathode. Hence, trace metals within the mercury were oxidized and came into solution in the electrolyte (0.1M KCl). The process was carried out at +0.300 V vs Ag/AgCl for 12 hours, by which time the meter indicated zero current flow. Impurities of 1.5 gr were collected from three lbs. of Hg.

The electrolysis was powered by the potentiostat Hewlett-Packard, Series STB, Model 6113A, and the potential was monitored by Metrohm E 300-B pH/mV meter.

C-3 Blank Evaluation: 0.1 M KCl Supporting Electrolyte

Initial CV scans of the supporting electrolyte within the needed working range (-0.30 to -0.60 Volts) indicated the following. First, the shape of the polarogram was not affected by the sweeprate (other than a proportional decrease in size). Second, as can be seen from Figure C-1, the switching potential (E_{switch}) also did not affect the general shape of the i-E curve. Finally, the residual current (the upper plateau in Figure C-1) is parallel to the zero current baseline.

Based on these observations, it was decided

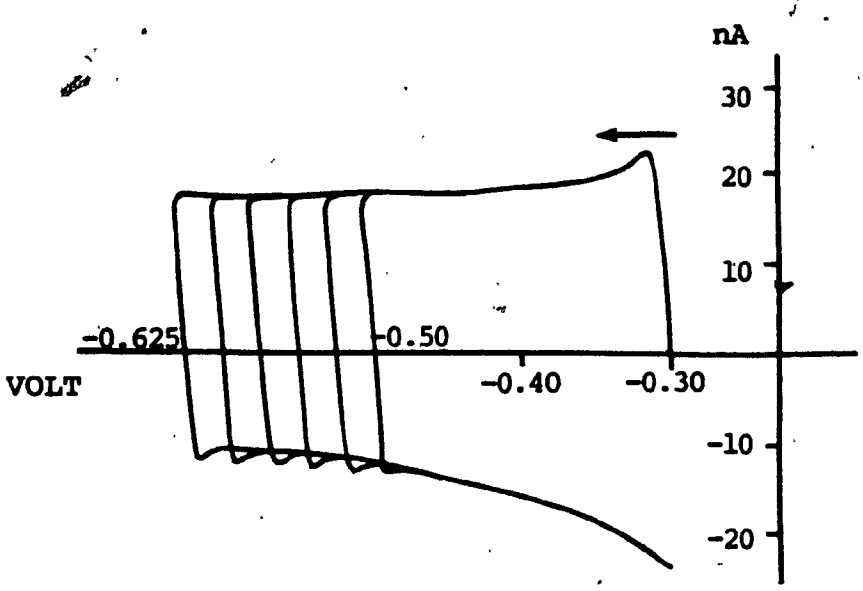

Figure C-1: CV scan of 0.1M KCL supporting electrolyte (blank).

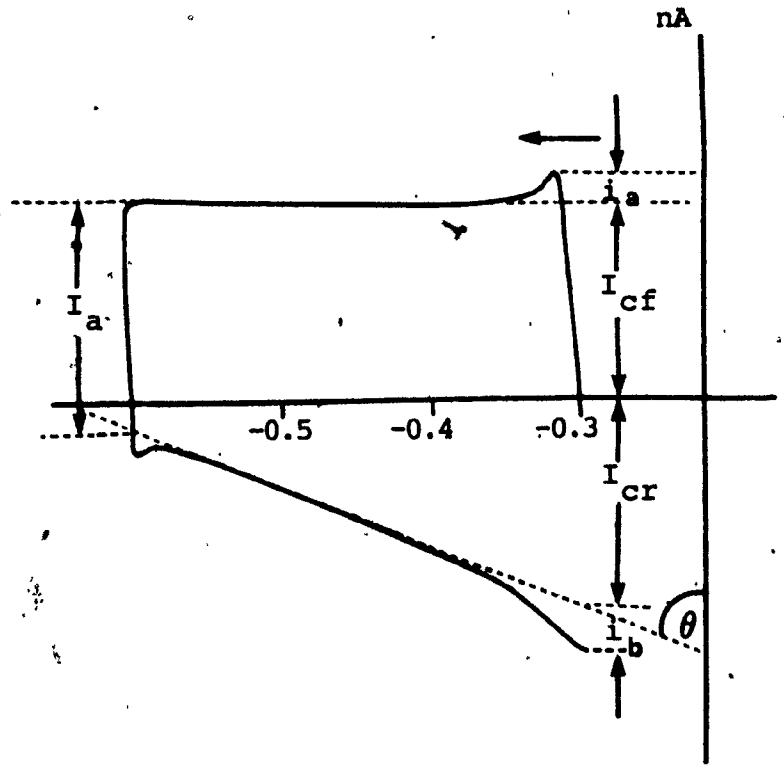

Figure C-2: Measurable parameters from blank (0.1M KCl).

to construct a theoretical "blank" Polarogram which in turn could be used in the evaluation of the $Cr(bipy)_3$ polarograms. The construction of the theoretical curves was based on the measurement of the parameters indicated in Figure C-2. These were measured at different scan-rates, four polarograms at each scan-rate with three different samples. The data, summarized in Table C-1, represent the final averages for the pertinent measurements. The bulk of the data, as obtained from the three samples, is listed in Tables C-2, C-3, and C-4. Figure C-3 shows the polarograms constructed from the above data (Table C-1). It should be noted here that the quantities I_{cf} and i_a represent the charging currents (see Figure 5-2) for the cathodic (reduction) portion of the sweep, and that their magnitude is the only parameter which does not change with the addition of the analyte to the supporting electrolyte. Hence, in the cases where the computed blank did not fit a given $Cr(bipy)_3$ polarogram, a new blank was constructed based on the measurement of the scan $I_{cf} + i_a$ and its relation (ratios) to the other parts of the model.

SCAN RATE V/S	$i_{a(cm)}$	$I_{a(cm)}$	$I_{cf(cm)}$	$I_{cr(cm)}$	I_a/I_{cf}	I_{cr}/I_{cf}	θ
0.10	0.49±0.04	3.48±0.06	2.30±0.08	2.44±0.14	0.213	1.061	11.5°
0.09	0.42±0.08	3.07±0.09	2.12±0.08	2.15±0.08	0.201	1.014	11.0°
0.08	0.38±0.07	2.68±0.07	1.89±0.06	1.96±0.07	0.201	1.037	11.0°
0.07	0.29±0.11	2.37±0.05	1.70±0.06	1.70±0.09	0.171	1.00	9.5°
0.06	0.21±0.05	2.02±0.03	1.47±0.08	1.47±0.09	0.143	1.00	9.0°
0.05	0.14±0.04	1.68±0.03	1.29±0.07	1.24±0.07	0.109	0.961	8.0°
0.04	0.05	1.34±0.03	1.06±0.06	1.01±0.05	0.05	0.953	7.0°

TABLE C-1: Summary of DATA Needed for the Construction of Theoretical Blank

GRAPH NO.	POLARO-GRAM	SCAN RATE V/S	i_a	i_b	I_{cr}	I_{cf}	I_a
Ia	1	0.10	0.50	0.60	2.40	2.20	3.55
Ia	2	0.10	0.45	0.55	2.40	2.20	3.45
Ia	3	0.10	0.50	0.50	2.40	2.20	3.40
Ia	4	0.10	0.50	0.50	2.35	2.25	3.45
Ia	1	0.09	0.30	0.45	2.15	2.10	3.00
Ia	2	0.09	0.45	0.45	2.10	2.00	3.00
Ia	3	0.09	0.35	0.45	2.05	2.00	3.00
ia	4	0.09	0.40	0.40	2.15	2.00	2.95
Ib	[illegible]	0.08	0.35	0.45	1.90	1.80	2.65
Ib	2	0.08	0.30	0.40	1.90	1.85	2.65
Ib	3	0.08	0.35	0.40	1.90	1.85	2.65
Ib	4	0.08	0.35	0.40	1.90	1.80	2.60
Ib	1	0.07	0.15	0.35	1.70	1.70	2.35
Ib	2	0.07	0.20	0.40	1.70	1.60	2.35
Ib	3	0.07	0.25	0.35	1.65	1.60	2.35
Ib	4	0.07	0.20	0.30	1.65	1.65	2.35
Ic	1	0.06	0.25	0.40	1.40	1.35	2.05
Ic	2	0.06	0.20	0.40	1.40	1.30	2.00
Ic	3	0.06	0.20	0.35	1.20	1.45	2.00
Ic	4	0.06	0.15	0.30	1.35	1.40	2.00
Ic	1	0.05	0.15	0.30	1.20	1.15	1.65
Ic	2	0.05	0.05	0.25	1.20	1.20	1.70
Ic	3	0.05	0.05	0.25	1.20	1.25	1.65
Ic	4	0.05	0.00	0.20	1.25	1.25	1.65
Ic	1	0.04	0.00	0.25	1.05	1.00	1.30
Ic	2	0.04	0.00	0.25	1.05	1.00	1.30
Ic	3	0.04	0.05	0.15	0.95	1.00	1.30
Ic	4	0.04	0.00	0.15	0.95	1.00	1.30

TABLE C-2: Measured Dimensions from Blanks at Different Scan Rate: Sample 1

GRAPH NO.	POLARO-GRAM	SCAN RATE V/S	i_a	i_b	I_{cr}	I_{cf}	I_a
IIIa	1	0.10	0.55	0.50	2.65	2.30	3.50
IIIa	2	0.10	0.50	0.50	2.70	2.30	3.45
IIIa	3	0.10	0.45	0.55	2.55	2.40	3.45
IIIa	4	0.10	0.45	0.50	2.55	2.40	3.50
IIIa	1	0.09	0.35	0.60	2.20	2.20	3.25
IIIa	2	0.09	0.40	0.45	2.25	2.20	3.15
IIIa	3	0.09	0.40	0.30	2.20	2.20	3.10
IIIa	4	0.09	0.35	0.40	2.25	2.20	3.10
IIIb	1	0.08	0.35	0.45	2.05	1.90	2.75
IIIb	2	0.08	0.30	0.45	2.00	1.90	2.75
IIIb	3	0.08	0.40	0.45	2.05	1.95	2.75
IIIb	4	0.08	0.30	0.45	2.05	2.00	2.80
IIIb	1	0.07	0.35	0.35	1.90	1.70	2.40
IIIb	2	0.07	0.25	0.45	1.85	1.75	2.40
IIIb	3	0.07	0.20	0.45	1.70	1.80	2.45
IIIb	4	0.07	0.20	0.50	1.70	1.75	2.45
IIIc	1	0.06	0.15	0.30	1.65	1.55	2.05
IIIc	2	0.06	0.15	0.40	1.60	1.45	2.05
IIIc	3	0.06	0.20	0.40	1.45	1.50	2.05
IIIc	4	0.06	0.20	0.35	1.55	1.50	2.00
IIIc	1	0.05	0.10	0.15	1.30	1.35	1.65
IIIc	2	0.05	0.10	0.20	1.20	1.35	1.70
IIIc	3	0.05	0.05	0.30	1.20	1.30	1.70
IIIc	4	0.05	0.10	0.25	1.30	1.35	1.70
IIIc	1	0.04	0.05	0.20	1.05	1.10	1.35
IIIc	2	0.04	0.00	0.20	1.10	1.00	1.35
IIIc	3	0.04	0.05	0.25	1.00	1.10	1.40
IIIc	4	0.04	0.05	0.30	1.05	1.05	1.35

TABLE C-3: Measured Dimensions from Blanks at Different Scan Rate: Sample 2

GRAPH NO.	POLARO-GRAM	SCAN RATE V/S	i_a	i_b	I_{cr}	I_{cf}	I_a
Va	1	0.10	0.75	0.70	2.35	2.35	3.55
Va	2	0.10	0.75	0.75	2.35	2.30	3.45
Va	3	0.10	0.75	0.75	2.30	2.40	3.60
Va	4	0.10	0.65	0.65	2.30	2.30	3.45
Va	1	0.09	0.45	0.55	2.20	2.10	3.00
Va	2	0.09	0.55	0.50	2.15	2.15	3.05
Va	3	0.09	0.55	0.50	2.00	2.15	3.15
Va	4	0.09	0.50	0.50	2.10	2.15	3.05
Vb	1	0.08	0.45	0.55	1.85	1.90	2.70
Vb	2	0.08	0.45	0.55	2.00	1.90	2.65
Vb	3	0.08	0.50	0.70	1.65	1.95	2.65
Vb	4	0.08	0.40	0.40	2.00	1.95	2.60
Vb	1	0.07	0.40	0.50	1.65	1.70	2.35
Vb	2	0.07	0.45	0.50	1.65	1.70	2.30
Vb	3	0.07	0.45	0.50	1.60	1.70	2.35
Vb	4	0.07	0.40	0.50	1.60	1.75	2.30
Vc	1	0.06	0.30	0.80	1.45	1.50	2.00
Vc	2	0.06	0.25	0.50	1.40	1.50	2.05
Vc	3	0.06	0.20	0.30	1.50	1.55	2.00
Vc	4	0.06	0.25	0.30	1.50	1.55	2.00
Vc	1	0.05	0.15	0.20	1.35	1.30	1.70
Vc	2	0.05	0.20	0.30	1.30	1.30	1.65
Vc	3	0.05	0.15	0.35	1.10	1.40	1.70
Vc	4	0.05	0.15	0.30	1.25	1.30	1.70
Vc	1	0.04	0.05	0.20	1.00	1.10	1.35
Vc	2	0.04	0.10	0.20	1.05	1.10	1.35
Vc	3	0.04	0.05	0.20	0.95	1.15	1.35
Vc	4	0.04	0.10	0.20	0.95	1.10	1.35

TABLE C-4: Measured Dimensions from Blanks at Different Scan Rate: Sample 3

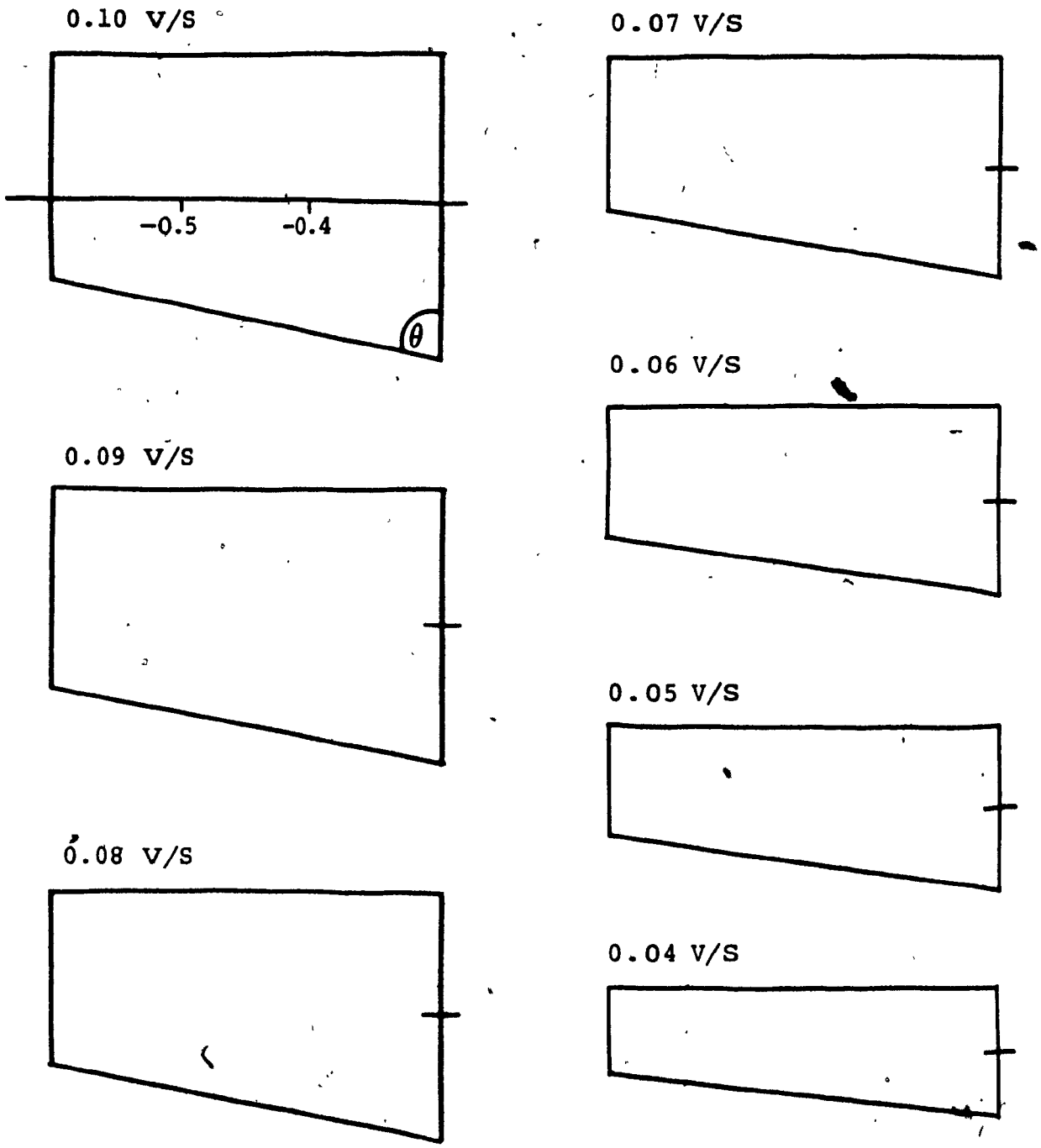

Figure C-3: Theoretical construction of blank.

C-4 Baseline for Anodic Peak Measurements

Although the superimposed blank provided an excellent baseline for the cathodic peak and a good baseline for the apparent anodic peak current measurements, it did not solve the problem of the switching current (i_{sw} in Figure 5-1). The capacitance effect at the switching point did not correlate to that of the "blank (I_a)" and in addition I_a did not have a logical baseline. It was also impossible to decide whether I_a should be measured to a point before or after the capacitance effect. Hence, the theoretical model ended up providing only the baseline for the true cathodic peak, and it was decided not to use Nicholson's technique. Consequently, a new method had to be developed in order to evaluate the true value of the anodic peak--to replace the apparent anodic and switching currents used in Nicholson's equation of ratios.

There are several techniques for the establishment of the proper baseline for anodic measurements (34, 69). These involve stopping the scan upon completion of the cathodic portions and allowing the current to decay to a point of electrochemical equilibrium at the switching potential. A horizontal line (parallel to the zero current line) passing through this point becomes the base-

line for the anodic peak, since this point is the location from which the anodic scan begins to give the oxidation portion of the CV polarogram. This technique is reliable and, although several minutes are required to complete a CV cycle, it is an excellent method for the evaluation of uncomplicated reactions. However, in complex reactions, as in the case of $Cr(bipy)_3$ where an electron transfer is followed by an irreversible chemical reaction, this technique cannot be applied directly. Stopping the scan at the end of the cathodic (reduction) portion will permit the irreversible process (Equation 5-7) to dominate and consequently distort the shape and size of the anodic peak. This, however, does not affect the equilibrium (current) at the switching potential, since Equation 5-7 does not involve electron transfer (i.e. the catalytic reaction is not detected by the electrode system). Consequently the following procedure was adopted. Each determination involved two scans. The first produced the full cycle, and the second scan was used only cathodically and yielded the equilibrium point which was used in the measurement of the true anodic peak (Figure 5-9).

C-5 Rate of Reaction (K_f) Results for Aqueous $[Cr(bipy)_3]^{+3}$

Tables C-5 and C-6 list the pertinent data and the computed values of K_f at different scan rates for both samples (duplicates) at 23°C. The data were extracted from CV polarograms obtained for $5.5X10^{-5}M$ $[Cr(bipy)_3]^{+3}$ in 0.1M KCl pH 3.5, at the HMDE (radius = 0.265 mm) vs SCE saturated KCl.

Table C-7 lists results for the same samples at 25°C.

In these tables, the values for the cathodic and anodic currents (I_c and I_a) are listed in units of length (cm.) rather than the proper "amperes." The reason for this lies in the fact that the main interest here is to obtain an accurate ratio of these values (I_a/I_c), and since conversion to current units might introduce new errors, it was decided against it. Nevertheless, the amplitude conversion factor for these parameters is

1.17 cm. = 10 nAmperes

Table C-5: Data from sample 1; aqueous $Cr(bipy)_3$ at 23°C

Scan rate (V/S)	E_{start} (V)	$E_{c.p.}$ (V)	$E_{\frac{1}{2}}$ (V)	$E_{sw.}$ (V)	i_C (cm)	i_A (cm)	$\frac{i_A}{C}$	$K_f\tau$	τ (sec)	K_f (sec-1)
0.040	-0.300	-0.503	-0.475	-0.575	6.98	3.90	0.559	0.750	2.50	0.300
0.040	-0.300	-0.503	-0.475	-0.575	6.80	3.82	0.562	0.740	2.50	0.296
0.040	-0.300	-0.503	-0.480	-0.575	6.57	3.85	0.586	0.665	2.38	0.279
0.040	-0.300	-0.503	-0.480	-0.575	6.35	3.70	0.583	0.670	2.38	0.282
0.040	-0.300	-0.503	-0.478	-0.575	6.10	3.63	0.595	0.640	2.55	0.251
0.040	-0.300	-0.503	-0.478	-0.575	6.30	3.65	0.579	0.685	2.55	0.269
0.040	-0.300	-0.503	-0.478	-0.575	6.37	3.55	0.557	0.750	2.55	0.294
0.050	-0.300	-0.500	-0.478	-0.575	7.90	4.98	0.630	0.548	1.94	0.283
0.050	-0.300	-0.500	-0.475	-0.575	7.50	4.70	0.627	0.550	2.00	0.275
0.050	-0.300	-0.500	-0.478	-0.575	7.42	4.70	0.633	0.540	1.94	0.278
0.050	-0.300	-0.500	-0.477	-0.575	7.85	4.78	0.609	0.600	1.96	0.306
0.050	-0.300	-0.503	-0.475	-0.575	7.60	4.65	0.612	0.595	2.00	0.298
0.050	-0.300	-0.503	-0.475	-0.575	7.55	4.63	0.613	0.594	2.00	0.297
0.050	-0.300	-0.503	-0.475	-0.575	7.53	4.60	0.611	0.597	1.96	0.305
0.050	-0.300	-0.503	-0.475	-0.575	7.37	4.45	0.604	0.610	1.94	0.314
0.090	-0.300	-0.525	-0.497	-0.600	9.97	7.75	0.777	0.270	1.14	0.237
0.090	-0.300	-0.525	-0.497	-0.600	9.90	7.45	0.753	0.305	1.14	0.268
0.090	-0.300	-0.525	-0.495	-0.600	10.15	7.20	0.709	0.377	1.17	0.322
0.090	-0.300	-0.523	-0.495	-0.600	10.20	7.60	0.745	0.320	1.17	0.274
0.090	-0.300	-0.523	-0.495	-0.600	10.25	7.25	0.707	0.385	1.17	0.329
0.090	-0.300	-0.520	-0.495	-0.600	9.90	7.40	0.748	0.313	1.17	0.268

Table C-6: Data from sample 2; aqueous $Cr(bipy)_3$ at 23°C

Scan rate (V/S)	E_{start} (V)	$E_{c.p.}$ (V)	$E_{\frac{1}{2}}$ (V)	$E_{sw.}$ (V)	i_C (cm)	i_A (cm)	$\frac{i_A}{C}$	$K_f\tau$	τ (sec)	K_f (sec-1)
0.070	-0.300	-0.500	-0.475	-0.580	8.10	5.63	0.695	0.405	1.50	0.270
0.070	-0.300	-0.500	-0.475	-0.580	7.97	5.43	0.681	0.432	1.50	0.288
0.070	-0.300	-0.500	-0.475	-0.580	8.15	5.40	0.663	0.470	1.50	0.313
0.070	-0.300	-0.500	-0.475	-0.580	8.05	5.34	0.663	0.470	1.50	0.313
0.070	-0.300	-0.500	-0.475	-0.580	7.95	5.32	0.669	0.455	1.50	0.303
0.070	-0.300	-0.500	-0.475	-0.580	8.00	5.30	0.663	0.470	1.50	0.313
0.070	-0.300	-0.500	-0.475	-0.580	7.95	5.35	0.673	0.445	1.50	0.297
0.070	-0.300	-0.500	-0.475	-0.580	8.00	5.40	0.675	0.435	1.50	0.290
0.100	-0.300	-0.508	-0.478	-0.580	10.07	7.58	0.753	0.307	1.02	0.301
0.100	-0.300	-0.508	-0.478	-0.580	9.95	7.37	0.741	0.326	1.02	0.320
0.100	-0.300	-0.508	-0.478	-0.580	10.00	7.40	0.740	0.327	1.02	0.321
0.100	-0.300	-0.508	-0.475	-0.580	9.90	7.35	0.742	0.325	1.05	0.310
0.100	-0.300	-0.508	-0.475	-0.580	9.95	7.33	0.737	0.335	1.05	0.319
0.100	-0.300	-0.508	-0.475	-0.580	9.80	7.39	0.754	0.305	1.05	0.291

Table C-7: Data from samples 1 and 2; aqueous $Cr(bipy)_3$ at 25°C

Scan rate (V/S)	E_{start} (V)	$E_{c.p.}$ (V)	$E_{\frac{1}{2}}$ (V)	$E_{sw.}$ (V)	i_C (cm)	i_A (cm)	$\frac{i_A}{i_C}$	$K_f\tau$	τ (sec)	K_f (sec-1)
0.060	-0.300	-0.500	-0.475	-0.575	8.55	5.45	0.638	0.525	1.67	0.314
0.060	-0.300	-0.500	-0.475	-0.575	8.65	5.33	0.616	0.583	1.67	0.349
0.060	-0.300	-0.503	-0.475	-0.575	8.45	5.48	0.649	0.500	1.67	0.299
0.060	-0.300	-0.503	-0.475	-0.575	8.57	5.27	0.615	0.585	1.67	0.350
0.070	-0.300	-0.499	-0.475	-0.575	9.00	6.00	0.666	0.463	1.43	0.324
0.070	-0.300	-0.499	-0.473	-0.575	9.22	5.85	0.635	0.535	1.46	0.366
0.070	-0.300	-0.499	-0.471	-0.575	9.15	5.80	0.634	0.535	1.49	0.359
0.060	-0.300	-0.503	-0.475	-0.575	8.67	5.65	0.652	0.495	1.67	0.296
0.060	-0.300	-0.503	-0.475	-0.575	8.72	5.50	0.627	0.555	1.67	0.332
0.060	-0.300	-0.503	-0.475	-0.575	8.65	5.45	0.630	0.548	1.67	0.328
0.070	-0.300	-0.500	-0.473	-0.575	9.05	5.90	0.652	0.495	1.46	0.339
0.070	-0.300	-0.500	-0.473	-0.575	9.10	5.90	0.648	0.500	1.46	0.342
0.070	-0.300	-0.500	-0.475	-0.575	9.00	5.95	0.661	0.475	1.43	0.332
0.100	-0.300	-0.520	-0.495	-0.595	10.33	7.90	0.765	0.289	1.00	0.285
0.100	-0.300	-0.520	-0.490	-0.595	10.90	7.60	0.697	0.395	1.05	0.376
0.100	-0.300	-0.520	-0.490	-0.595	10.60	7.70	0.726	0.350	1.05	0.333
0.100	-0.300	-0.520	-0.493	-0.595	11.10	7.70	0.694	0.405	1.02	0.397
0.100	-0.300	-0.520	-0.493	-0.595	10.80	7.80	0.722	0.357	1.02	0.350

C-6 Rate of Reaction Results for Aqueous $[Cr(me_2\text{-}bipy)_3]^{+3}$

Tables C-8 and C-9 show the pertinent data and the computed values of K_f at different scan rates for the duplicate samples of $Cr(me_2\text{-}bipy)_3$ at 25°C. The data were extracted from CV polarograms obtained for:

5.5×10^{-5}M $[Cr(me_2\text{-}bipy)_3]^{+3}$ in 0.1M KCl
pH 3.5, at the HMDE (radius = 0.265 mm)
vs SCE saturated KCl

E506: 1×10^{-9} A/mm, D.C., $mm/t_{drop} = 0.25$,
$t_{drop} = 6$ sec

E612: U = -0.450 & -.500 V, ΔU = -0.745 to -0.760 (according to need), Scan rates: 0.04, 0.08 and 0.10 Volt/sec

X-Y Recorder: X = Y = 0.05 V/cm

From Y = 0.05 V/cm and sensitivity 1×10^{-9} A/mm, one obtains for the current axis:

8.51×10^{-9} A/cm or 1117 cm = 10 nAmperes.

Table C-10 lists the results obtained for Sample 1 at different temperatures. The temperature was controlled by passing hot water through the outer shell of the analytical cell, the water being supplied from a thermostatically controlled source. The data were collected under the same experimental

Table C-8: Data from sample 1; aqueous $Cr(me_2\text{-}bipy)_3$ at 25°C

Scan rate (V/S)	E_{start} (V)	$E_{c.p.}$ (V)	$E_{\frac{1}{2}}$ (V)	$E_{sw.}$ (V)	i_C (cm)	i_A (cm)	$\frac{i_A}{i_C}$	$K_f\tau$	τ (sec)	K_f (sec-1)
0.100	-0.450	-0.680	-0.653	-0.755	7.59	5.27	0.694	0.405	1.02	0.397
0.100	-0.450	-0.680	-0.653	-0.755	7.50	5.32	0.709	0.377	1.02	0.370
0.100	-0.450	-0.680	-0.653	-0.755	7.48	5.28	0.706	0.386	1.02	0.378
0.100	-0.450	-0.680	-0.653	-0.755	7.55	5.32	0.705	0.385	1.02	0.377
0.080	-0.450	-0.676	-0.650	-0.755	6.50	4.50	0.692	0.410	1.31	0.313
0.080	-0.450	-0.675	-0.650	-0.755	6.28	4.40	0.701	0.394	1.31	0.300
0.080	-0.450	-0.677	-0.650	-0.755	7.00	4.33	0.619	0.575	1.31	0.439
0.080	-0.450	-0.676	-0.650	-0.755	6.65	4.30	0.647	0.505	1.31	0.385
0.060	-0.450	-0.670	-0.642	-0.750	4.75	2.85	0.600	0.623	1.80	0.346
0.060	-0.450	-0.670	-0.642	-0.750	5.20	3.20	0.615	0.585	1.80	0.325
0.060	-0.450	-0.670	-0.642	-0.750	5.18	2.97	0.573	0.700	1.80	0.389
0.060	-0.450	-0.670	-0.643	-0.750	5.05	3.00	0.594	0.640	1.80	0.360

Table C-9: Data from sample 2; aqueous $Cr(me_2\text{-bipy})_3$ at 25°C

Scan rate (V/S)	E_{start} (V)	$E_{c.p.}$ (V)	$E_{\frac{1}{2}}$ (V)	$E_{sw.}$ (V)	i_C (cm)	i_A (cm)	$\frac{i_A}{i_C}$	$K_f\tau$	τ (sec)	K_f (sec-1)
0.100	-0.500	-0.680	-0.653	-0.760	8.30	5.80	0.699	0.396	1.07	0.370
0.100	-0.500	-0.680	-0.653	-0.760	8.00	5.70	0.713	0.370	1.07	0.346
0.100	-0.500	-0.680	-0.653	-0.760	8.15	5.82	0.714	0.368	1.07	0.344
0.100	-0.500	-0.680	-0.653	-0.760	8.12	5.90	0.727	0.348	1.07	0.325
0.080	-0.500	-0.678	-0.653	-0.755	7.10	4.70	0.662	0.473	1.28	0.369
0.080	-0.500	-0.675	-0.653	-0.755	7.00	4.80	0.686	0.422	1.28	0.330
0.080	-0.500	-0.678	-0.653	-0.755	7.15	4.80	0.678	0.435	1.28	0.340
0.080	-0.500	-0.678	-0.653	-0.755	7.00	4.87	0.696	0.403	1.28	0.315
0.040	-0.450	-0.665	-0.645	-0.745	3.78	2.05	0.542	0.810	2.50	0.324
0.040	-0.450	-0.665	-0.645	-0.745	3.75	2.03	0.541	0.815	2.50	0.326
0.040	-0.450	-0.665	-0.645	-0.745	3.80	2.00	0.526	0.870	2.50	0.348
0.040	-0.450	-0.665	-0.645	-0.745	3.79	1.98	0.522	0.890	2.50	0.356

Table C-10: Data from sample 1;
effect of temperature on the rate of reaction (K_f) of aqueous $Cr(me_2\text{-}bipy)_3$

Temp. (°C)	Scan rate (V/S)	E_{start} (V)	$E_{c.p.}$ (V)	$E_{\frac{1}{2}}$ (V)	$E_{sw.}$ (V)	i_C (cm)	i_A (cm)	$\frac{i_A}{i_C}$	$K_f\tau$	τ (sec)	K_f (sec-1)
22.0	0.100	-0.500	-0.682	-0.655	-0.760	8.43	6.62	0.785	0.257	1.05	0.245
22.0	0.100	-0.500	-0.683	-0.655	-0.760	8.29	6.45	0.778	0.267	1.05	0.259
22.0	0.100	-0.500	-0.683	-0.655	-0.760	8.20	6.40	0.780	0.265	1.05	0.252
22.0	0.100	-0.500	-0.682	-0.655	-0.760	8.37	6.52	0.779	0.266	1.05	0.253
29.0	0.100	-0.500	-0.675	-0.650	-0.750	9.05	5.23	0.578	0.685	1.00	0.685
29.0	0.100	-0.500	-0.675	-0.648	-0.750	8.65	5.15	0.595	0.638	1.02	0.625
29.0	0.100	-0.500	-0.675	-0.650	-0.750	8.45	5.03	0.595	0.638	1.02	0.638
29.0	0.100	-0.500	-0.673	-0.650	-0.750	8.32	5.02	0.603	0.613	1.02	0.603
32.5	0.100	-0.500	-0.675	-0.650	-0.745	8.12	4.19	0.578	0.685	0.95	0.720
32.5	0.100	-0.500	-0.673	-0.650	-0.745	8.12	4.90	0.603	0.615	0.95	0.647
32.5	0.100	-0.500	-0.673	-0.650	-0.745	8.10	4.56	0.563	0.735	0.95	0.774
32.5	0.100	-0.500	-0.675	-0.650	-0.745	8.17	4.65	0.569	0.715	0.95	0.753
35.0	0.100	-0.500	-0.655	-0.633	-0.735	7.18	3.55	0.494	1.000	0.02	0.980
35.0	0.100	-0.500	-0.657	-0.633	-0.735	7.25	3.65	0.503	0.965	0.02	0.946
35.0	0.100	-0.500	-0.657	-0.633	-0.735	7.40	3.70	0.500	0.975	0.02	0.956
35.0	0.100	-0.500	-0.657	-0.633	-0.735	7.45	3.75	0.503	0.965	0.02	0.946

parameters as described above (for 25°C).

The baselines for the measurements of I_a and I_c, however, were slightly different from those used for $Cr(bipy)_3$. While the anodic peak (I_a) was measured again from a point of equilibrium at half cycle, the cathodic peak (i_c) had to be measured from an inclined baseline. Figure C-4 shows a polarogram of the supporting electrolyte in the analytical working range at a scan rate of 0.10 V/S. It was observed that, at this scan rate as well as at 0.080 and 0.060 Volt/sec, the upper plateau of the residual current had an inclination angle of 3.5°. This angle had to be used when the baseline for the cathodic peak was traced. At scan rates slower than 0.050 V/S, the observed angle was 2.5°.

For the polarograms obtained at the higher temperature, it was difficult to reproduce the blanks (supporting electrolyte) at exactly the same temperature. Consequently, the baseline for the cathodic peak had to be constructed with respect to its position relative to the equilibrium point at half-cycle as it was observed at 25°C.

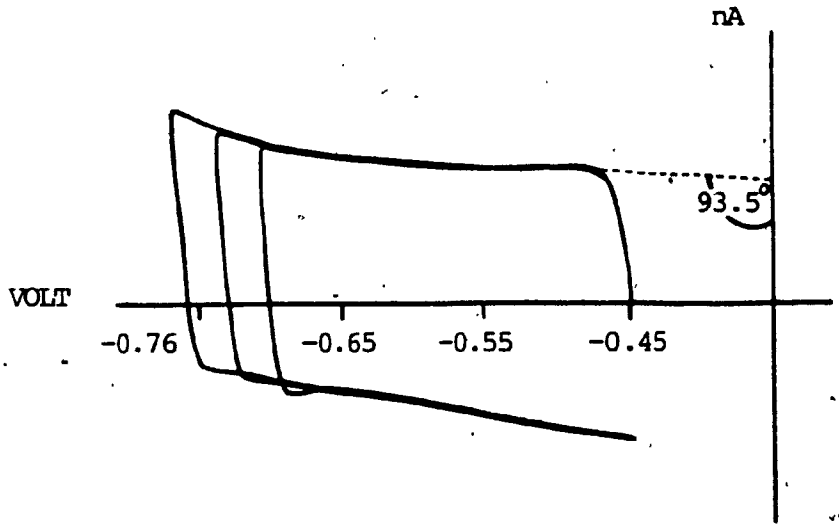

Figure C-4: CV scan of 0.1M KCl supporting electrolyte (blank).